BONE SAWING AND MILLING IN COMPUTER-ASSISTED TOTAL KNEE ARTHROPLASTY

by:

Christopher Plaskos
B.E.Sc., University of Western Ontario, 1999

THESIS SUBMITTED IN PARTIAL FULFILLMENT OF
THE REQUIREMENTS FOR THE DEGREE OF
MASTER OF APPLIED SCIENCE

in

THE FACULTY OF GRADUATE STUDIES
(Department of Mechanical Engineering)

We accept this thesis as conforming

to the required standard

THE UNIVERSITY OF BRITISH COLUMBIA

March 2002

In presenting this thesis in partial fulfilment of the requirements for an advanced degree at the University of British Columbia, I agree that the Library shall make it freely available for reference and study. I further agree that permission for extensive copying of this thesis for scholarly purposes may be granted by the head of my department or by his or her representatives. It is understood that copying or publication of this thesis for financial gain shall not be allowed without my written permission.

Department of Mechanical Engineering

The University of British Columbia
Vancouver, Canada

Date April 9, 2002

Abstract

In total knee arthroplasty, poor limb alignment has been correlated to early failures requiring revision surgery. This thesis therefore addresses three questions: (1) How repeatable and accurate is the conventional sawing process? (2) Could a milling tool produce better results? (3) How can we optimize the milling process for clinical application?

(1) Based on 85 resections performed by eight orthopaedic surgeons on 19 cadaveric femurs and tibias, I estimate the varus/valgus alignment variability associated with making two bone cuts to be ~0.8° SD for expert surgeons and ~1.4° SD for less experienced surgeons (taking $\sqrt{2}$ × the variability associated with a single cut at 95% confidence). In flexion/extension, alignment precision is estimated to be worse at over 2° SD for the group. A significant bias of ~1° in extension due to saw-blade defection on open guide surfaces was detected. Slotted cutting guides eliminated the bias in the sagittal plane but did not significantly improve frontal plane alignment variability.

(2) A novel milling technique is designed and developed to improve cutting precision. Six operators performed a total of 62 cuts on 25 porcine femurs and tibias with the milling technique. The overall varus/valgus alignment variability is estimated to be ~0.6° SD ($\sqrt{2}$ × °SD at 95% confidence) with the milling instrumentation, regardless of the experience of the operator. Similar improvements were observed in flexion/extension, with an estimated alignment variability of ~1.2° SD (compared with >2°) and no significant bias for the milling instrumentation.

(3) A bone-milling model was formulated based on the specific cutting energy of cortical bone, which I estimated from orthogonal cutting tests in the literature. A non-linear model was used to estimate resection accuracy under several different conditions, by solving for the quasi-static deflection of the tool in the direction normal to the cutting surface. Simulation results indicated that resection accuracy could potentially be improved by simply optimizing the surgical parameters of the cutting technique (for example, increasing the feed rate – depth of cut ratio). Alternatively, one could maintain accuracy while improving cutting time.

Table of Contents

Table of Figures

List of Tables

Acknowledgments

First thanks goes to my wonderful and tolerant partner, Sara, who endured more neglect than she deserved during the course of this work.

Thanks to my supervisor, Dr. Antony Hodgson, who provided me with enthusiastic advice and direction. I would also like to acknowledge Drs. Thomas Oxland, Yusuf Altintas, and Wayne Vogl for providing an excellent learning experience through their inspirational lectures. Thanks also to Drs. Robert McGraw, Bassam Masri, and all other surgeons who took time out of their busy schedules to participate in this study and offer their insightful clinical perspectives.

Finally, a very special thanks goes out to Scott Illsley, Paul MacBeth, and Cameron Shute for their technical and moral support, and for donating several hours of their time to the gruelling experimental work detailed here.

Chapter 1: Bone Cutting in Total Knee Arthroplasty

1.0 Objectives

In total knee arthroplasty (TKA), the surgeon aims to restore limb alignment by resecting the damaged bone surfaces and replacing them with a knee implant. Several TKA surgeons have noted that the current cutting technique used to resect the bone surfaces is sub-optimal in terms of resection accuracy and repeatability [Cooke 1985, Lennox 1988, Laskin 1991, Krackow 1991, Minns 1992, Toksvig-Larsen 1994a 1994b, Mont 1997]. In particular, there are many potential sources of error associated with the technique and therefore it is not uncommon for cutting errors to occur in surgery, especially when the surgeon does not have a great deal of experience in TKA.

Cutting errors are important because they can affect the alignment (or orientation) of the implant, which alters how forces are transferred through the patient's knee during weight-bearing activity. Clinically, improper alignment can cause complications and early failure of the prosthesis and lead to revision surgery [Lotke 1977, Moreland 1988, Jeffery 1991, Ritter 1994].

In this thesis, I make three contributions to the field of bone cutting in TKA. Specifically, I complete the following studies:

(1) First, I determine the how much variability the conventional bone sawing technique contributes to knee implant alignment.

(2) Second: I design a novel milling technique that has fewer potential sources of error, and compare it to the conventional technique to determine the relative improvements.

(3) Third: I model the bone milling process and demonstrate how this model can be used to optimize the surgical parameters and cutting tool designs to further reduce alignment variability and/or cutting time. I use a quasi-static tool deflection model to estimate the accuracy of the new milling technique under standard and optimal surgical conditions.

Although study (3) above was undertaken to analyse and further develop the new milling technique presented in (2), it not limited to TKA resections and can be used in almost any orthopaedic procedure that uses bone-cutting tools.

1.1 Background and Literature Review

There are at least five basic bone resections required to perform a standard tricompartmental TKA. These are the proximal tibial resection, the distal femoral resection, the anterior femoral resection, the posterior femoral resection, and the patellar resection (figure 1.1, patellar resection not shown). Supplementary cuts are often required for particular implant designs to allow for chamfers in the femoral component, for intercondylar prominences (especially in posterior stabilized implants), and for fixation stems or pegs [Laskin 1991].

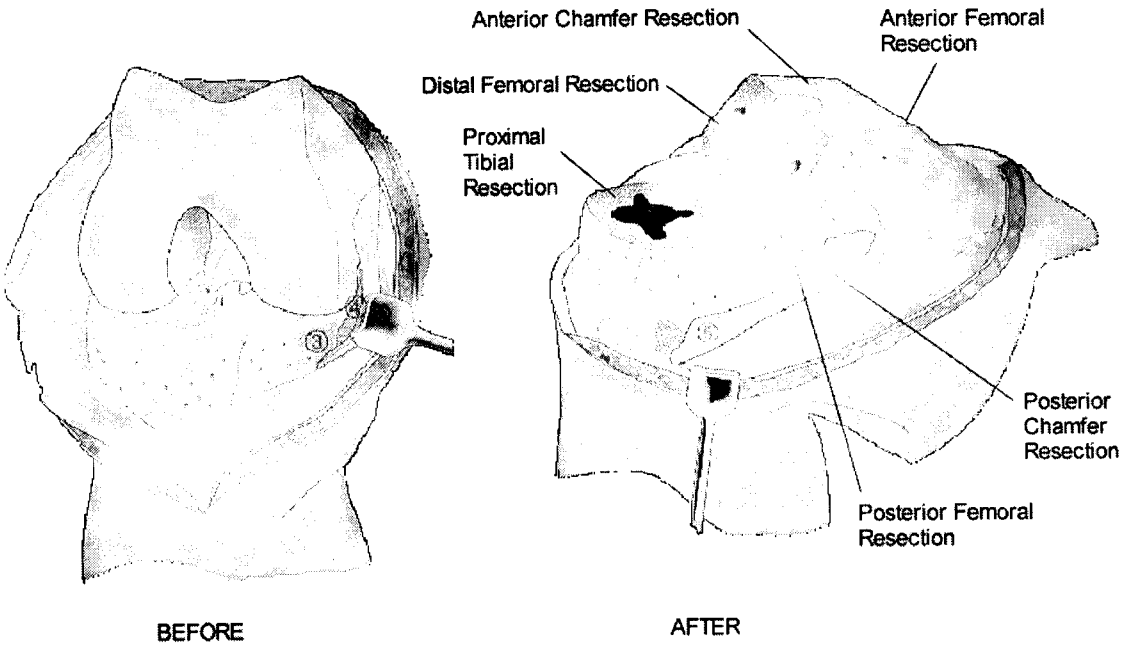

Figure 1.1 Bone cuts made in TKA (Johnson & Johnson Orthopaedics).

Implant alignment is primarily determined by proximal tibial, distal femoral, and anterior and posterior femoral resections, and therefore these are evaluated in this study. Although the patellar resection may have a significant effect on the postoperative function of the knee (for instance, not removing enough bone may lead to extreme tightness, limited flexion and pain), it is not considered in this study. Nor are any supplementary resections such as femoral chamfer cuts or intercondylar notches considered, although these could also affect knee function if not performed correctly (for example, a chamfer cutting error which removes too little bone may lead to distal placement of the femur and 'overstuffing' of the joint).

Typical proximal tibial and distal femoral resections are illustrated in figures 1.2 and 1.3 using the conventional sawing technique currently used in TKA. A cutting guide (also called a cutting block) is used to guide the oscillating saw-blade as it progresses through the bone. Either the slot or the open surface of the cutting block can be used to guide the saw-blade (figure 1.3).

Once the cuts are completed, the components are fixed to the resected bone surfaces either with or without the use of bone-cement (polymethylmethacrylate, or PMMA). Most cementless designs rely on the concept of biological fixation in which bony ingrowth into a porous coating stabilizes the prosthesis, whereas cemented implants rely on a 2-3mm layer of PMMA infused into the cancellous bone for fixation. The use of cementless implants in TKA demands an even higher level of accuracy and planarity from the cutting technique. Not only is the final alignment of the implant important to restore normal loading conditions, but the bone surface must also be sufficiently flat so that a close fit (0.3-0.5mm [Carlsson 1988]) is obtained between the bone and the prosthesis to permit bony ingrowth and fixation to occur [Toksvig-Larsen 1994a]. However, in this study we are primarily concerned with the effects of cutting errors on implant alignment variability, so bone surface flatness is not directly evaluated. In addition, it should be recognised that the cementing process may introduce another source of variability to implant alignment, but this contribution to the overall alignment variability is not measured in this study.

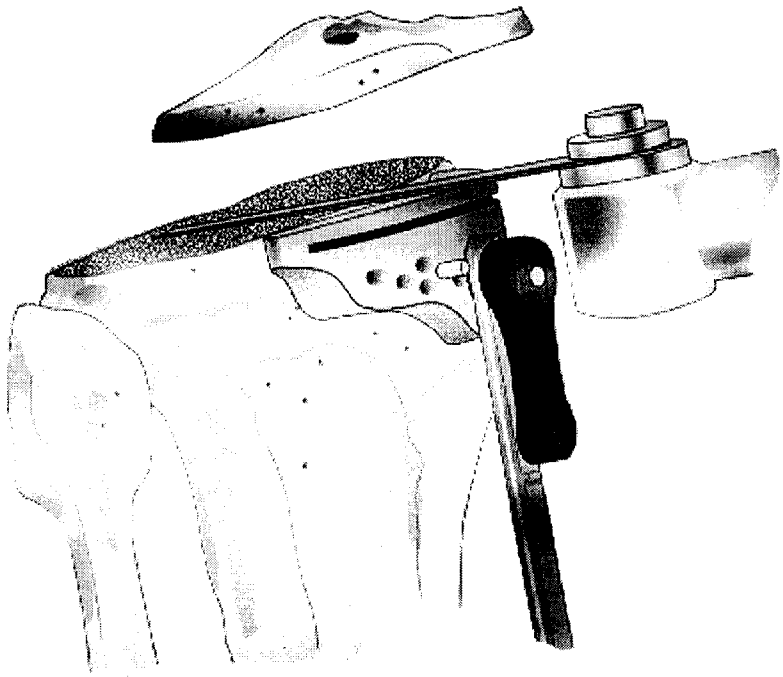

Figure 1.2 Proximal tibial cut (Johnson & Johnson Orthopaedics).

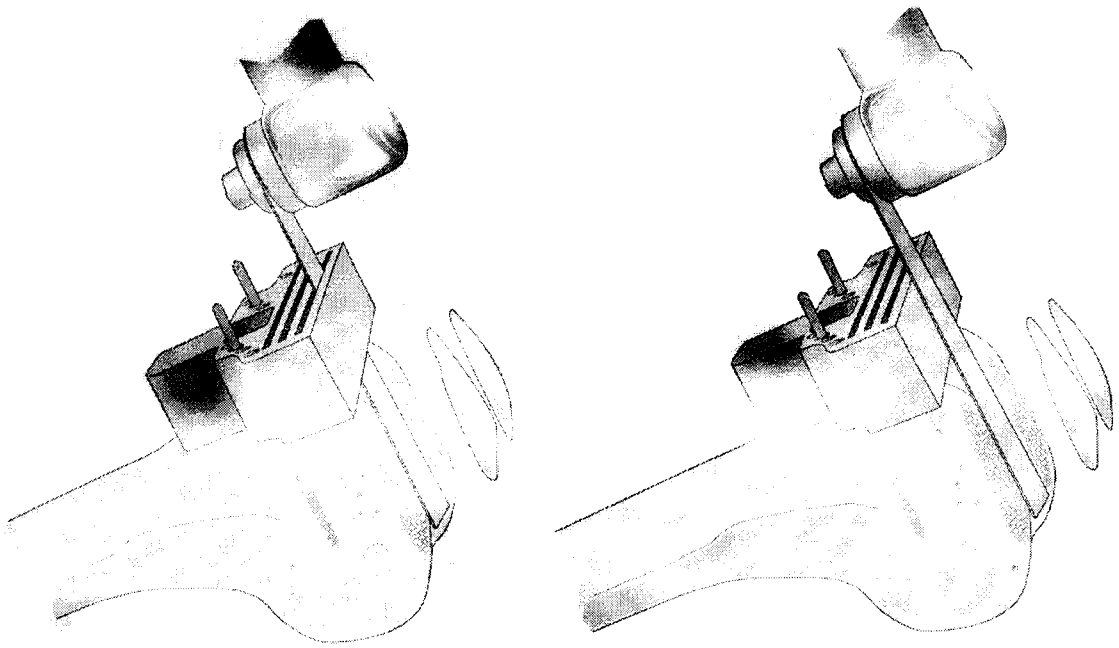

Figure 1.3 Distal femoral cut made with slotted (left) and open (right) cutting guide (Johnson & Johnson Orthopaedics).

1.1.1 Implant Alignment and Cutting Errors

The bone cuts made in TKA are typically referenced to the 'mechanical axis' of the limb, which is defined as the line joining the hip and ankle centres. A cutting error can affect the orientation of the implant relative to this axis in the frontal, sagittal, and transverse planes (varus/valgus, flexion/extension and internal/external rotational alignment errors). The frontal plane is normal to the anterio-posterior direction (figure 1.4), the sagittal plane is normal to the medio-lateral direction, and the transverse plane is normal to the proximal-distal direction.

1.1.1.1 Frontal plane alignment

The importance of proper frontal plane implant alignment in TKA has long been recognised and numerous clinical studies spanning several decades have correlated varus/valgus malalignment, in particular, to early failure [Lotke 1977, Moreland 1988, Jeffery 1991, Ritter 1994]. Proximal tibial or distal femoral cutting errors in the frontal plane directly affect the varus/valgus alignment of the leg. In addition, anterior or posterior femoral cutting errors in the transverse plane can

create an uneven gap between the femoral component and the distal cut surface, affecting alignment in both the frontal and sagittal planes.

Varus or valgus malalignment alters the loading distribution and kinematics at the knee. The intersection point between the knee joint line and the limb's mechanical axis shifts medially in varus, and laterally in valgus (figure 1.4). This results in overloading of the corresponding compartment and an accelerated breakdown of the bone-prosthetic or bone-cement interface. The contact between the tibial and femoral components may shift from both condyles to a single condyle, effectively changing the knee to a ball and socket joint which would result in rotational and anterior/posterior instabilities [Hungerford 1985]. These unstable loading conditions may result in component loosening, excessive wear, subsidence, and ultimately revision TKA [Insall 1985, Moreland 1988, Jeffery and Morris 1991].

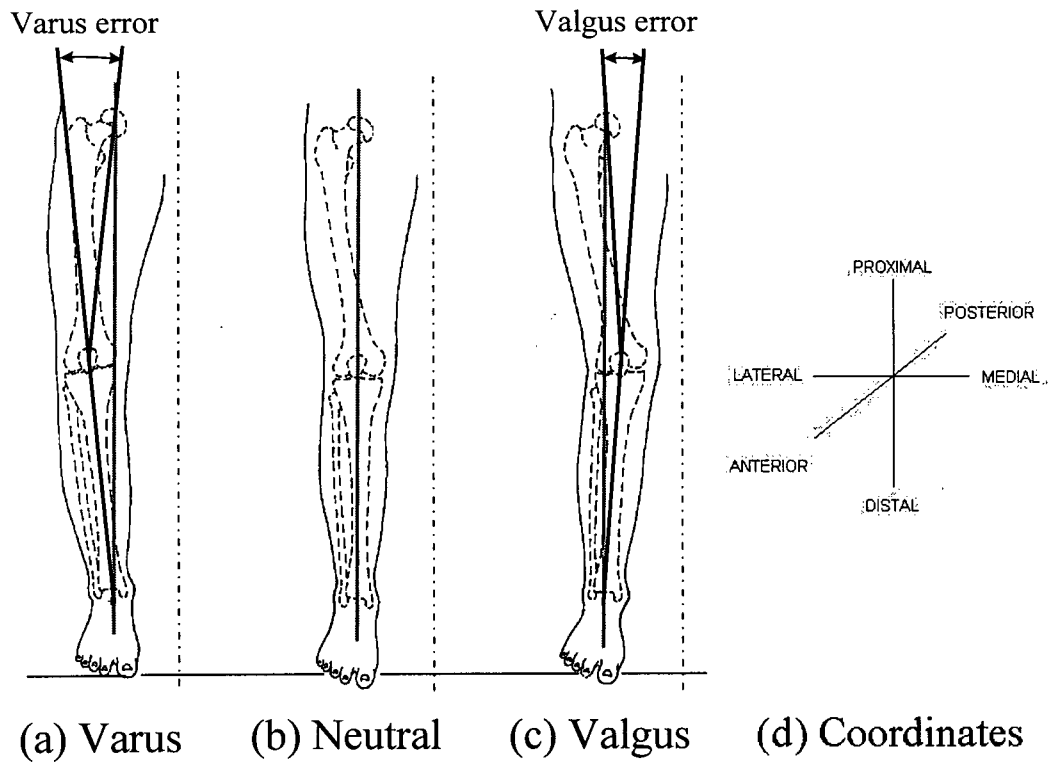

Figure 1.4. Frontal plane alignment errors:
a) Varus malalignment, the mechanical axis shifts medially
b) Neutral alignment, the mechanical axis passes through the knee centre
c) Valgus malalignment, the mechanical axis shifts laterally
d) Anatomic coordinate system, anterior direction out of the page

Although the precise degree of tolerable malalignment is somewhat controversial, many authors maintain that a 2°–3° window in the frontal plane is needed to ensure high success rates in TKA [Insall 1985, Moreland 1988, Hsu 1989, Jeffery 1991, Ritter 1994]. Varus malalignment is generally known to produce worse outcomes and has been reported to be the most common cause of aseptic loosening in TKA [Insall 1985]. Radiographic studies report significant increases in loosening with tibial components placed in varus, and therefore surgeons are advised to aim for neutral or a slight amount of valgus alignment to give the patient the best chance for long-term survival [Kagan 1977, Dorr 1986, Hsu 1989, Windsor 1989, Brugioni 1990].

1.1.1.2 Sagittal plane alignment

Cutting errors in the sagittal plane influence flexion/extension alignment, which can also result in abnormal knee kinematics, soft tissue imbalances, and component subsidence [Hofmann 1991, Bai 2000]. The anterior and posterior femoral cuts are usually keyed from the distal femoral cut by placing the cutting guide directly on the resected distal femoral surface. Therefore a distal femoral cutting error in the sagittal plane will result in incorrectly referenced anterior and posterior resections, and flexion/extension malignment of the femoral component. Extension errors on the anterior cut (i.e. removing too much bone) can cause notching of the anterior femoral cortex, which results in a stress concentration and increased risk of femoral fracture. Flexion errors can result in a fixed flexion contracture [Hungerford 1985].

The tibial plateau in the natural knee is sloped posteriorly and distally 5°–10° to assist femoral 'roll back' on the tibia as the knee is flexed. Typically, the tibia is cut parallel to the natural plateau (~7°), although many tibial implants have a built-in slope and require a cut perpendicular to the mechanical axis in the sagittal plane. Hofmann [1991] found that the load carrying capacity of the tibia is increased by 40% and the stiffness by 70% when cutting parallel to the tibial slope, as opposed to perpendicular to the axis. Although the attitude of the posterior slope cut may vary with the instrumentation set, it is generally agreed that an anteriorly sloped cut should be avoided [Laskin 1991]. An anteriorly sloped tibial cut can decrease the flexion range of motion and diminish the size of the flexion space posteriorly causing posterior wedging and increased polyethylene wear or even anterior lift-off of the tibial component [Dorr 1986, Walker 1991, Bai 2000].

1.1.1.3 Rotational alignment

The orientations of the anterior and posterior femoral bone cuts determine the rotational alignment of the femoral component (about the mechanical axis). Excess bone excised on one of the posterior condyles can cause the femoral component to be rotated in that direction, which may produce instability on that side while the other side is too tight in flexion (flexion contracture) [Hungerford 1985]. Rotation of the anterior femoral surface may produce a malalignment between the patellofemoral groove and the extensor mechanism, which can lead to excessive pain, wear, or dislocation.

After femoral component rotation is determined, tibial component rotation may be fixed with screws or by preparing recess holes to correspond to the stems or pegs of the tibial component. Improper position of these holes can cause also cause premature wear of the bearing surfaces, poor patellar tracking, or instability.

1.1.2 Accuracy of Conventional Cutting Techniques

There have been few published studies that quantify the accuracy and/or precision of the cutting instrumentation used in TKA. Most of the available papers describe the roughness and flatness characteristics of bone surfaces prepared for cementless implants. Others subjectively describe some common cutting errors that occur when using conventional cutting guides in the operating room.

Toksvig-Larsen [1994a] measured the surface characteristics of 26 tibial resections made *in vivo* using thin (1mm) and thick (2mm) saw-blades and cutting guides from a cementless implant system. Tibial plateau surfaces that the surgeon deemed to be clinically 'flat' and acceptable for noncemented insertion were found to be uneven with maximum roughness of 2.5mm (defined as the distance between the uppermost and lowermost measured points) and flatness of 0.38mm (defined as the standard deviation of the measured points). Interestingly, the surface prepared by the thick saw-blade was inferior to that created by the thin blade. They also reported a consistent lack of flatness in the central region in front of the posterior cruciate attachment and a wavy pattern where the cut surface transfers from a hard sclerotic area to an area with normal cancellous bone. They did not, however, measure how these parameters affected the alignment of the implant.

In a similar study using cadaver tibiae, the authors made two attempts to improve surface flatness: (1) with a semi-rotating saw, and (2) with a secondary cutting operation, where a thin layer of bone is 'shaven off' after the initial cut is made [Toksvig-Larsen 1994b]. The semi-rotating saw produced somewhat smoother surfaces than the oscillating saw, though these findings have not resulted in the widespread use of the instrument. They also found that the primary cut surfaces could not be improved with subsequent cuts with either saw type, which demonstrates the importance of achieving an accurate resection on the first attempt.

Krackow [1991] identified several tendencies that are present when making bone cuts in TKA, including the tendency for the saw-blade to 'deep skive' (i.e., to deflect) as a result of dense subchondral bone (figure 1.5). The relatively dense bone in the medial compartment commonly found in varus deformity cases can cause thinner saw-blades to deflect distally, resulting in a varus cutting error. The presence of the extensor mechanism laterally also created a tendency to displace the cutting guide and saw-blade in a proximal direction, further contributing to varus malalignment.

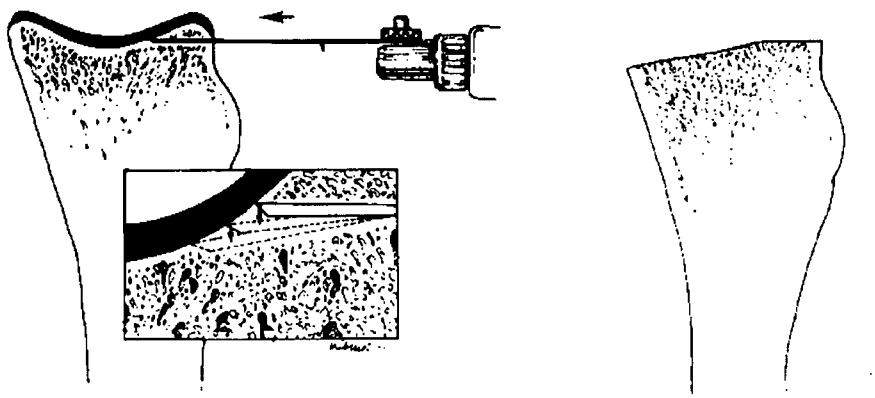

Figure 1.5 "Deep skiving" of saw blade under dense subchondral bone, [Krackow 1991].

Minns [1992] conducted a survey to assess the accuracy of proximal tibial and distal femoral cuts made with slotted and open surface cutting guides. Although no quantitative results were given, slotted cutting guides were noted to produce more accurate cuts than open surface guides. Open surface guides allowed for more error because of the lack of constraint placed on the blade. The blade can easily lift off the guide surface whilst only travelling on the leading or trailing edge of

the guide, resulting either in leaving excess bone uncut or removing excess bone relative to the resection plane (figure 1.6). When cutting the femoral condyles (distal femoral cut) with their sharply curved surfaces and hard sclerotic bone (commonly seen in patients with osteoarthritis), the surgeon often angled the blade downwards to gain purchase into the bone to start a cut. Since the surface of the guide allows this, there is a risk of the blade continuing to bear along the trailing edge of the guide and produce an incorrectly angled cut. When the saw blade encountered the hard subchondral bone after the cut was started, it was seen to deflect and produce a curved surface regardless of the guide type used. The blade can also be lifted on its side whilst moving the saw laterally, which gives an undesired tilt to the cut surface in the frontal plane (varus/valgus error). Other common cutting errors observed included making the cut in the incorrect plane or direction and making multiple cuts over the surface in slightly different planes (for example, excess bone remaining on one side of the transection and removed on the other).

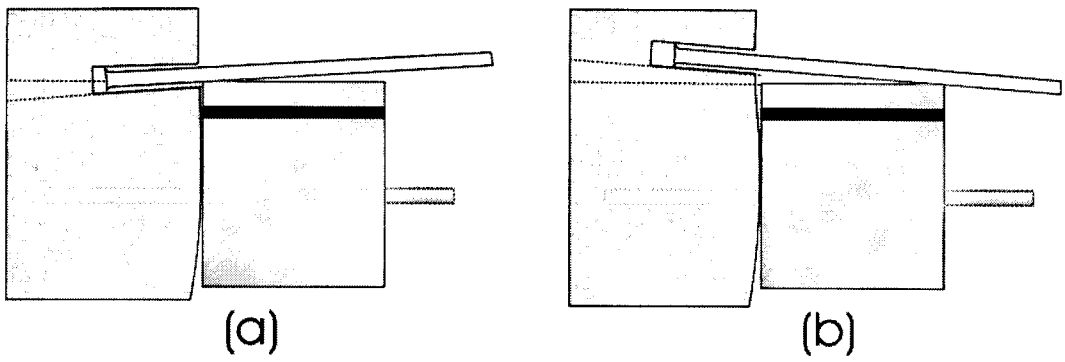

Figure 1.6 Common cutting errors in the sagittal plane: (a) blade traveling on the trailing edge of guide surface removing excess bone (b) blade traveling on the leading edge, leaving excess bone on cut surface

Accurate bone cuts on the femur are of particular importance since many femoral components rely on an interference fit or 'press fit' between the bone and implant for fixation. However, many surgeons note that precise femoral resections are difficult to achieve in the clinical setting and the component is often left improperly seated on the bone surface. Lennox [1988] demonstrated the patterns of femoral component malposition that result from errors in various femoral bone cuts. When excess bone remained on an anterior cut the impacted femoral component assumed a flexed position with asymmetric gaps between the anterior chamfer and distal femoral cuts, while the opposite occurred when excess bone was left on posterior resections (figure 1.7). These cutting errors can cause damage to the posterior or anterior aspect of the femur due to the prosthesis 'digging' into the bone during impaction, and thus should be revised before complete impaction.

Imprecise cuts where excess bone is removed (causing a gap to form between the cut and the implant) are more difficult to correct, and although it is recommended that these errors be filled with bone graft, this is clearly sub-optimal. Lennox also noted a tendency to cut the distal femur asymmetrically (leaving excess bone on the medial or lateral side), causing the component to toggle with symmetric gaps appearing on one side only. Repairing this frontal plane alignment error necessitates revision of the distal femoral cut and the anterior and posterior chamfer cuts.

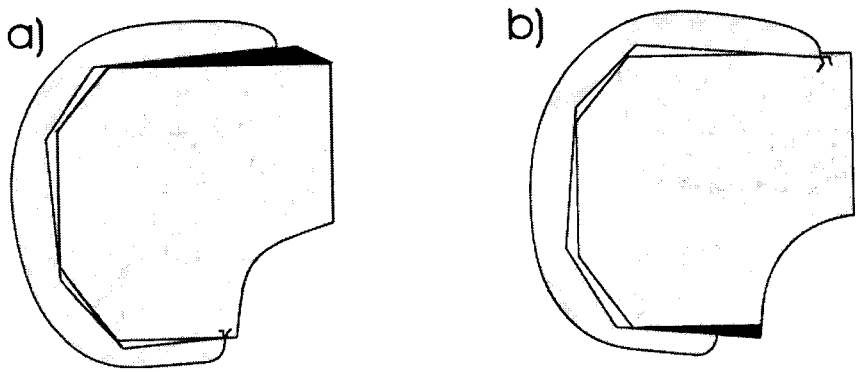

Figure 1.7 Excess uncut bone (black area) on an anterior (a) and posterior (b) femoral cut.

Otani [1993] measured the sagittal plane cutting error caused by toggle of the saw blade in the slot (of width 1.5mm) of an anterior/posterior femoral cutting guide using standard (1.2mm) and thick (1.4mm) saw-blades. The maximum cutting errors measured in balsa wood blocks at a cutting depth of 55mm were on the order of ~0.9 mm for the standard blades and ~0.5 mm for the thicker blades. The maximum toggle angles of the saw-blade in the slot were 0.9° and 0.3° with the 1.2mm and 1.4mm thick blades, respectively. The authors noted that these toggle angles could be caused by displacements of as little as ~2mm at the hand of the surgeon, and since it is very difficult to avoid displacements of this magnitude during cutting with an oscillating saw, the measured maximum errors are likely to be common in clinical practice.

Otani [1993] also measured the relative motion between an anterior/posterior femoral cutting guide and the distal femur during bone cutting with several different types of fixation methods. Pin fixation that relied only on the cancellous bone beneath the cutting guide could not provide tight fixation, allowing over 1 mm of motion. This motion was reduced when combined fixation methods were used (for example, augmenting fixation with an intramedullary rod).

Mont [1997] used an intramedullary goniometer to intraoperatively measure the angle of the distal femoral cut referenced to the medullary canal in the frontal plane. Twenty-five out of the fifty cuts measured (50%) had varus/valgus errors over 1° (and 38% were over 2°) and had to be revised during the procedure. Two resections (4%) had frontal plane errors over 4°, indicating that significant cutting errors can occur even for expert TKA surgeons.

Most of the described studies illustrate the difficulty in producing accurate cuts repeatedly with conventional sawing instrumentation, and many authors note that TKA resections often have to be recut due to cutting errors [Lennox 1988, Minns 1992, Mont 1997]. This can make the procedure more difficult for the surgeon and increase the period of anaesthesia for the patient. Furthermore, a cutting error of 1° or 2° is not visually obvious in the patient and could easily go unnoticed. Therefore, it is important for a cutting technique to be repeatable, permitting the surgeon to consistently achieve accurate resections on the first attempt.

1.1.3 Non-Conventional Cutting Instrumentation

Some researchers have attempted to reduce the number of potential sources of error and improve alignment precision with 'constraint-based' designs of guidance instrumentation. Cooke [1985] introduced a mechanical jig that pinned to the femur and tibia and used sliders to passively guide a conventional oscillating saw (figure 1.8). Guiding the saw instead of the blade eliminated the problems associated with blade–template contact, including blade damage and debris generation [Minns 1992, Wevers 1987]. However, the blades often deflected out of the resection plane upon engaging the hard, rounded cortical bone at the start of the cut. Adapting the blades with 'stiffeners' that were removed after the cut was started reduced this 'vertical whip' or deflection. Although the authors stated that precision and fit was within 1° and 1mm, the accuracy and repeatability of the cutting technique was not directly measured.

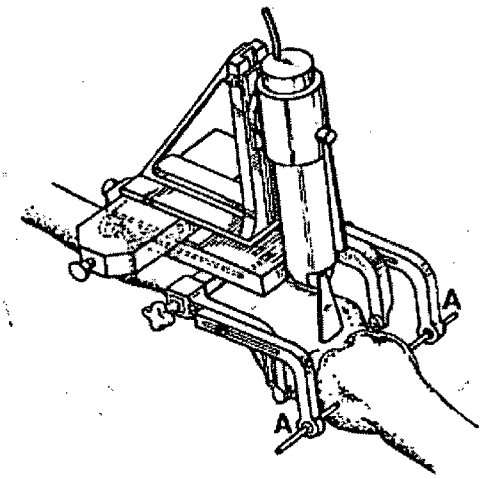

Figure 1.8 "Universal Bone Cutting Device" [Cooke 1985]

Other researchers have taken a more sophisticated approach to reduce cutting errors. Moctezuma [1997] completely redesigned the oscillating saw so that it could be used in conjunction with a robotic arm. The poor ability to start a cut and the high reaction forces needed to support the oscillating saw during cutting motivated its redesign. The new device incorporated a second blade that rotated counter to the first, reducing the lateral forces at the cutting teeth. Although the device was reported to improve surface roughness, no experiment was undertaken to assess the alignment variability of the cutting technique.

Matsen [1993] used a robotic arm to position a specially designed cutting guide for performing distal femoral resections. The saw guide was constructed in a curved configuration so that it could be applied closely to the femur and the surgeon could make the cuts in the correct plane from any of several different approaches. The robot arm was equipped with a stiffening link to reduce the flexibility of the system during the manual sawing process, and this contributed an average of ~4 minutes to the total preparation time (~22 minutes). To test the accuracy of the system and its ability to produce congruent surfaces, five experienced TKA surgeons made distal, anterior, and posterior femoral resections and the angles of the anterior and posterior resections were measured relative to the distal cut. Each surgeon performed the cuts on four plastic femurs: two with a commercially available guide system and two with the robotic system. Even though the guide positioning capability of the robot was determined to be ±0.025mm, forty percent of the cuts made with the system had an angular error of ±2° or more (range ±5°). The system did however improve the cutting accuracy of the conventional guides, which had seventy percent of

errors equal to or larger than ±2° (range -15°–9°). The orientation of the distal femoral cut relative to the cutting guide orientation was not measured.

Thus far, only robot-guided TKA cutting techniques have demonstrated improved resection accuracy with respect to surface flatness and orientation. Instead of using an oscillating saw to make the bone cuts, these systems typically use milling tools coupled with passive, semi-active, or active robotic guidance [Davies 1997, Delp 1998, Fadda 1998, Van Ham 1998]. Fadda [1998] used porcine femurs and tibiae to demonstrate that robot-assisted milling is capable of producing bone surfaces within the roughness and flatness limits necessary for bone integration into cementless implants. Van Ham [1998] used porcine and cadaveric tibiae to demonstrate that sub-degree precision is attainable with robotic guidance, though their system required the tibial and femoral condyles to be sawed off first with a conventional cutting block and oscillating saw. Accurate resections were subsequently obtained by performing a finishing operation where the robot guided a milling tool over the cut surface, removing ~2mm of bone.

The orientation of the milling tool relative to the bone axis is also an issue in TKA. Most milling systems (including one commercially available manual TKA instrumentation set, Zimmer NextGen Knee System) orient the mill so that the tool axis is perpendicular to the resection plane [Davies 1997, VanHam 1998]. This creates a tendency to cut more bone than is strictly necessary and increases the production of bone dust in the patient. In addition, access to the bone surfaces becomes difficult (especially for the posterior femoral resection and the tibial resection with its posterior slope) and therefore these systems often require larger incisions and more invasive surgical techniques.

Although robotic systems have demonstrated the ability to position tools accurately and perform resections repeatedly, they are generally not well suited for the operating room as they often require increased operating time in terms of equipment set-up and cutting time. Most of the abovementioned studies have used slow feed rates that would result in clinical resection times of over 5 minutes per cut. In addition, the capital cost associated with robotic systems used in the operating room has been approximately US$500,000 [Delp 1998], which is a major limitation of this technology. The safety concerns associated with robot-aided surgery have also inhibited their widespread use in orthopaedic surgery. Some authors have developed sophisticated control strategies in hopes of establishing clinical acceptance and reducing the inherent risks of surgeon/robot/patient interaction. For instance, Davies [1997] developed an active constraint robot (or ACROBOT) that restricts the movement of the cutting tool to pre-programmed regions

in the distal femur. Van Ham [1998] designed a hybrid force-velocity control scheme to constrain the robot's motion to a predefined trajectory within the cutting region. However, since robotic instrumentation suffers from increased time and cost, as well as safety issues, it is not likely that they will be a feasible alternative for most clinics.

1.1.4 Alignment Accuracy in Conventional and Computer-Assisted TKA

Passive computer-assisted TKA techniques have been recently introduced into the operating room in hopes of improving the implant alignment variability that is associated with manual instrumentation. These systems typically use infrared cameras that track reference frames pinned to the femur and tibia, and kinematic or digitization methods to accurately register the mechanical axis to the patient [Krackow 1999, Saragaglia 2001, Inkpen 2000]. Once the registration stage is complete, cutting guides are precisely oriented relative to the mechanical axis under computer guidance and conventional sawing is used to resect the bone ends [Leitner 1997].

Unfortunately, these systems have only demonstrated a marginal improvement in alignment variability [Jenny 2001, Mielke 2001, Saragaglia 2001]. Jenny used long leg radiographs to compare 80 knees implanted with computer-assisted vs. manual instrumentation and found 7 (18%) and 9 (23%) knees, respectively, with frontal plane alignment errors outside a 6° window (3° varus to 3° valgus). Mielke also found no statistically significant improvement in mechanical axis alignment with a computer-assisted procedure. Saragaglia reported the frontal plane alignment variability in 50 knees implanted with computer-assisted vs. manual instrumentation and found only a marginal improvement (2.53 vs. 2.72° SD).

Since these systems have reported excellent registration capabilities (mechanical axis definition <0.5°SD) [Leitner 1997, Krackow 1999, Inkpen 2000], there is a possibility that the sawing technique is contributing a high percentage of the total alignment variability. Inkpen [1999] assessed the variability associated with registering the mechanical axis with various computer-assisted techniques. He also conducted a pilot study to assess the alignment variability associated with the conventional sawing technique. From a total of 20 test cuts made by one expert surgeon (8 cuts) and four operators with no TKA experience (12 cuts), he estimated that the contribution of cutting errors to frontal plane alignment variability was over 90% (figure 1.9). It is worth noting that the cuts made by the expert surgeon were considerably less variable than those made by the inexperienced operators, although the difference was not statistically significant due to the small number of cuts measured.

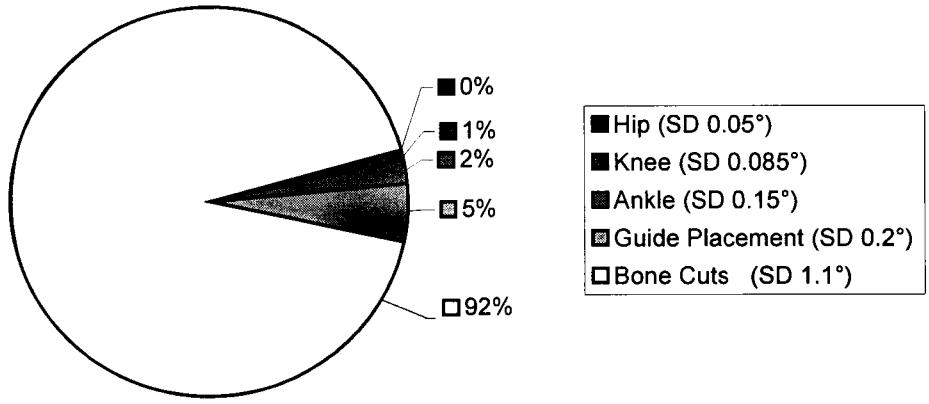

Figure 1.9 Contributions to overall varus/valgus alignment variance in computer-assisted TKA.

To accurately estimate the contribution that a conventional sawing technique would introduce into a computer-assisted procedure, a representative population of TKA surgeons should be evaluated. If this variability is as high as Inkpen's pilot study suggests, a computer-assisted procedure that aims for sub-degree alignment variability will have to consider alternative cutting techniques, such as milling [Delp 1998]. Although robot guided milling has demonstrated improved resection accuracy in TKA, a cutting technique that does not suffer from such high instrumentation costs, increased resection times, or other drawbacks would be of great value to such a system. For example, if a milling technique could be implemented manually and the surgical parameters determined so that resection accuracy and time are optimized, perhaps computer-assisted TKA instrumentation will make a more significant improvement to implant alignment variability.

1.2 Thesis Overview

Chapter 1: Objectives, background and literature review.

Chapter 2: Evaluation of the conventional sawing technique: Eight orthopaedic surgeons with varying TKA experience are recruited to make 85 cuts on 19 cadaveric femurs and tibiae and the alignment accuracy of each cut is measured.

Chapter 3: Evaluation of a novel hand-operated milling technique for TKA: Six operators make a total of 97 cuts manually (62 with milling and 35 with sawing) on 40 porcine femurs and tibiae and the alignment variability is compared for each technique.

Chapter 4: Model development of the bone milling process: In order to analyse the milling technique developed in Chapter 3, a force prediction model of the bone milling process is formulated using the specific cutting energy of bone. The accuracy of the milling technique is estimated (by modelling the cutting tool as an elastic beam) under a variety of cutting conditions and optimal surgical parameters are determined based on these results.

Chapter 5: Conclusions and future work.

Appendix A: Determining the resonant frequencies and optimal cutting speeds for bone milling.

Appendix B: A Passive Bone Milling Guide for Computer-Assisted Knee Replacements.

Chapter 2: Bone Sawing Errors in Total Knee Arthroplasty

2.0 Chapter Summary

Although achieving precise implant alignment is critical for producing good outcomes in total knee arthroplasty, the contribution of the bone cutting process to overall variability has not previously been measured. Eight orthopaedic surgeons of varying TKA experience performed eighty-five resections on 19 cadaveric femurs and tibias and the planes of the resulting cut surfaces were compared to the guide planes. Frontal plane cutting variability ranged from 0.4° SD [95% CI: 0.33°-0.55°] and 0.8° SD [95% CI: 0.68°-0.97°] for expert and trainee surgeons, respectively. Sagittal variability was 1.3° SD [95% CI: 1.13°-1.53°] for both surgeon groups. A tendency for the saw blade to deflect away from the guide surface in the sagittal plane for cuts made with open guides resulted in a bias of ~1°. Slotted cutting guides reduced the variability and eliminated the bias in the sagittal plane for experienced surgeons but did not significantly improve frontal plane alignment variability. Guide movement correlated with cutting errors for all cut types ($p<0.01$), but contributed less than 25% of the total cutting error for proximal tibial and distal femoral resections. For A/P resections, guide movement contributed ~40% of total errors, indicating that addition fixation techniques may be necessary.

2.1 Introduction

It has long been known that accurate component positioning is essential to the success of total knee arthroplasty (TKA) [Insall 1985, Dorr 1986, Moreland 1988, Whiteside 1988, Hofmann 1991]. Achieving this requires the surgeon to identify and register the tibial and femoral mechanical axes, align and mount cutting guides to these axes, and perform the bone cuts. Although several studies have compared and evaluated different registration and guide positioning techniques [e.g., Brys 1991, Teter 1995], the effects of conventional bone cutting techniques on overall TKA alignment accuracy and precision are not well known. In particular, we are not aware of any published studies in which the angular difference between the cutting guide surface and the resulting cut bone surface has been measured.

We do know that conventional sawing techniques produce uneven bone surfaces with gaps large enough to affect the fixation and position of the implant [Lennox 1988, Toksvig-Larsen 1994a, 1994b]. Modern TKA instrumentation incorporates various features (such as narrow slots to guide saw-blades) which are designed to improve resection accuracy. Nevertheless, making precise bone cuts in the clinical setting remains difficult [Lennox 1988, Minns 1992] and

varus/valgus cutting errors as high as 4° [Mont 1997] and flexion/extension errors as high as 10° [Ewald 1985] have been reported. Minns [1992] noted that slotted guides appear to increase cutting precision, but did not provide experimental results supporting this observation.

Computer-assisted TKA techniques have been developed more recently and have had good success in reducing registration errors [Delp 1998, Krackow 1999], but whole-system results have been somewhat disappointing [Saragaglia 2001]. This suggests that perhaps variability due to the cutting process dominates the variability of the overall procedure (among other possibilities). Milling has been shown to be more accurate than sawing [Fadda 1998, Van Ham 1998], but it tends to involve more cumbersome equipment and may possibly increase the risk of injury to the patient and surgeon, so it is not clear whether or not computer-assisted registration procedures need to be paired with milling to reduce the overall alignment variability significantly.

This study therefore examines the specific contributions of tibial and femoral cutting errors to implant alignment in the frontal and sagittal planes. In particular, we address the following questions:

(1) Do cutting errors referenced from a positioned guide surface contribute significant variability to implant alignment? If so, is this variability affected by:

(2) surgical experience,

(3) guide type (open or slotted), or

(4) guide movement relative to the bone?

2.2 Materials and Methods

2.2.1 Experimental Procedure

Eight orthopaedic surgeons performed a total of eighty-five bone cuts on 19 fresh frozen human bone specimens (12 femora and 7 tibia). The surgeons were drawn from two populations: expert surgeons, who had performed more than 500 total knee arthroplasties (TKA's) each (3 surgeons: A-C) and less experienced surgical residents (trainees), each of whom had performed fewer than 50 TKA's (5 surgeons: D-H). The surgeons used the PFC™ Total Knee Instrumentation (DePuy, Warsaw, IN. USA) to implement proximal tibial (PT), distal femoral (DF), and anterior/posterior

(AP) femoral resections (Table 2.1). On each specimen, the surgeon made one primary resection and two to three recuts at an average resection depth of 2 to 4 mm. The bones (12 male: 83.9 ± 10.5 years, 61.9 ± 17.4 kg; 4 female: 72.3 ± 1.5 years, 56.0 ± 4.7 kg; 3 unknown), which had all soft tissues removed, had no obvious abnormalities in bone quality, and they were allocated randomly to each surgeon.

Table 2.1. Distribution of cuts by surgeon experience, cut type and guide type

	Experts n=3	Trainees n=5
Primary*	25	38
Secondary+	12	10
Open Guide	22	27
Slotted Guide	15	21

*Primary = proximal tibial and distal femoral cuts
+Secondary = anterior and posterior femoral cuts

The PFC™ instrumentation enables surgeons to use either slotted or open surface guides for the three cut types tested (PT, DF, and AP; chamfer cuts were not measured). Guide type was allocated at random with open guides used for 49 cuts and slotted guides for the remainder. All cuts were made with a 1.19mm thick, 90mm long saw blade (Johnson & Johnson #26-6050) except for 8 cuts made with a 0.8mm thick, 75mm long blade (Synvasive 'Stablecut' #11-0470). Blades were renewed at the surgeons' request. The resections made with the 0.8mm blade (5 distal femoral and 3 anterior femoral) were made by one expert surgeon (surgeon A) and were measured and reported in a pilot study reported elsewhere [Inkpen 1999].

Bone specimens were rigidly clamped to a table in positions approximating those encountered in the operating theatre. Prior to each cut, the surgeon pinned the guide to the specimen and we measured the orientation of the cutting guide using an optoelectronic localizer (described below). The surgeon then made the cut and did any trimming and checking they would normally do in live surgery. We then re-measured the guide to check for any change in orientation. We also measured the plane of the bone cut by placing an appropriately sized dummy implant on the cut bone surface and measuring its orientation relative to the original cutting guide position. This orientation was characterized by two fixed frame rotations corresponding to varus/valgus tilt and posterior slope (see figure 2.1). The dummy implants were flat aluminium plates without stems or pegs and with profiles and distal footprints matching the tibial and femoral components of the Johnson & Johnson PFC implants.

2.2.2 *Measurement Technique and Precision*

We measured the orientations of the cutting guides and the cut bone surfaces using a custom-built planar probe instrumented with an array of infra-red emitting diodes (IREDs). An optoelectronic localizer (Flashpoint 5000, Image Guided Technologies, Boulder, CO, USA) measured the three-dimensional positions of these IREDs and we applied a coordinate transformation obtained during a calibration procedure to infer the location of the plane on which the probe rested. We estimated the measurement variability by repeatedly (30 times) placing a dummy implant on a fixed cut bone surface and measuring its orientation. For the particular position of the localizer relative to the experimental setup, the resulting standard deviation (SD) was <0.10° for varus/valgus errors and <0.17° for flexion/extension errors (upper bound of the 95% confidence interval on the standard deviation estimate).

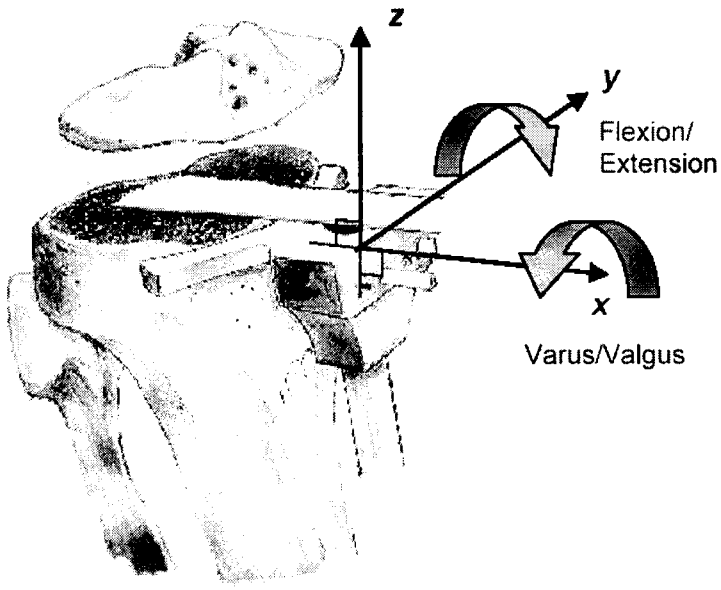

Figure 2.1. The bone–cutting error is defined as two fixed frame rotations between the cutting guide and dummy implant.
Flexion/extension errors (about y) are in the sagittal plane and varus/valgus errors (about x) are in the frontal plane (transverse plane for secondary resections).

2.2.3 *Statistical Analysis*

We assumed that frontal and sagittal plane cutting errors were uncorrelated, and analyzed these errors independently in a repeated measures ANOVA with the following two factors: surgical experience (expert and trainee) and guide type (open and slotted). We pooled proximal tibial and distal femoral cuts and anterior and posterior cuts, analyzing them as two separate groups (cut types PT/DF and A/P, hereafter referred to as primary and secondary cuts). For intra-surgeon and group variability estimates, we used exclusive means for each combination of individual surgeon, guide type and cut type to calculate residuals. For box-plots, we provide variability estimates for the group mean for each surgeon or group of surgeons. The guide movement and implant error results were correlated in an ANCOVA that tested for significance of experience level and guide type for each cut type. The confidence intervals on the squared correlation coefficient r^2 were calculated assuming that $\ln((1+r)/(1-r))/2$ is a normally distributed random variable with variance $1/(n-3)$, where n is the number of data points used to calculate r.

2.3 Results

2.3.1 *Overall Variability*

Figure 2.2 shows the results of all primary cuts made, regardless of cutting guide type, grouped by surgeon. The standard deviations associated with individual surgeons ranges from 0.35° to ~1.0° (varus/valgus: V/V) and from 0.8° to ~2.0° (flexion/extension: F/E), and varus/valgus alignment is significantly less variable for the majority of surgeons. For all but one surgeon (C), there is no significant bias in varus/valgus alignment, while three surgeons exhibit a bias towards extension (A, C, E). The maximum errors relative to the cutting guide are in the range of 1.5-2.0° (V/V) and 3.0-4.0° (F/E).

2.3.2 *Effect of Surgical Experience*

The expert group exhibited significantly less variance in frontal plane alignment than did the trainee group (0.4° SD [95% CI: 0.33°-0.55°] and 0.8° SD [95% CI: 0.68°-0.97°] respectively, $p<0.01$, figure 2.3). The experts were able to limit their varus/valgus cutting errors to under ±1° (range, -0.94°–0.66°, positive = varus), whereas each of the trainee surgeons had at least one cut outside the ±1° range (range, -1.56° – 2.13°). The mean cutting error in the frontal plane for each

surgeon group was -0.15° and 0.3° (expert and trainee grand mean, primary cuts with both guide types).

Cutting precision in the sagittal plane (flexion/extension error) was significantly worse for both surgeon levels ($p<0.0005$), with several resections having errors over 2°. Experts and trainees exhibited similar sagittal plane cutting variability for primary resections, with equivalent group variances of ~1.3° SD (figure 2.3). The mean cutting error in the sagittal plane for each surgeon group was 0.86° and 0.16° (expert and trainee grand mean, primary cuts with both guide types).

2.3.3 Effect of Cutting Guide Type

When using open cutting guides, both surgeon groups tended to leave excess bone at the back of the cut for primary and secondary resections, resulting in a sagittal plane bias which, surprisingly, was greater for expert surgeons than for trainees (1.4° vs. 0.6°), although this was not a significant difference ($p=0.19$). This bias was largely eliminated for all cuts across both surgeon groups when resections were carried out with slotted guides (figure 2.4), although the effect on trainee surgeons was not statistically significant ($p = 0.13$); expert surgeons reduced their bias from 1.4° to 0.2° ($p<0.02$), whereas trainee surgeons reduced their bias from 0.6° to -0.1°.

Slotted cutting guides did not significantly improve frontal plane cutting variability for either surgeon group (figure 2.4, experts: $p = 0.40$, trainees: $p = 0.78$), nor did they improve sagittal variability within the trainee group (1.52° SD [95% CI: 1.24–1.98°] and 1.58° SD [95% CI: 1.27–2.13°] for open and slotted guides, respectively; $p = 0.69$). They did, however, significantly reduce variability in flexion/extension from 1.60° [95% CI: 1.28–2.15°] to 0.64° SD [95% CI: 0.49–0.93°] for the expert surgeons ($p < 0.02$).

Only one out of 22 secondary resections (A/P) had over 1° of error in the transverse plane (internal/external rotation of femoral component – analogous to varus/valgus alignment for a primary cut). For the expert surgeons, slotted guides significantly reduced variability in the transverse plane from 0.8° SD [95% CI: 0.57–1.76°] to 0.2° SD [95% CI: 0.15–0.47°] ($p<0.05$, figure 2.4). This improvement, however, was not seen in the trainee group who had similar cutting variability (~0.5° SD) with both guide types.

2.3.4 *Effect of Cutting Guide Movement*

The cutting errors correlated with the guide movement measurements for primary and secondary resections in all cardinal planes ($p<0.01$, figure 2.5). For primary cuts, guide movement contributed 18.3% [95% CI: 16.0%–21.2%] (r^2 = sum of squares ratio) of the total error variance in the frontal plane and 10.8% [95% CI: 8.9%–12.9%] in the sagittal plane. For secondary cuts, guide movement contributed 30.1% [95% CI: 22.1%–38.4%] and 39.5% [95% CI: 31.4%–47.6%] of error variance in the transverse and sagittal planes, respectively. Surgical experience or guide type did not significantly affect the guide movement/implant error relationship for primary cuts in the frontal plane, or for secondary cuts in either plane. For primary cuts in the sagittal plane the tendency for the blade to deflect with open guides is evident, with the open guide regression line intercept (0° guide movement) almost 1° higher than the slotted guide intercept.

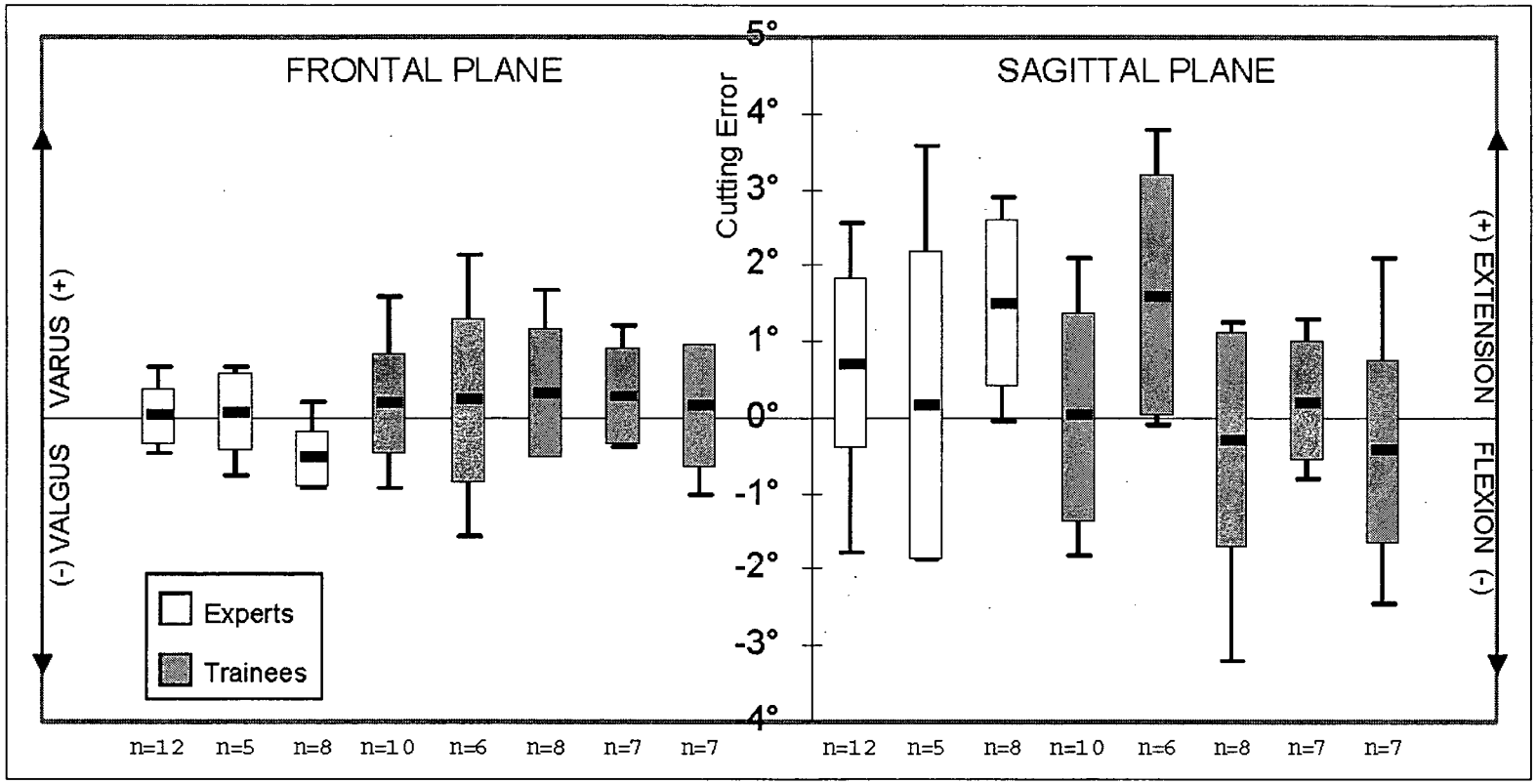

Figure 2.2: Frontal (varus/valgus) and sagittal (flexion/extension) plane cutting errors (°) for each surgeon (proximal tibial and distal femoral cuts with open and slotted guides).

[bold line = mean, box length = ± SD, error bars = range]

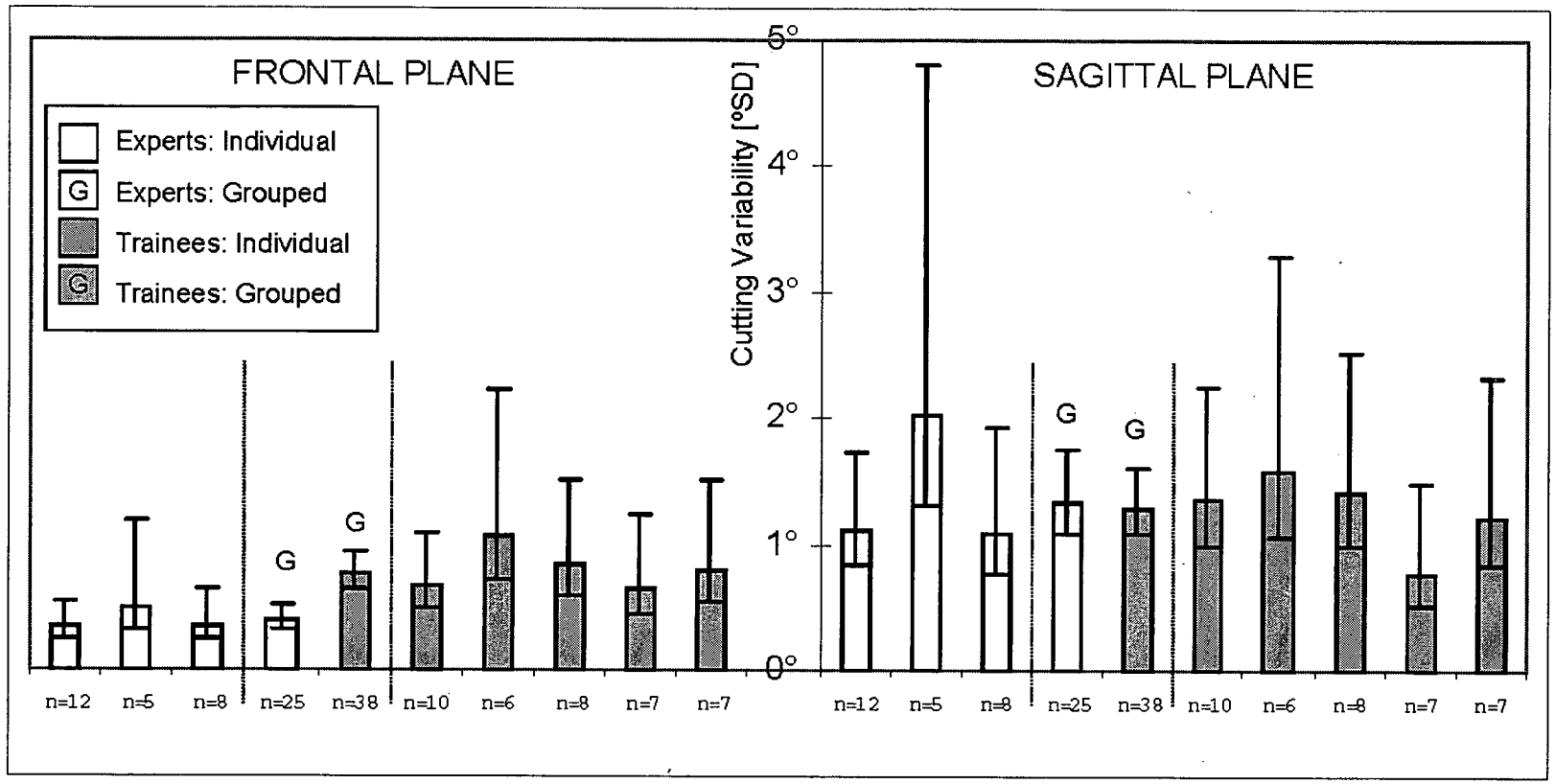

Figure 2.3. Intra-surgeon and grouped cutting variability (°SD) in the frontal and sagittal planes for expert and trainee surgeons (proximal tibial and distal femoral cuts with open and slotted guides).

[error bars = 95% confidence intervals]

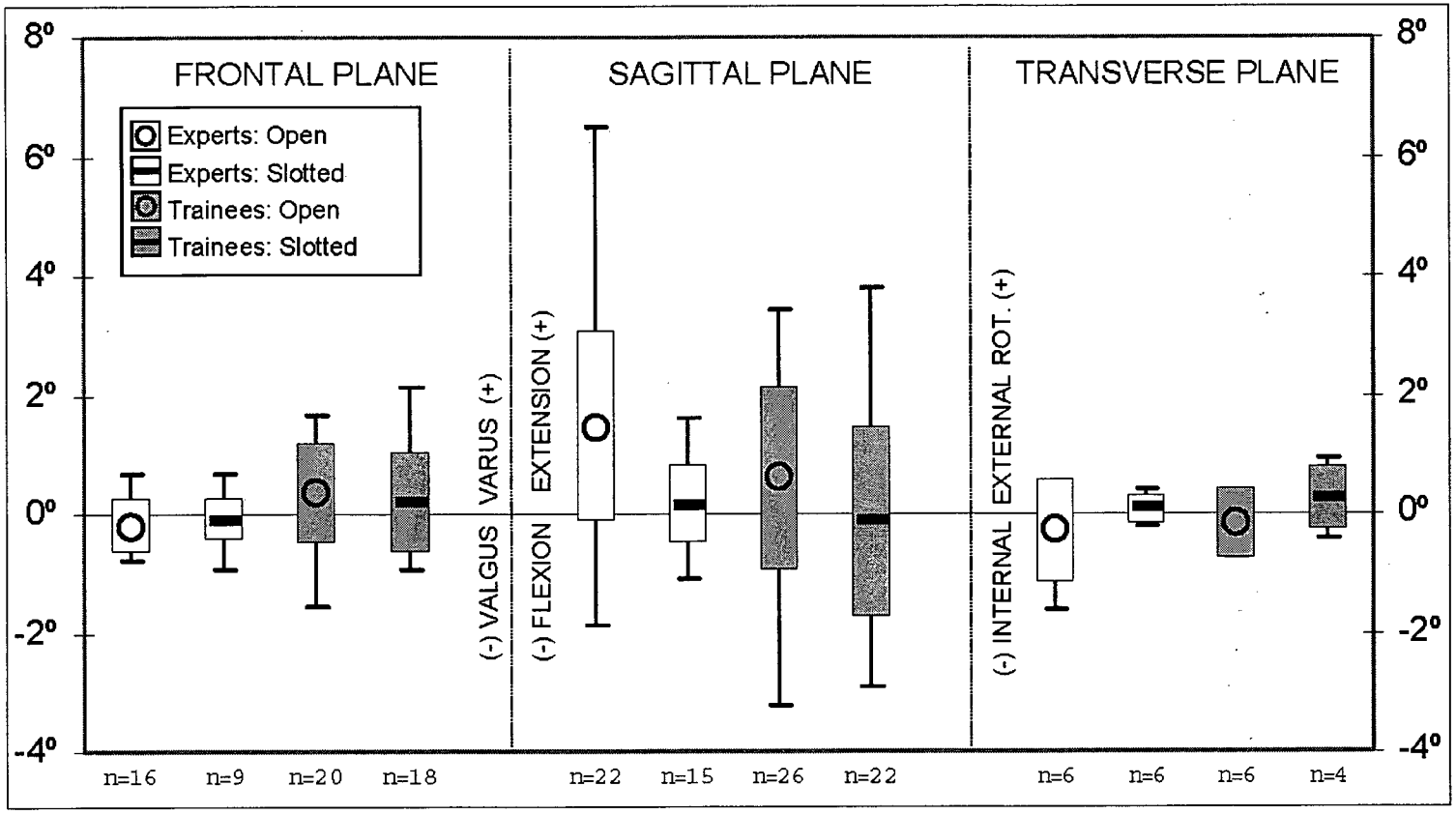

Figure 2.4. Cutting errors with open and slotted cutting guides in the frontal (primary cuts), sagittal (primary and secondary cuts) and transverse (secondary cuts) planes for expert and trainee surgeons.

[line/circle = mean, box length = ±SD, error bars = range]

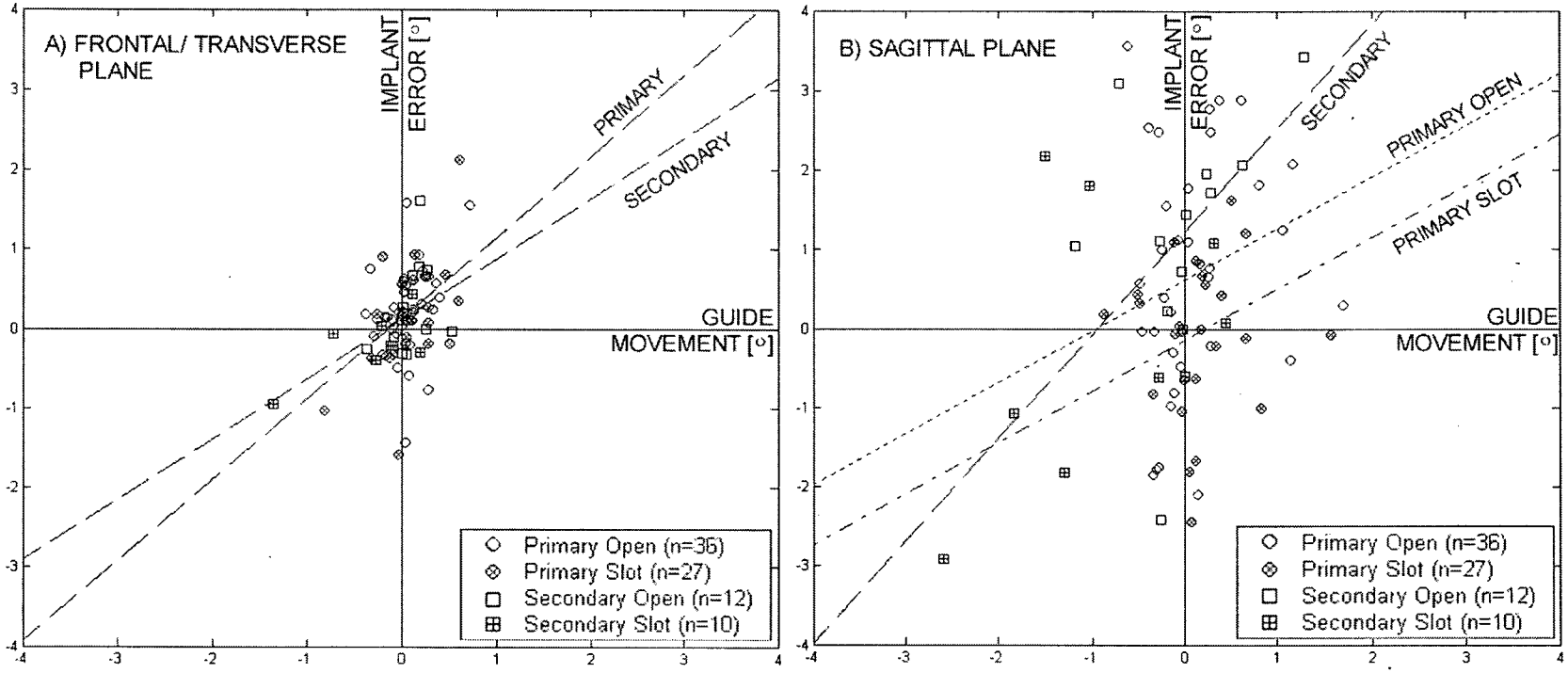

Figure 2.5. Implant error vs. guide movement [scale = 1°] in the a) frontal/transverse and b) sagittal planes for all cuts.

Dashed lines represent lines of best fit ($p<0.01$). Surgical experience or guide type did not significantly affect the guide movement/implant error relationship for primary cuts in the frontal plane, or for secondary cuts in either plane. In the sagittal plane, open guides (dotted line) had a significant biasing effect over slotted guides (dash-dot line) for primary cuts ($p<0.05$). Note: guide movement data was unavailable for 3 primary resections, and guide movement/implant errors exceeded +4° in the sagittal plane for 2 cuts

2.4 Discussion

Exceeding the narrow limits of optimal implant alignment can result in unstable loading conditions, component loosening, wear and subsidence, and may often necessitate revision in TKA [Insall 1985, Moreland 1988, Jeffery 1991]. The precise limits of acceptable alignment relative to the mechanical axis are somewhat controversial, though many authors suggest a 2° – 3° window in the frontal plane for the highest success rate [Insall 1985, Moreland 1988, Hsu 1989, Jeffery 1991, Ritter 1994]. In this study only 4 cuts (6%) had varus/valgus errors of greater than 1.5° (two such cuts would be required to produce an overall alignment error greater than 3°, which would be a relatively rare occurrence). However, these errors represent only those produced in the cutting process itself and do not include any errors in positioning the guide relative to the mechanical axis. Since many essential bony landmarks are concealed with only the ends of the bones exposed to the surgeon, precise guide positioning is extremely difficult [Windsor 1989]. We estimate that the variability associated with two bone cuts made with saws (one on the tibia and one on the femur) would be on the order of ~0.8°-1.5° SD in varus/valgus and over 2.0° in flexion/extension (taking $\sqrt{2}$ times the variability associated with a single cut at 95% confidence). If we wish to produce alignments which are consistently within the 3° window mentioned above, we would need to reduce the variability in the overall procedure to <1° SD. The variability associated with bone cuts alone would nearly always prevent us from attaining this goal, even if our guide alignment were perfect.

Despite reports of significant increases in loosening with tibial components placed in varus [Kagan 1977, Dorr 1986, Hsu 1989, Windsor 1989, Brugioni 1990], some authors suggest that 3° varus placement of the tibial component better restores physiologic loading conditions [Hungerford 1982]. Clinical attempts to achieve a 3° varus tibial cut have, however, resulted in an average (±SD) varus cut of 4.6° ± 3.3° [Rand 1985]. Interestingly, some reviews report that even when attempting to cut perpendicular to the mechanical axis the average result is almost 2° of varus [range 8° valgus to 12° varus], with radiolucent lines appearing in tibial components averaging 4.8° varus [Ewald 1985]. Mont [1997] designed an intraoperative goniometer to measure the varus/valgus angle of distal femoral resections referenced to the medullary canal. Even with resections performed by expert surgeons, 50% of cuts measured had >1° error (and 38% >2°) and were recut. The reported accuracy of these cuts does not include errors associated with approximating the mechanical axis by an offset from the medullary canal or errors introduced by placing the intramedullary rod [Nuno-Siebrecht 2000].

Implant alignment in the sagittal plane has been shown to influence knee kinematics [Whiteside 1988, Piazza 1998, Hofmann 1991, Walker 1991] and postoperative subsidence of the tibial component [Hofmann 1991, Bai 2000]. Computer simulations identify tibial component sagittal plane tilt as the most important surgical variable determining postoperative range of motion [Piazza 1998, Walker 1991]. Many authors and commercially available implant systems recommend a posterior slope tibial cut of 0° (perpendicular to the mechanical axis) [Whiteside 1988, Bai 2000] while others feel a more anatomic slope of up to 10° is more suitable [Hofmann 1991]. Our study revealed a tendency to leave excess bone posteriorly due to blade deflection when open guides were used, with several cuts (25%) having errors over +2°. Leaving excess bone posteriorly would result in an anteriorly sloped cut for a guide positioned perpendicular to the mechanical axis. An anteriorly sloped cut can greatly decrease the flexion range of motion [Dorr 1986, Walker 1991] and diminish the size of the flexion space posteriorly causing posterior wedging and increased posterior polyethylene wear. In a biomechanical study, Bai [2000] showed that an anteriorly sloped cut led to significantly increased posterior micromotion of the tibial polyethylene component and increased tensile strains in the anterior tibia (anterior lift-off).

Inaccurate anterior or posterior resections in the transverse or sagittal planes can prevent proper seating of cementless femoral components (causing large gaps that inhibit bony ingrowth) and produce uneven cement mantles in cemented systems (which may result in early loosening) [Lennox 1988]. Upward deflections on an anterior cut will settle the prosthesis into a slightly flexed position, whereas a similar deflection on the posterior cut will result in the prosthesis taking on an extended position [Lennox 1988]. Significant upward deflections of both anterior and posterior cuts were found with open cutting guides, which can also lead to distal placement of the femoral component and a resulting loss of extension.

When using an open surfaced guide, the surgeon has an unobstructed view of the cutting progress and, with a small biasing force, can hold the saw blade flat against the guide surface [Hungerford 1982, Laskin 1991]. If this force exceeds the stiffness of the saw blade, however, the blade will bend and rest along the front edge of the guide (figure 2.6), causing the blade to deflect upwards (+ error). In our study, over 50% of the cuts made with open guides had positive sagittal plane errors >1° and 26% >2°, while slot guided resections had only 18% of the cuts >+1° and 6% >+2°. Slotted guides also reduced the variability in the sagittal plane by 1° for the experts (from 1.6° to 0.6° SD, figure 2.4). This variability, however, is still over twice that seen in the frontal plane. This may be intrinsic to the design of the cutting guide. Since guides mount anteriorly and have the greatest length in the mediolateral direction and the smallest in the AP direction, more

consistent guidance is provided from medial to lateral than from anterior to posterior. As the saw-blade moves posteriorly, the distance between the cutting teeth and the guide surface increases; in contrast, this distance does not change when traveling mediolaterally.

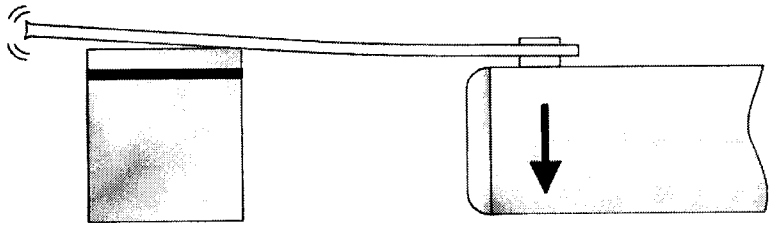

Figure 2.6. Saw-blade deflecting up in sagittal plane with open cutting guide.

Forces transferred between a vibrating saw blade and metal guide can generate motion of the cutting block [Otani 1993] as well as metal debris [Minns 1992]. The guide movement measurements correlated with the implant errors in all planes regardless of cut type, indicating that guide movement has a significant effect on cutting errors, although the size of this effect is modest for primary cuts. The contribution of guide movement to cutting error variance was significantly higher for secondary resections than primary resections in both planes (~40% vs. ~10% in the sagittal plane and ~30% vs. ~20% in the frontal plane). Otani [1993] measured the relative motion between the cutting guide and distal femur during A/P and chamfer cuts with various combinations of guide fixation. Fixation with pins alone allowed cutting guide displacements over 1.2 mm with small pins and 0.8 mm with larger pins. These values are comparable to our angular displacements for the A/P cuts, which were larger than for the distal femoral and proximal tibial cuts. The A/P cutting guides used in this study are fixed with 2 small nails that insert directly into the cancellous bone exposed by the distal femoral cut, obtaining no cortical bone purchase. Distal femoral and proximal tibial cutting guides pin directly into the anterior cortical bone with 2 long pins. These guides were often seen sliding on the pins towards the surgeon, increasing the unsupported length of the blade. Pins alone, particularly those without cortical bone purchase, may not be optimal and surgeons should consider combined fixation methods [Otani 1993].

Whether cutting errors warrant more sophisticated cutting techniques that eliminate cutting blocks altogether is dependent on the relative improvement, speed, convenience and feasibility of the new techniques. Oscillating saws are quick and easy to handle and are favoured by most

TKA surgeons and supported by most instrumentation systems. However, limited accuracy, poor surface planarity and other drawbacks [Toksvig-Larsen 1994a 1994b, Wevers 1987] leave room for significant improvement. We believe that the significant contribution of cutting errors to the variability of overall implant alignment (here estimated at 0.8-1.5° in varus/valgus and >2° in flexion/extension) has not been sufficiently recognized. The cutting accuracy and precision we have found is likely better than would be the case in the operating room due to better stability of the bone and better visibility of and access to the bone in the laboratory set-up. Furthermore, surgeons and residents may subconsciously take more time and care with the cuts under test conditions, thereby introducing an unavoidable experimental bias towards better results in the lab. This comparatively high level of variability in the cutting process may partially explain the somewhat disappointing results of early computer-assisted TKA procedures which focused only on improving placement of the guide blocks, but which used conventional bone-sawing techniques. For example, Saragaglia [2001] found only marginal improvements in implant alignment for a computer-assisted technique over manual techniques (2.53° vs. 2.72° frontal plane variability), which suggests that improvements in the bone cutting process itself, perhaps by using a milling tool instead of a saw [Delp 1998], will be required to achieve sub-degree alignment variability.

Chapter 3: A New Bone Milling Technique for Total Knee Arthroplasty

3.0 Chapter Summary

Conventional sawing techniques produce variable and uneven bone surfaces that affect the alignment and fit of implants in TKA. Moreover, the accuracy of the technique seems to be sensitive to the amount of experience the surgeon has with the instrumentation. In this study, we present a novel, manual approach to making TKA resections using a milling tool and instrumentation designed to be more accurate and less sensitive to operator experience. To assess the alignment accuracy of the milling technique, six operators, none of whom had any previous experience with the technique (two were expert TKA surgeons and four had no surgical training), made a total of 62 resections (50 proximal/distal and 12 anterior/posterior) on 25 porcine femurs and tibiae. The untrained operators also made a total of 35 cuts on 15 porcine femurs and tibiae with the conventional sawing technique. Resection accuracy, evaluated by measuring the orientation of a knee implant positioned on the bone cut, was markedly improved for all untrained operators in both frontal and sagittal planes with the milling instrumentation. For sawing, cutting variability for the untrained group was ~1° and 1.2° in the frontal and sagittal planes, respectively. For the milling technique, resection accuracy was very consistent for all the operators tested, with a group variability of 0.31° [95% CI: 0.27–0.37°] and 0.68° [95% CI: 0.58–0.81°] in the frontal and sagittal plane, respectively. The results show that sub-degree accuracy in the frontal plane can be achieved with a manual milling technique even by persons with no experience with the instrumentation. This represents a considerable improvement in variability over the sawing technique currently used in surgery.

3.1 Introduction

Accurate alignment of prosthetic components is essential for good outcomes in total knee arthroplasty (TKA) [Moreland 1988, Windsor 1989, Jeffery 1991, Ritter 1994]. Although there are many contributors to alignment variability (eg. registration of the mechanical axes and positioning of the cutting guides), the conventional sawing process alone can exclusively contribute over 1° and 2° of variability in the frontal and sagittal planes, respectively [Plaskos 2002]. Thus, the variability intrinsic to the cutting technique can prevent a surgeon from

consistently aligning implants within the narrow 2°–3° window that many authors recommend for the highest success rate in TKA [Hsu 1989, Jeffery 1991, Ritter 1994]. This poor precision is due to the many potential sources of error that are inherent to the technique and, although expert TKA surgeons are able to produce more repeatable resections, those who perform fewer TKA's are more susceptible to these sources of error [Plaskos 2002]. Indeed, many authors note that inaccurate bone cuts frequently occur in surgery [Krackow 1991, Minns 1992], especially when the surgeon does not have extensive experience with the instrumentation [Lennox 1988, Matsen 1993].

Precise bone cuts on the femur are of particular importance since many cementless femoral components are of a 'press fit' design, where a close fit between the bone and the implant is necessary for achieving bony ingrowth and fixation. Cementless fixation has produced better results in the femur than in the tibia or patella [Collier 1991], though surgeons often note that making femoral resections that are precisely oriented relative to one another is difficult with conventional instrumentation [Otani 1993, Matsen 1993]. If one of the cuts is made in the incorrect plane the bone surface will not be congruent with the profile of the component, which will result in large gaps between the bone and malpositioned prostheses [Lennox 1988].

To produce congruent cuts, most femoral instrumentation systems are designed to guide a saw-blade in the correct planes through narrow slots or on flat surfaces. However, even small motions of the surgeon's hand (which is very difficult to avoid when using an oscillating saw) can cause the saw-blade to toggle in the slot or deviate from the open guide surface [Otani 1993, Laskin 1991]. A jig that captures the saw with sliders can prevent motion of the saw relative to the bone, though cutting errors can still result from deflection of the long saw-blade [Cooke 1985, Krackow 1991, Minns 1992].

Robot-assisted milling has demonstrated improved resection accuracy in TKA [Delp 1998, Fadda 1998, Van Ham 1998], though these systems are typically still in the research and development phase. A noted drawback to these milling systems is the relatively large amount of bone chips dispersed into the operating site (since the approach typically involves machining away the entire bone end with milling tools of relatively large diameter [Davies 1997, Fadda 1998, Malsavi 2000]). Ideally, the milling tool should be slender like a saw-blade so that a minimal amount of bone is machined permitting quick resections [Giraud 1991], though the tool must be also sufficiently stiff to limit deflection under the cutting forces. Robotic milling processes also tend

to take longer, the equipment costs more, and there are non-trivial safety issues to be addressed, so it is not likely that they will be a feasible alternative for most clinics.

The purpose of this study, therefore, was to investigate whether a manual milling technique that uses a relatively slender milling tool could produce more consistent bone cuts than an oscillating saw (with respect to implant alignment and fit of the femoral component) without requiring extensive experience with the instrumentation. Also, the advantages and disadvantages of milling and sawing with respect to cutting accuracy, temperature, and safety are discussed.

3.2 Materials and Methods

3.2.1 Experimental Procedure

Six operators made a total of 97 cuts on 40 porcine femurs (n=25) and tibia (n=15). Two operators had extensive TKA experience (experts E1 and E2), while the others had no TKA experience (novices A, B, C, and D; C was the author). The expert and novice groups each made a total of 24 and 38 resections with the milling technique, respectively. None of the six operators had any experience with the milling instrumentation. To estimate the relative improvement in precision, the novices also made a total of 35 cuts with the conventional sawing technique. Distal femoral and proximal tibial cuts were evaluated with 1 primary and 1-2 revision resections performed on each bone and the resection time noted for each cut. One expert surgeon (E2) and two novices (A and C) also performed a primary distal, anterior and posterior femoral resection sequence on 6 femurs (2 each) with the milling technique. In four knees, the posterior cruciate and collateral ligaments and the posterior aspect of the knee joint capsule were retained to assess the feasibility of using a milling tool in the presence of these critical soft tissues. All other bones were stripped of soft tissues. The specimens had no abnormalities in bone quality and were allocated randomly to each operator.

The alignment accuracy and variability of each technique was assessed by measuring the orientation of a dummy implant placed on the prepared bone surface. Dummy implants without stems or pegs were machined from flat metal plates by copying the profile of the tibial trays and the distal footprints of the femoral components from a Johnson & Johnson PFC™ implant series. An implant placed on a perfect resection will have the same orientation as the guide reference surface (0°).

The bone cutting error for proximal tibial and distal femoral resections (hereafter referred to as primary cuts) is defined as the difference in orientation between the initial guide position and the dummy implant, described using two fixed frame rotations (figure 3.1a). The first is about the mediolateral (ML) axis (sagittal plane error). The second is about the anterioposterior (AP) axis (frontal plane error). The AP axis is defined by the vector perpendicular to the front face of the cutting guide. The ML axis is defined by the cross-product of the AP axis and the normal to the guide reference surface (Z axis).

The fit of the femoral component is determined by the relationship of the three basic cuts: anterior, distal, and posterior. The bone cutting error for anterior and posterior femoral resections (hereafter referred to as secondary cuts) is expressed as the absolute difference between the angle of the secondary cut measured from the distal cut, and the angles built in to the cutting guide (figure 3.1c).

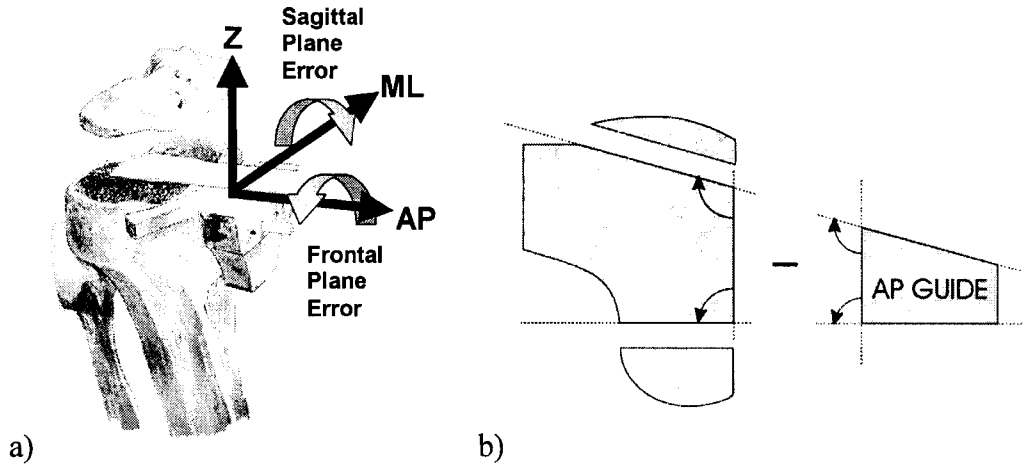

Figure 3.1. The bone–cutting error for a) primary cuts, and b) secondary cuts.
For primary cuts, frontal plane errors are about the AP axis and sagittal plane errors are about the ML axis. For secondary cuts, the cutting error is measured from the distal cut surface, minus the angle of the cutting guide.

3.2.2 Measurement Technique and Precision

An optoelectronic localizer (Flashpoint 5000, Image Guided Technologies, Boulder, CO, USA), equipped with a custom-built and calibrated planar probe with reference frame rigidly attached, was used to measure the plane of each bone cut and orientation of the cutting guides.

Measurements (the average of 30 sequentially obtained samples per measurement) of both the guide position before and after cutting and the dummy implant on the bone cut were recorded relative to a local reference frame pinned rigidly to the tibia/femur. All reference frames were triangular (120 mm on a side with 3 infrared emitters). The variability associated with placing a dummy implant on a bone cut and measuring its orientation was determined by making 30 repeated placements and measurements on a single bone cut. The resulting standard deviation (SD) was <0.10° and <0.17° in the frontal and sagittal planes, respectively.

3.2.3 Milling Instrumentation

A distal femoral/proximal tibial cutting guide was manufactured with an expanded platform (or constraint surface, figure 3.2). A sleeve accurately machined with a square outer surface fits over the mill attachment piece and functions as a flat skate or slider on the guide platform. An anterior/posterior femoral cutting guide was constructed to mount directly on the distal femoral cut surface. The instrumentation permits the surgeon to manually constrain the mill to the guide surface with one hand, while manoeuvring the cutter with the other. The pneumatic mill (Medtronic, Midas Rex, TX, USA) was operated at 120psi and equipped with a double fluted side cutter, 3.1mm in diameter, ~100mm in length with straight cutting flutes extending ~35mm along the axis (#M-10, figure 3.3). The mill was used with long (65mm) and short (45mm) attachments (types 'M' and 'O') to cut the anterior and posterior regions of the bone, respectively. Each novice operator used one new cutting tool, while 3-4 tools were available for each expert operator.

3.2.4 Sawing Instrumentation

Cutting guides from a commercially available knee system (PFC Total Knee Instrumentation, DePuy, Warsaw, IN, USA) were used to evaluate the conventional sawing technique (figure 3.4). Open guides were used for all cuts. Resections were performed with an oscillating pneumatic bone saw (HALL Series 4 Oscillator) supplied with nitrogen at 100psi. and equipped with a 86mm long, 1.27mm thick saw-blade (HALL Oscillator Blade #5071-181, figure 3.3). Each novice operator used one new saw-blade.

3.2.5 Guide Fixation and Movement

Fixation of all cutting guides was augmented with additional pins and/or screws to minimise relative motion between the guide and the specimen and reduce the influence of guide movement

on cutting errors [Otani 1993]. The milling guides were typically fixed with two screws that inserted directly into the anterior cortical bone of the femur/tibia or the cancellous bone in distal femur, while the sawing guides were all fixed with at least four long pins (since we could not find screws narrow and long enough to fit in the holes of the cutting guides). Movement of the cutting guides was measured for each cut by digitizing the guide reference surface with the planar probe immediately after each resection. The guide movement is calculated in the same manner as the bone cutting errors, using two fixed frame rotations referenced from the initial guide position.

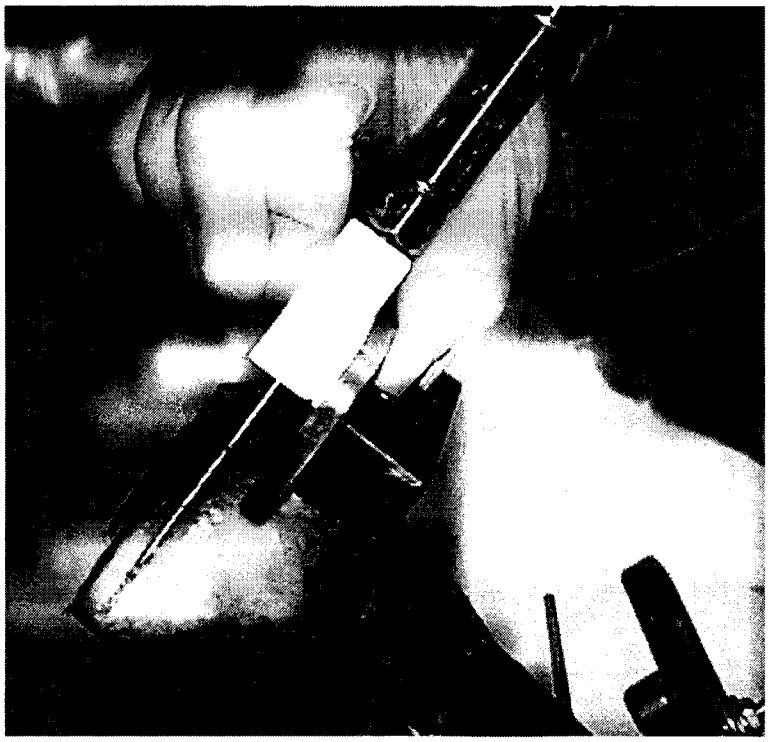

Figure 3.2. Manual milling instrumentation, shown with short attachment.

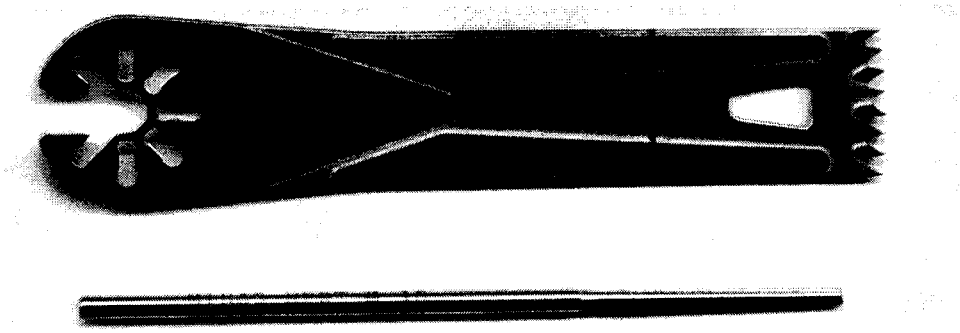

Figure 3.3. Saw-blade (HALL Oscillator Blade #5071-181) and milling tool (Midas Rex, #M-10).

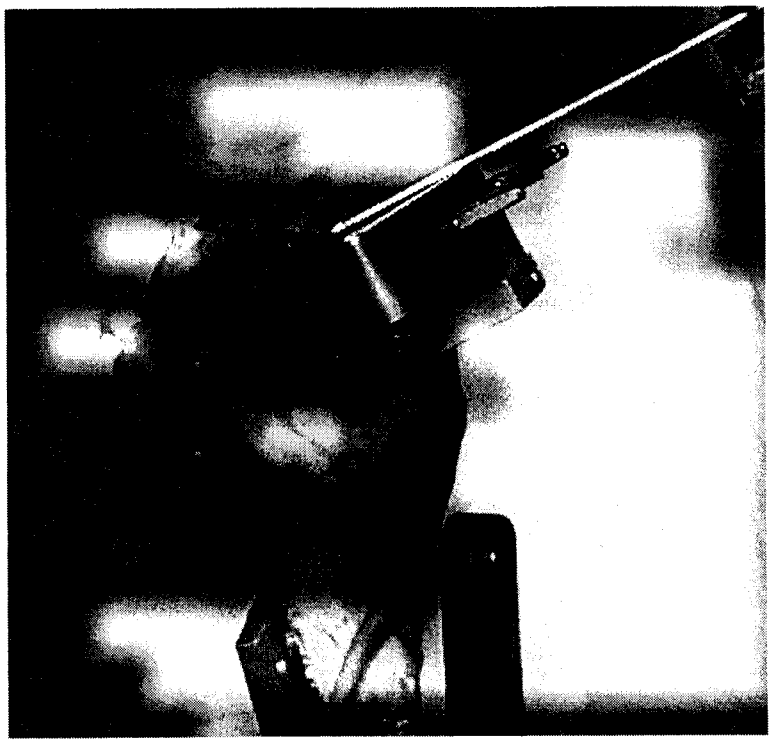

Figure 3.4. Conventional sawing instrumentation (open guide).

3.3 Results

3.3.1 Intra-Operator Frontal Plane Accuracy and Variability

Figure 3.5 shows the results of all primary resections, grouped by operator and cutting technique. In the frontal plane the standard deviations associated with individual operators ranges from ~0.15°-0.4° SD for the new milling technique, and from ~0.75°-1.25° SD for the conventional sawing technique. For all novices, the cutting variability in the frontal plane is significantly less with milling than with sawing ($p_{A,C}<0.05$ and $p_{B,D}<0.005$, F-test). The maximum errors relative to the guide in the frontal plane for each operator are in the range of ~0.5°-0.65° for milling and ~1.4°-2.5° for sawing, with no significant bias for either technique.

3.3.2 Intra-Operator Sagittal Plane Accuracy and Variability

The variability in the sagittal plane is typically higher for both cutting techniques for all operators (except for B with milling). For milling, the intra-operator variability ranges from ~0.3°-0.9° SD, and for sawing, from ~0.8°-1.5° SD. The milling technique reduced the sagittal plane variability for operators B, C, and D, and this difference is statistically significant for operator B ($p<0.0001$, F-test). Although the milling technique was not effective in reducing the sagittal plane variability of operator A (0.8° SD), it did significantly reduce the operator's mean error from over 2.0° to under 0.5° ($p<0.002$, t-test). Milling also significantly reduced the mean error for operator B (2.6° vs. 0.0°, $p<0.001$, t-test). Two novices (A and B) had over 60% of cuts over +2.0° with sawing, resulting in significant sagittal plane biases ($p<0.001$), while one expert (E2) had a significant negative bias in the sagittal plane with milling ($p<0.01$). The maximum errors in the sagittal plane for each operator are in the range of ~0.3-1.5° and ~1.0-4.8° for milling and sawing, respectively.

3.3.3 Effect of Surgical Experience and Group Variability

There were no significant differences in frontal or sagittal plane alignment variability between the experts (0.31° and 0.71° SD) and the novices (0.32° and 0.65° SD) for milling, and therefore the data were pooled into one group. However, for the novice group there was a significant difference in both frontal ($p=0$) and sagittal ($p<0.001$) plane alignment variability between milling (0.32° and 0.65° SD) and sawing (0.99° and 1.22° SD). For each group standard deviation, the residuals are calculated about each operator mean, summed, and divided by the total number of cuts minus one for each operator (figure 3.6). For an operator (expert or novice)

with no experience with the milling technique, the estimated variability associated with making a single cut is 0.31° [95% CI: 0.27–0.37°] and 0.68° [95% CI: 0.58–0.81°] in the frontal and sagittal planes, respectively. For sawing, the variability of a novice operator is estimated to be higher at 0.99° [95% CI: 0.83–1.25°] in the frontal plane and 1.22° [95% CI: 1.02–1.53°] in the sagittal plane.

In the frontal plane, there was no significant bias for either operator group or cutting technique (experts milling: 0.08°, novices milling: -0.01°, novices sawing 0.16°). For milling in the sagittal plane, the mean error for the experts was larger than for the novices (-0.55° vs. -0.02°, p=0.012). For milling and sawing in the sagittal plane, there was a significant difference in the mean error for the novices (-0.02° vs. 1.35°, p=0.0).

3.3.4 Accuracy of Surgical Fit of Femoral Component

For secondary resections, the mean (±°SD) errors relative to the guide position in the frontal and sagittal planes were 0.06 ± 0.35° and –0.20 ± 0.46° for anterior cuts, and 0.40 ±0.26° and 0.40 ± 0.93° for posterior cuts, respectively. The relative orientations of the femoral resection surfaces determine the fit of the component. The absolute errors for the secondary resections referenced from the distal femoral cut are shown in figure 3.7. The mean (±°SD) error for anterior and posterior resections is ~0.5 ± 0.4 °SD, with maximum errors in the range of 1°–1.3°.

3.3.5 Effect of Cutting Guide Movement

The cutting errors correlated with the guide movement measurements for milling in the frontal ($p<0.01$) and sagittal ($p<0.005$) planes and for sawing in the frontal plane ($p<0.005$) (figure 3.8). Guide movement data was unavailable for 7 resections due to disturbance of the reference frame or instability of the operating system during cutting (the cutting error for these resections is calculated from the final guide position). One sawing error exceeds 4° in the sagittal plane, though the guide movement for this resection is <0.25°. The standard deviation of all of the guide movement measurements was higher in the frontal than in the sagittal plane for both milling (0.33° and 0.21° SD) and sawing (0.39° and 0.24° SD).

For milling, guide movement contributed 14.3% [95% CI: 11.7%–17.0%] (r^2 = coefficient of determination) of the total error variance in the frontal plane and 17.3% [95% CI: 14.6%–20.2%] in the sagittal plane. For sawing, guide movement contributed 24.8% [95% CI: 20.1%–29.7%]

and 0.0% [95% CI: 0.0%–0.5%] of variance in the frontal and sagittal planes, respectively. The tendency for the saw-blade to deflect in the sagittal plane is evident with a regression line intercept above 1°.

3.3.6 Resection Time, Bone Volume Removal Rate, and Soft Tissue Results

For primary resections, the mean milling time (±SD) was significantly lower for the experts (~ 80 ± 15 sec.) than for the novices (~215 ± 50 sec). The mean sawing time for the novices (~100 ± 30 sec.) was also significantly lower than the novice milling time. For secondary resections, the mean milling time was ~35 ± 15 sec. grouped aver all operators.

The average rate of bone removal (i.e. average volume of bone removed per cut divided by cut time) is compared for each cutting technique for the novices. The average volume of bone removed per cut (estimated by multiplying the average bone resection area by the cutter kerf) is ~10,735 mm^3 for milling and ~4,370mm^3 for sawing. There is no significant difference between the milling (55 ± 15mm^3/s) and sawing (49 ± 14mm^3/s) bone removal rates ($p>0.1$).

No soft tissues were cut or damaged in the milled specimens that had ligaments and joint capsules retained.

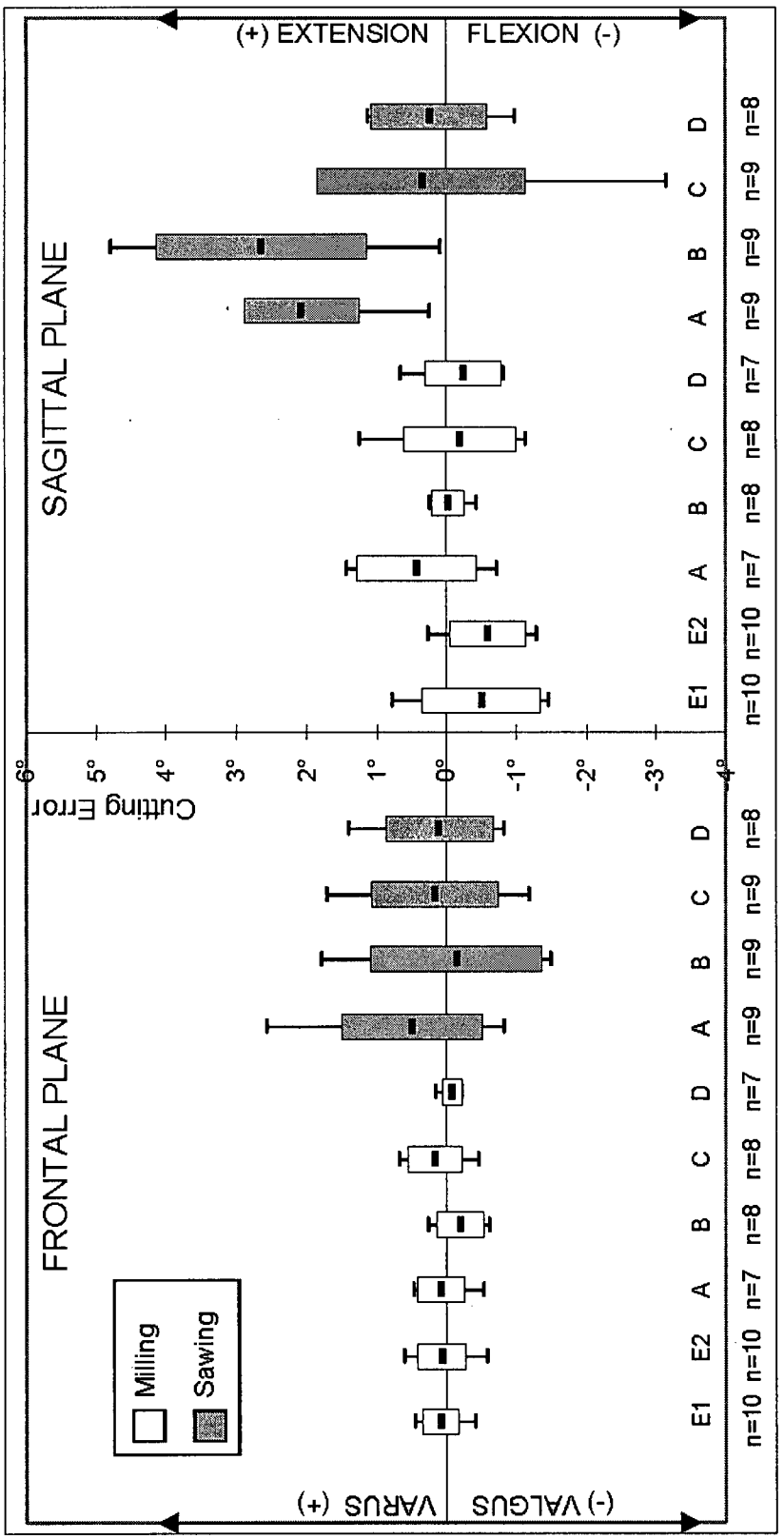

Figure 3.5. Frontal (varus/valgus) and sagittal (flexion/extension) plane cutting errors (°) for each operator for milling and sawing (proximal tibial and distal femoral cuts).

[bold line = mean, box length = ± SD, error bars = range]

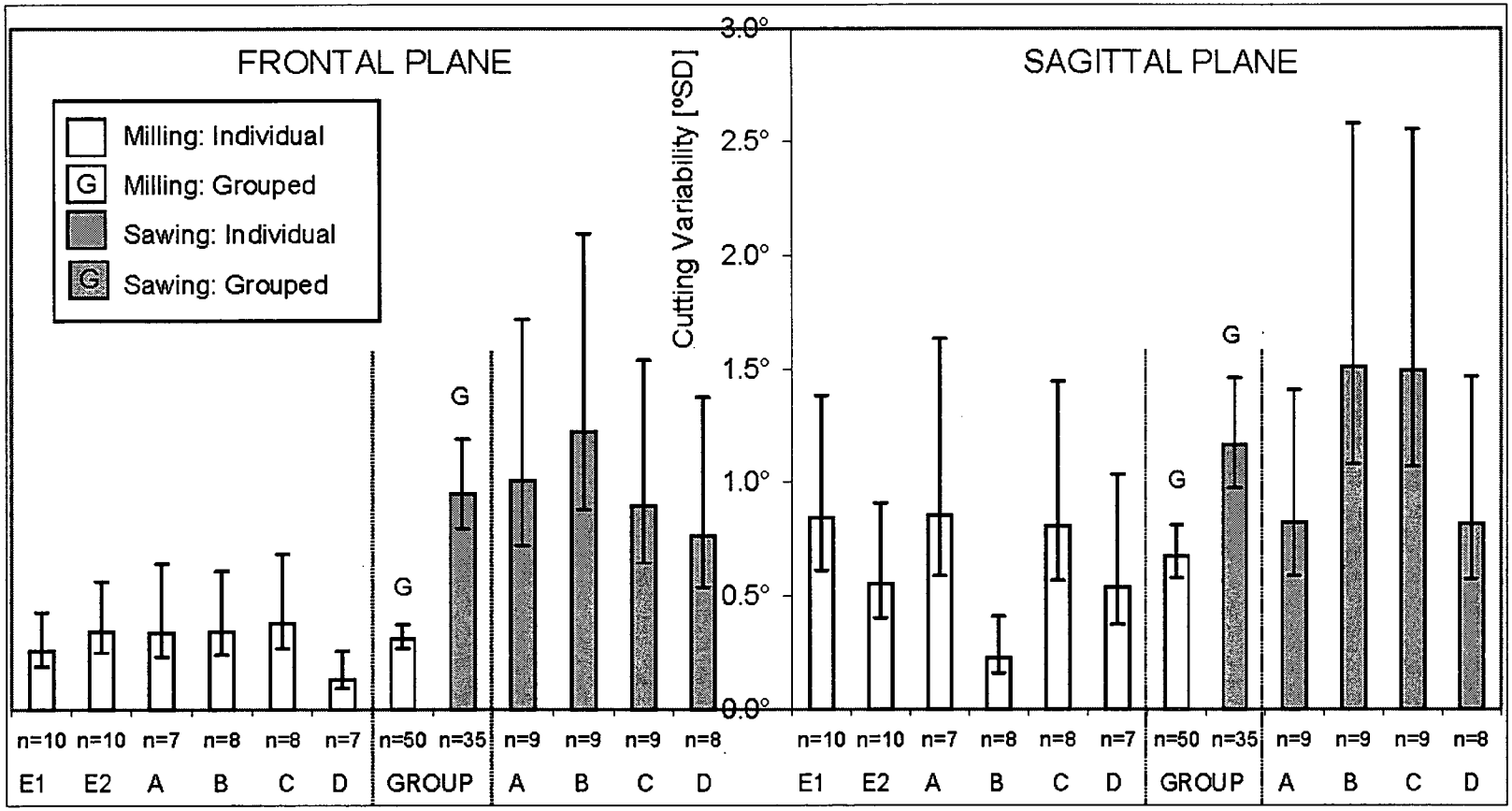

Figure 3.6. Intra-operator and grouped cutting variability (°SD) in the frontal and sagittal planes for milling and sawing (proximal tibial and distal femoral cuts).

[error bars = 95% confidence intervals]

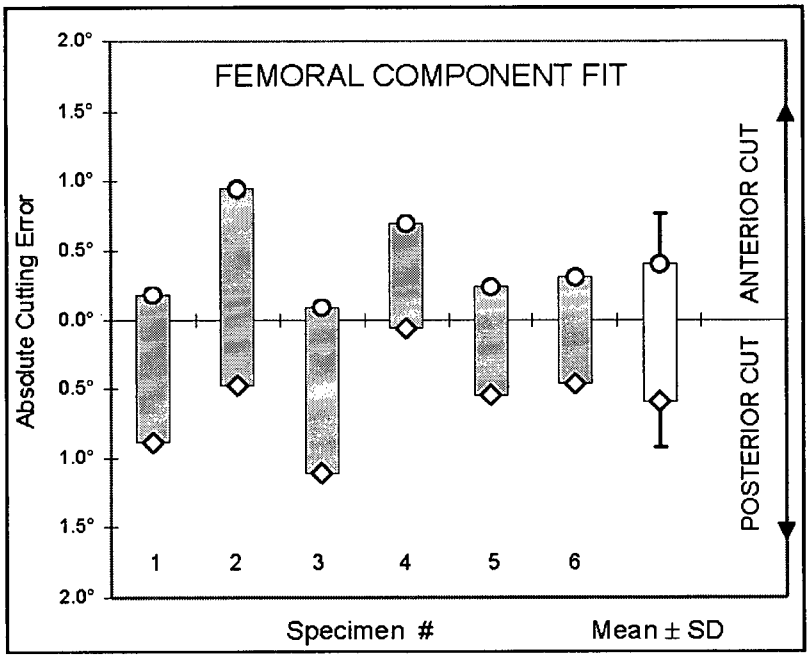

Figure 3.7. Absolute angular error (sagittal plane) for anterior and posterior femoral cuts (n=12) with milling, measured relative to the distal femoral cut surface.

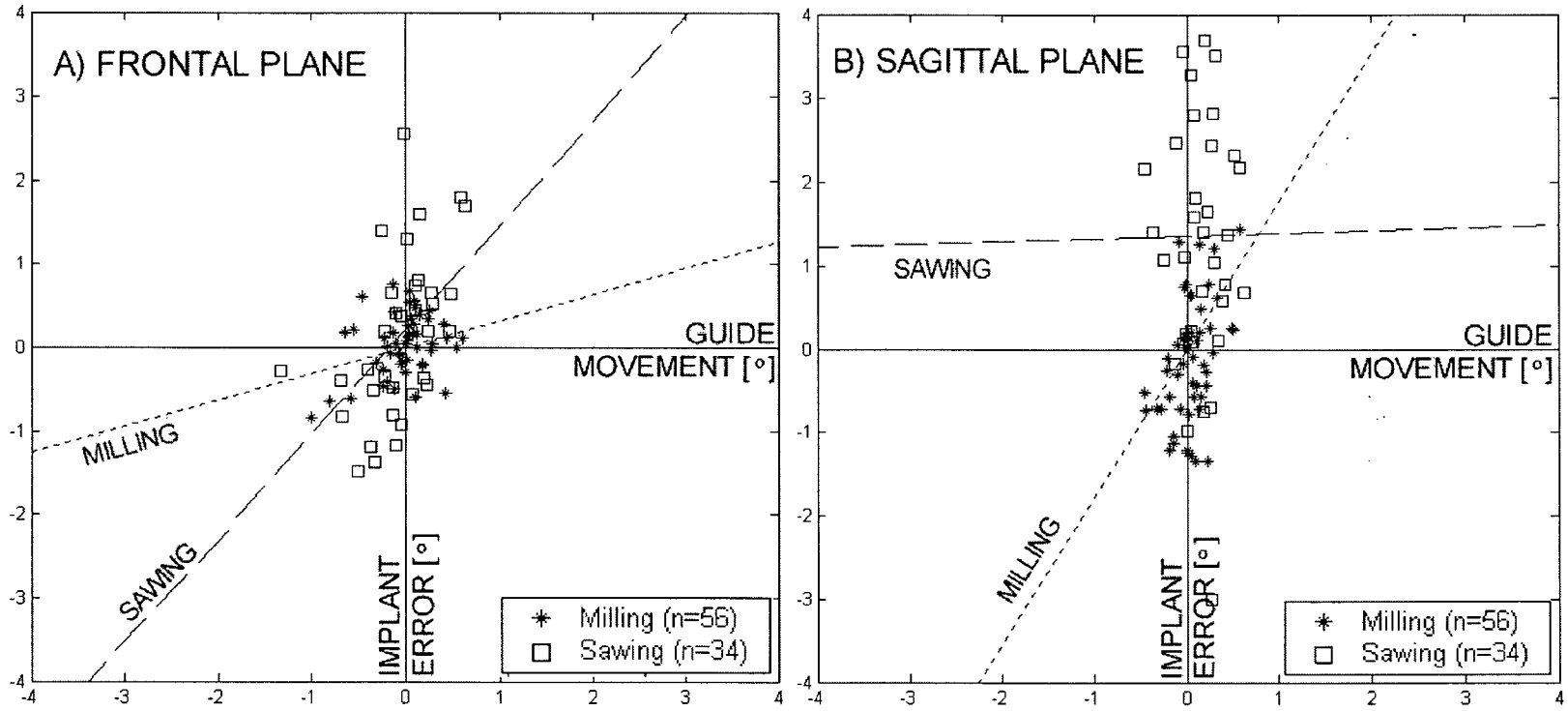

Figure 3.8. Cutting error versus guide movement [scale = 1°] in the (a) frontal/transverse and (b) sagittal planes for both cut types (primary and secondary) and cutting techniques (milling and sawing). Significant correlations were found for milling in the frontal and sagittal planes and for sawing in the frontal plane ($p<0.01$). Note: guide movement data was unavailable for 7 resections, and one cut had an error exceeding +4° in the sagittal plane for sawing.

3.4 Discussion

Several clinical studies have found that alignment outside a 2°–3° window in the frontal plane significantly increases the probability of early failure in TKA [Moreland 1988, Windsor 1989, Hsu 1989, Jeffery 1991, Ritter 1994]. To consistently achieve alignments within this narrow window, the surgeon must be able to install implants with a standard deviation in alignment of ~1°. If the operator has no experience with an oscillating saw, the contribution of cutting errors alone toward overall alignment variability would be over 1.5° in the frontal plane and over 2° in the sagittal plane (taking $\sqrt{2}$ times the variability associated with a single cut at the upper 95% confidence bound). However, the variability associated with two bone cuts made with the milling technique (one on the tibia and one on the femur) would be on the order of ~0.6° in the frontal plane and ~1.2° in the sagittal plane ($\sqrt{2}$ x SD at 95% confidence), regardless of the surgeon's experience with the technique. Although achieving sub-degree alignment precession wouldn't be possible with manual bone cuts made with a saw even if the guide positioning were perfect, this goal is attainable with the new milling instrumentation even for surgeons who do not regularly perform TKA.

With the use of press-fit femoral components, the importance of precise resections in TKA is increased. Inaccurate anterior or posterior resections can prevent proper seating of cementless femoral components (causing large gaps that inhibit bony ingrowth) and produce uneven cement mantles in cemented systems (which may result in early loosening) [Lennox 1988]. However, many authors have noted that it is difficult to consistently attain precisely congruent surfaces on the distal femur with conventional instrumentation [Lennox 1998, Otani 1993, Matsen 1993]. Matsen [1993] compared the accuracy of conventional sawing instrumentation with a specially designed slotted saw-guide that was positioned with a robotic arm. Five experienced TKA surgeons each made distal, anterior and posterior femoral resections on two plastic femurs with each technique, and the angles of the anterior and posterior cuts were measured relative to the distal cut. With the conventional instrumentation, 70% of the RMS errors were ≥2°, with several cuts in the 5°–15° range. Although the robotic system limited these errors to the ±5° range, 40% of the cuts made with the system had an angular error ≥2°. Plaskos [2002] measured the cutting errors relative to the guide plane for 8 orthopaedic surgeons of varying TKA experience using oscillating saws and found that over 30% of anterior/posterior resections had errors ≥2° (range -3°–6.5°). In this study, three operators (none of which had any experience with the milling

instrumentation) made anterior and posterior resections on two femurs each using our milling device and all resections had <2° of error.

Several other researchers have used milling tools to improve resection accuracy in TKA, though these systems typically incorporate robotic instrumentation to guide the milling tool [Marcacci 1996, Davies 1997, Fadda 1998, Van Ham 1998]. Milling tools are better suited for robotic-assisted procedures than are oscillating saws because of their smaller size and mass, and their lower vibration levels and cutting forces. Although robotic systems can position tools accurately and perform resections repeatably, they are generally not well suited for the operating room as they often require increased set-up and cutting time. In addition, the capital cost associated with robotic systems used in the operating room has been approximately US$500,000 [Delp 1998], which is a major limitation of this technology.

In this study, simple open cutting guides (similar to those used in conventional TKA) were used to guide the mill's housing, in contrast to the conventional technique where the guide is in direct contact with the saw blade. A saw-blade that is oscillating at high frequency in contact with a metal template creates a risk for blade damage and the generation of debris in the operating site [Wevers 1987, Minns 1992]. Moreover, it is difficult to keep the vibrating saw-blade constrained to the surface as the blade can vibrate on or deflect off the guide surface [Laskin 1991]. Although slotted cutting guides can limit this deflection [Otani 1993, Plaskos 2002], cutting errors can still occur since there must be enough clearance to prevent the blade from binding in the slot. Even when the saw is constrained to the bone, the sharply curved condyles of the femur and the dense subchondral bone in the tibia can create high cutting forces which can cause the blade to deflect out of the resection plane during cutting [Cooke 1985, Krackow 1991, Minns 1992]. If the operator pushes down on the saw to keep the blade on the guide surface, there is a risk of the blade bending and travelling on the front edge of the guide (which is difficult to detect from the anterior view), resulting in a positive sagittal plane cutting error [Plaskos 2002]. In this study, over 30% of resections made with the sawing technique had errors >2° in the sagittal plane.

In contrast, the milling instrumentation allows the surgeon to directly constrain the mill to the cutting plane by simply 'clamping' the mill to the guide platform with one hand. This reduces the likelihood of the operator lifting the mill off the guide surface while cutting, and can prevent excessive load transfer to the bone pins or screws. Optimal design or selection of the cutting tool is therefore of considerable importance since cutting errors are largely limited to the defection of the slender milling tool under the cutting load. Different tool forms have been shown to increase

cutting forces by as much as 300% [Jacobs 1976] and temperatures by 200% [Saha 1982] in bone drilling, and this is commonly extended to bone milling. Because this is a new milling technique, it was difficult to select a suitable milling tool that could be used the appropriate attachment pieces. Ideally, the tool should be designed with an optimal form and stiffness, and it should be used with one attachment of adjustable length that the surgeon can quickly adjust (for example, an attachment equipped with threaded couple that is extended or shortened axially when rotated).

Another important consideration is the rate at which the surgeon moves the tool through the bone (i.e. the feed rate) and the depth at which the surgeon inserts the tool (i.e. the axial cutting depth). Krause [1982] found that milling forces increased with cutting depth and feed rate, and bone temperatures increased with cutting depth but decreased with feed rate. In this study, the cutting depth was observed to be more or less constant for both groups though the experts used significantly higher feed rates than the novices, which resulted in shorter cutting times and probably lower temperatures. However, we would therefore expect the loading on the tool to be higher for the experts, which would result in larger tool deflections in the transverse and sagittal planes [Kline 1982]. This may explain the negative sagittal plane bias of ~0.5° found with the experts (i.e. excess bone consistently removed in the posterior regions of the cut, where the tool is most flexible). This bias was, however, much lower than the mean sagittal plane bias of 1.35° found in this study, and the 1.4° found with experts in our previous study, when sawing with open guides [Plaskos 2002].

The temperature elevation during bone cutting is an important consideration in implant surgery, especially for cementless implants that rely on bone regeneration and ingrowth for fixation. The feed rate, cutting depth, rotational speed, and geometry of the tool all affect the forces and temperatures in bone cutting [Krause 1982], and although the interrelationships of these parameters are not well understood, it is well known that cutting forces increase dramatically as the tooth angle (or rake angle) changes from negative to positive [Jacobs 1974, Wiggins 1978, Krause 1987]. Saw-blades, however, have negative rake angles so that teeth will cut during the left and right motion of the oscillating blade, and this tends to push bone fragments into the uncut bone at the front of the tooth [Wevers 1987]. This bone chip removal mechanism can result in high cutting forces and temperature elevations exceeding the limit for thermal necrosis in TKA [Krause 1982, Toksvig-Larsen 1989]. Also, the velocity of the saw-blade is reduced to zero at the extreme right and left position of the tools' motion, which results in higher cutting forces and an overall decrease in cutting efficiency [Krause 1987, Giraud 1991]. In contrast, milling tools rotate in one direction only and so they can have positive rake angles and higher cutting

efficiency. Positive rake angles can help decrease temperature elevations due to lower cutting forces and better bone removal from the cutting site [Wiggins 1978, Malvisi 2000]. In this study, there was no significant difference between the novice milling and sawing bone removal rates. We would therefore expect that the energy deposition rate during sawing was higher and that the peak bone temperatures would be correspondingly higher during sawing than during milling.

The longer resection time for the novices with milling is still of some concern because not only is the operation time increased, but the potential risk for thermal damage may also be higher (since thermal necrosis is the combined result of the temperature and the period of time that the bone tissue is at the elevated temperature [Krause 1982]). However, a similar bone milling technique (in a robot-aided TKA study that used a similar milling tool [Malvisi 2000]) was found to produce temperatures under the limit for thermal necrosis even without the use of irrigation. Although a surgeon should always irrigate when cutting bone, this result is important since several studies have measured temperatures exceeding the thermal necrosis limit when sawing bone, even with irrigation [Toksvig-Larsen 1989, Krause 1982, Malvisi 2000]. The detrimental temperatures and the uneven surfaces produced by conventional sawing could potentially prevent successful bone ingrowth and fixation of cementless implants [Toksvig-Larsen 1989, 1994a, 1994b].

Milling tools can slip and damage adjacent tissues [Giraud 1991], and it is therefore essential that the cutter is under control at all times and no unplanned movements occur while cutting inside the patient. Some researchers advocating robot-assisted techniques have developed sophisticated control strategies to improve the surgeon's control of the mill in the cutting region. For instance, Davies [1997] developed an active constraint robot that restricts the movement of the cutting tool to pre-programmed regions in the distal femur. This system relies on rigid immobilization of the patient's bones and accurate registration of the CT model to define the pre-planned boundaries that separate the 'safe' cutting regions from the forbidden regions that include ligaments, nerves, and vascular structures. Other systems plan the explicit cutting trajectories from the preoperative CT images and program the manipulator to follow these paths [Marcacci 1996]. Van Ham [1998] designed a hybrid force-velocity control scheme to constrain the robot's motion to the predefined cutting plane, though no constraints are applied to restrict the motion of the cutting tool within the plane. In the milling technique presented here, the surgeon can manually control the lateral resistance of the cutter to resist slippage in the cutting plane. By increasing the applied clamping or squeezing force between the guide platform and mill sleeve, the surgeon can use the guide as a braking surface to prevent the cutter from unexpectedly slipping and entering any critical soft

tissue regions surrounding the joint. This control was demonstrated in the specimens with retained soft tissues, as none were damaged with the milling technique.

3.4.1 Study Limitations

In this study, only open surface guides were tested for both techniques, and no cuts were made with slotted cutting guides. Although both open and slotted cutting guides have been advocated as being optimal for conventional resection in TKR, many surgeons prefer open cutting guides in surgery [Laskin 1991, Mont 1997]. Open guides benefit from their simple, open design in the sense that the cutting surface provides a direct visual reference for the desired cut location and gives the surgeon a clear view of the cutting progress. Although slotted cutting guides can limit the deflection of the saw-blade, it has been our experience that they do not significantly reduce frontal or sagittal plane cutting variability for training surgeons (figure 2.4) [Plaskos 2002].

One could also criticize the use of animal bones for this study. However, because of their suitable size and availability, many other researchers have used porcine specimens to investigate both milling and sawing performance in TKA [Ark 1997, Fadda 1998, Van Ham 1998, Malvisi 2000]. Furthermore, the sawing results obtained in this animal study are comparable with those obtained using cadaver specimens cut by orthopaedic surgeons in training [Plaskos 2002]. In our previous study, the effect of surgical experience on sawing variability was evident -and the novice operators in this study performed slightly worse than the training surgeons and considerably worse than the expert surgeons from the previous study (1.0° vs. 0.8° vs. 0.4° SD, respectively in the frontal plane). Sagittal plane sawing precision was also consistent with the sawing trends found in cadaver bones, with a variability of ~1.2° SD and a significant bias of ~1° for all groups. Because the sawing errors made by the untrained operators in this animal study are consistent with sawing errors made previously in cadaver specimens by orthopaedic surgeons, we feel that the variability of each cutting technique is accurately represented here.

3.5 Conclusions

Our new bone milling instrumentation is simple and effective. The new milling technique significantly reduced frontal plane cutting variability for all novices tested in this study, and will likely allow surgeons of all skill levels to achieve levels of cutting precision substantially lower that 1°.

Chapter 4: A Generalized Model for Predicting Force and Accuracy in Bone Milling

4.0 Chapter Summary

No models currently exist for predicting forces or accuracy in bone milling operations, even though milling tools are routinely used in surgery to resect bone surfaces for implants. As a result resection parameters and tools are often arbitrarily selected, which can result in high cutting forces and temperatures, and poor bone surface quality. In this chapter, we formulated a model for predicting milling forces based on the specific cutting energy of cortical bone, which we estimated from orthogonal bone cutting studies in the literature. We modelled the cutting zone in front of the milling tool as a transversely orthotropic field of cortical bone with the predominate osteon direction aligned with the anatomic axis of the bone. We used both linear and non-linear models of the cutting process (the latter include the "size effect" phenomenon), along with corrections for the anisotropy of bone, to estimate the instantaneous cutting forces in milling operations as a function of the cutter orientation and other surgical parameters. We then integrated the instantaneous force values through a cutting cycle to estimate the average load on the tool. The two force models were compared with measured force values from bone milling experiments in the literature. The non-linear model correlated well with force data obtained at several different cutting depths, speeds, and feed rates (24 measurements, $r^2 = .87$), while the linear model failed to predict forces accurately at high cutting speeds ($r^2 = .32$).

We therefore used the non-linear model to estimate cutting forces and accuracy for two slender milling tools under various surgical conditions. The first was the milling tool that was used in the previous chapter (#M-10) while the second had twice as many cutting teeth. We modelled the tools as elastic cantilever beams and estimated resection accuracy by solving for the quasi-static deflection of each tool in the direction normal to the finished bone surface (i.e. the resection plane). The maximum tool deflection from the resection plane (at the tool tip) for the cutting conditions used in the previous chapter was ~0.5mm when cutting with the long attachment, and ~2.5mm when cutting with the short attachment (i.e. in the posterior regions of the cut). With optimized cutting conditions the large deflections estimated in the posterior regions of the bone were reduced by ~50%, by increasing the feed rate and the number of passes. Although the four-fluted cutting tool deflected less than the M-10 tool, the model predicted that this tool had a tendency to under-cut or over-cut bone, which could affect the alignment of the implant.

4.1 Introduction

Good bone cutting techniques are essential in implant surgery for attaining accurate placement and adequate fixation of components [Toksvig-Larsen 1989 1994a, Laskin 1991, Minns 1992]. The criteria, as reviewed by Giraudi [1991], that every bone cutting technique should satisfy is as follows. The duration of the cutting process is important to minimise operating time and reduce the period of anaesthesia, and the cutting technique should be relatively effortless so that the surgeon can keep instruments under control and not damage adjacent tissues. The extent of thermal damage due to the use of power osteotomes must be also be minimised as to not delay or prevent bone regeneration. The technique must not excise more bone tissue than required, and avoid its dispersion into the operating area. In cementless implant surgery, the accuracy of the resection is vital for maximizing contact area at the bone-implant interface so that bone integration into the prosthesis is not hindered [Carlsson 1986 1988, Toksvig-Larsen 1994a].

Although the criteria for good bone cutting techniques are specified [Giraudi 1991], few engineering analyses are available on the design of cutting instruments. Many bone cutting researchers have stated that cutting tools (i.e. milling tools and saw-blades) have generally just 'evolved', probably from common wood cutting tools, and little engineering has gone into their design [Wiggins 1978, Krause 1987, Giraudi 1991]. Before innovative cutting techniques are accepted clinically, the required cutting parameters and tools must be optimally engineered with respect to the surgical criteria. The inter-relationships of cutting force, depth, feed, speed, specific cutting energy, and tool geometry must be considered to optimize desired outputs such as resection accuracy, temperature and bone removal rate.

Aside from early fundamental works on orthogonal bone cutting [Jacobs 1974, Wiggins 1978, Krause 1987], most engineering analysis of actual orthopaedic cutting operations have been applied to the bone drilling process [Jacobs 1976, Wiggins 1976, Saha 1982]. Jacobs [1976] measured the torque and feed force while drilling at different rotational speeds (100-2360 RPM) and feed rates (25.4-127mm/min) with several surgical and industrial drill point geometries. They found that drilling force speed-feed relationship was of an asymptotic form in which the forces for each drilling tool tended to reach an asymptotic value at high rotational speeds. Since lower asymptote values indicated lower cutting forces, which are associated with lower cutting energies (and reduced thermal and physical damage [Matthews and Hirsch 1972]), these values were used to compare the performance of the various drill forms and select the optimal drill geometry. Wiggins and Malkin [1976] also employed a mechanistic approach to compare the performance

of several drill designs. They used an exponential formula to fit the measured feed rate-cutting force relationship for each drill tested. The empirical constants that were calibrated for each drill were then used to select the optimal bit.

Although there are several force and temperature studies on the drilling of bone, we could only find one investigation on the mechanical effects of the bone milling process. Krause [1982] measured the feed forces and temperatures during milling parallel to the axis of bovine femurs at various feed rates and cutting depths with high-speed rotary burrs. They found that generally the feed forces increased with cutting depth and feed rate, and decreased with cutting speed. Unfortunately, no mathematical force model was formulated to relate the measured values to the cutting conditions. Moreover, it is not clear how these values would change for milling tools of different geometry.

Hence, the primary objective of this paper is to develop a generalized force model for the orthopaedic process of bone milling. The model is general in the sense that it is not specific to any one particular milling tool design or milling path with respect to the anatomy of the bone. The secondary objective of this work is to predict the relative cutting accuracies of various slender milling tools for use in TKA. In particular, the force model will be used to design or select a milling tool that has:

(1) an optimal diameter and stiffness to limit the deflection of the tool under the applied cutting loads,

(2) minimal kerf to minimise the volume and dispersion of the bone chips generated and to minimise the resection duration,

(3) an optimal number of cutting teeth to maximize resection surface flatness and planarity.

The development of such a model would also facilitate specifying surgical parameters such as the feed rate and cutting depth for optimal resection accuracy and duration.

Since the secondary aim of this work is to develop an optimized milling technique for preparing the distal femur and proximal tibia for TKA, and since little quantitative cutting data exists for the complex bone structure at the knee, certain assumptions are made to simplify the model of the bony anatomy at the cutting site. However, the assumptions are expected to yield conservative estimates of resection accuracy and process time.

4.2 Model Formulation

The specific cutting energy of cortical bone is a measure of the energy required to remove a unit volume of bone by cutting [Wiggins 1978, Krause 1987], and provides the basis for the force prediction model developed here. Like other milling models, each cutting edge of the milling tool is partitioned into a series of small elements and for any cutter orientation the tooth elements that are actively engaged in cutting are identified [Tlusty, 1975. Devor 1983, Sutherland 1986, Feng 1996]. The milling forces are estimated by calculating the area of bone machined by each cutting edge as a function of the tools' angular rotation. The elemental cutting forces acting on each edge element are calculated from measured chip-force relationships and the orientation of the element with respect to the bone structure. The instantaneous cutting forces on the mill are then calculated by summing the contributions of all engaged cutting elements. The following sections discuss these steps in detail.

4.2.1 Determining the Specific Cutting Energy from Orthogonal Bone Cutting Tests.

Although many cutting processes are three dimensional and geometrically complex, the simple case of two-dimensional orthogonal cutting is commonly used to examine and quantify the general mechanics of the material removal process [Altintas 2000]. In an orthogonal cutting test the relationship between the force acting on a single cutting edge of a machine tool and the area of workpiece material being cut by the edge (uncut chip size) is examined. Typically, the measured cutting force ($\boldsymbol{F}$) and the uncut chip area (normal to the tool velocity) are normalized by the specimen width (w), and the cutting force components per unit width (F_t, F_r) are correlated to the depth of cut (t) for a particular cutting speed (v) and tool/workpiece combination (figure 4.1).

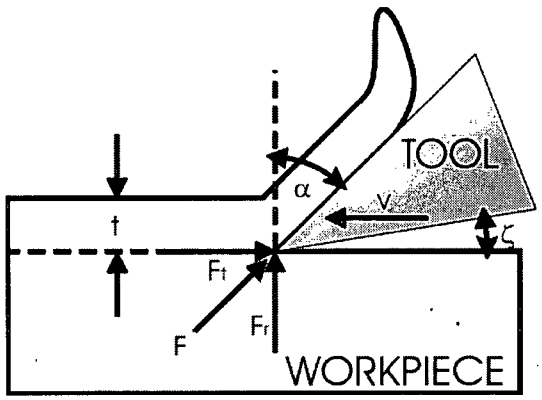

Figure 4.1 Orthogonal Cutting Test:
F – resultant cutting force; F_t – tangential cutting force; F_r – radial cutting force; t – depth of cut or uncut chip thickness; w – workpiece width into page; α – rake angle; ξ – clearance angle; v – cutting tool velocity.

For all machining operations, including orthogonal cutting, a specific amount of work is required to remove the material in front of the tool. This work can be separated into two components: the work used to cut the bone, and the work used to overcome the frictional forces between the bone and the tool [Krause 1987]. The sum of these two work terms represents the total amount of work done by the tangential cutting force. Although the radial force component is important as it may cause defection of the tool relative to the workpiece, it does no work in the actual cutting process.

The specific cutting energy of the material represents the amount of work expended per unit volume of material removed in the cutting process, and can be derived from the measured force components and the machining conditions. The specific cutting energy of any material is defined by the input cutting power ($F_t \times v$) divided by the material volume removal rate ($v \times w \times t$) [Oxley 1989, Puw and Hocheng 1996]. In orthogonal machining, this is simply equal to cutting force per unit cross-sectional area normal to the cutting direction:

$$E_c = \frac{F_t}{t} \qquad [\text{J/m}^3] \text{ or } [\text{N/m}^2] \quad (2)$$

where $F_t = F_t/w$. It should be noted that magnitude of the specific cutting energy (also called specific cutting pressure) can vary with the machining parameters such as cutting velocity, depth or tool geometry and so strictly speaking it is not a true material property. Since cutting temperatures are a function of energy expended, the magnitude of the specific energy also provides a relative indication of the temperature generated during machining [Wiggins 1978].

Jacobs [1974] were the first to investigate the chip-force relationship in bovine tibial shafts for various tool geometries. Cutting tests were performed at constant speed (v = 7.73 mm/s) and the resultant cutting forces (F) were plotted against the uncut chip thickness (t = 12—48 μm) for a series of tool rake angles (α = -5, 0, 15, 35, 45°; ζ = 10°) and cutting directions relative to the predominate osteon direction (transverse, parallel, and across, see figure 4.2). The cutting force curves increased linearly with uncut chip thickness (t) and intercepted the vertical axis at positive values when extrapolated. For any particular tool geometry and cutting depth, the cutting forces were highest when cutting transversely to the osteons, intermediate when cutting parallel, and lowest when cutting across to the osteon direction. The rake angle (α, shown as positive in figure 4.1) also had an influence; higher (positive) rake angles decreased the cutting forces in all cutting modes.

Other researches have also measured higher machining forces when cutting the osteons transversely and when cutting with decreased rake angles [Wiggins 1978, Krause 1987]. In the orthogonal bone cutting study performed by Wiggins [1978], bovine and human tibiae were cut at a constant speed (v = 8.47mm/s) with tools having rake angles of -30° to 40° and at six different orientations relative to the bone structure (in two normal directions within each of the three orthogonal planes). The depth of cut was varied from 10 – 500 μm and it was found that the relationship between cutting forces (F_t, F_r) and depth of cut (t) became increasingly non-linear with increasing cutting depth. For all cutting conditions, the cutting force increased at a rate less than in direct proportion to the uncut chip thickness. This trend has also been observed in cutting certain metal and composite materials, and has been termed the 'size effect' [Backer 1952, Oxley 1989]. The 'size effect' describes the sensitivity of the material to micro defects, where materials with high sensitivity require an increasingly lower amount of energy to remove larger amounts of the material [Puw 1996].

For orthogonal cutting in each of the principal directions relative to the predominate osteon direction, the cutting force components per unit width tangential (F_t) and normal (F_r) to the cutting velocity can be approximated by [Wiggins 1974]:

$$F_t = K_{tc} t^{n_t} + F_{te} \qquad \text{[N/mm]} \quad (2a)$$

$$F_r = K_{rc} t^{n_r} + F_{re} \qquad \text{[N/mm]} \quad (2b)$$

where t is the uncut chip thickness, n_t and n_r ($0<n<1$) are the constant parameters characterizing the 'size effect' of the particular workpiece material, K_{tc} and K_{rc} are the constant parameters which characterize the local cutting mechanics and are dependent on the tool geometry and cutting direction relative to the bone anisotropy. F_{te} and F_{re} are the residual force components per unit width at zero depth of cut (also referred to as edge forces) and are thought to be a result of friction between the tool clearance face and workpiece material [Oxley 1989]. Metal cutting force prediction models typically neglect these edge forces and express the force components as functions of the chip thickness and specific cutting pressure of the material. It can be seen from Equation 2 that when the cutting force/depth of cut relationship is linear and there are no edge forces (i.e. $n = 1$ and $F_e = 0$), the specific cutting energy is constant and equal to K_t. However, when $0<n<1$ or $F_e \neq 0$ the specific cutting energy decreases with t.

To determine these cutting parameters from the orthogonal cutting tests, the F/t data points from Jacobs [1973, 1974] and Wiggins [1974, 1978] were scanned, digitized using a MATLAB routine, and entered into a database. For the data of Jacobs [1973, 1974] where the force/chip relationship was reported to be linear, a least squares optimization (constrained to the form of Equation 2, with constraints $n=1$ and $F_e \geq 0$) was used fit to the data for each cutting mode (transverse, across, and parallel). For data of Wiggins [1974, 1978], the same optimization (with constraints $n>0$ and $F_e>0$) was used to determine each constant for each cutting mode. The data points from Jacobs (for $\alpha = 15°$) and Wiggins (for $\alpha = 10°$) and the fitted curves for each force component are plotted in figures 4.3 and 4.4. Note that for the transverse and across cutting modes measured by Wiggins, some force curves are different for each cutting direction within the cutting mode. For example, in the transverse cutting mode the radial force is higher when cutting in the 'rθ' direction compared to the 'θr' direction (cylindrical coordinate system: r – radial, θ – tangential, z – parallel to the bone axis, the first and second symbols indicate the directions parallel to the cutting edge and to the cutting velocity, respectively). Also note that for the transverse and parallel cutting modes measured by Wiggins, the edge forces F_e were determined to be zero. The non-linear and linear resultant force curves for large and small scales of uncut chip thickness are presented in figure 4.5 (average values used for the different force curves measured by Wiggins within each orthogonal direction). The specific cutting energy versus depth of cut, and the fitted curves from the orthogonal cutting data of Jacobs and Wiggins, are plotted on log-log coordinates in figures 4.6 and 4.7.

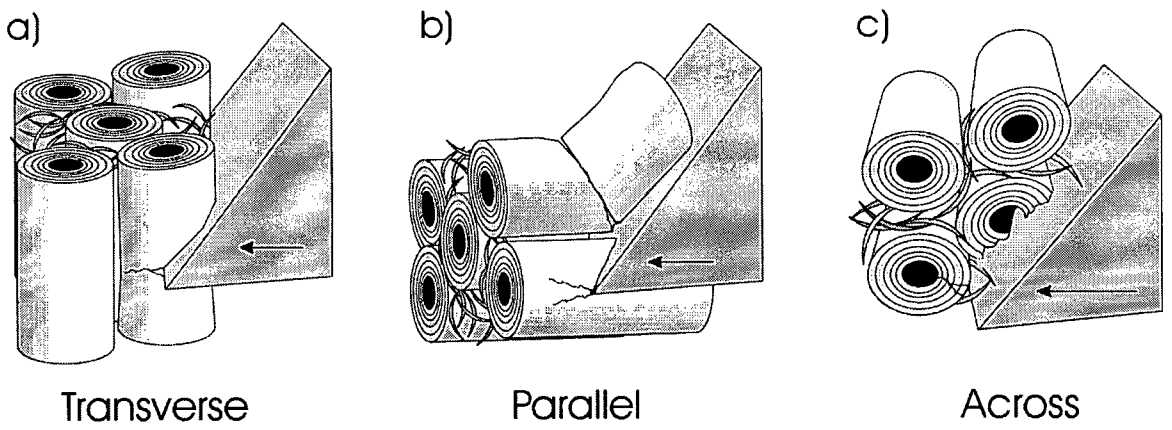

Figure 4.2. Illustrations of the a) Transverse, b) Parallel, and c) Across cutting modes.

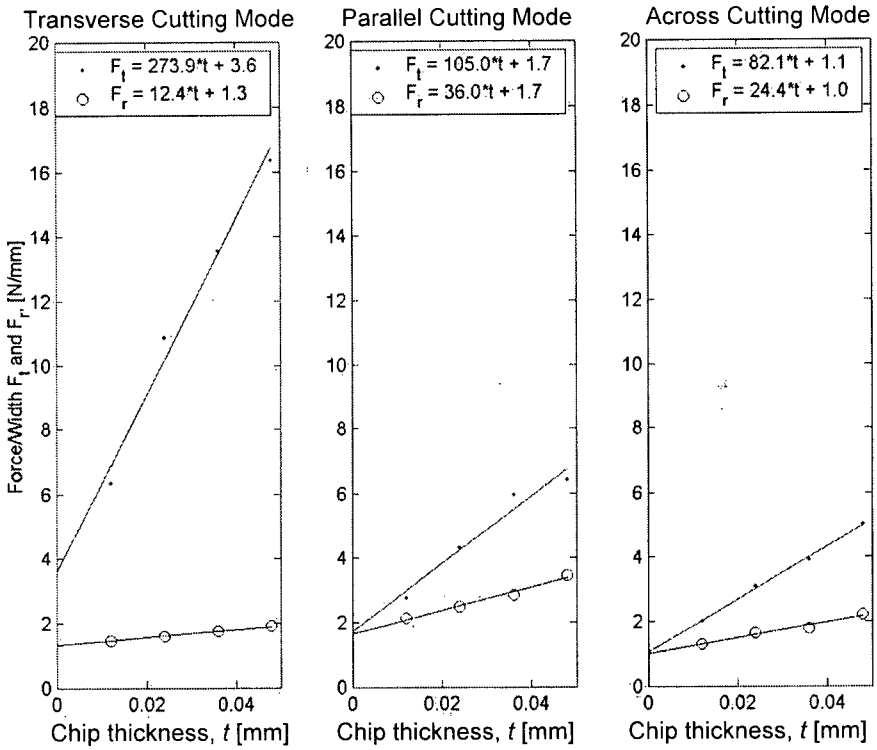

Figure 4.3 Orthogonal cutting data from Jacobs [1973, 1974] for $\alpha = 15°$.
Equations for lines of best fit. Least squares optimization used to fit data points.

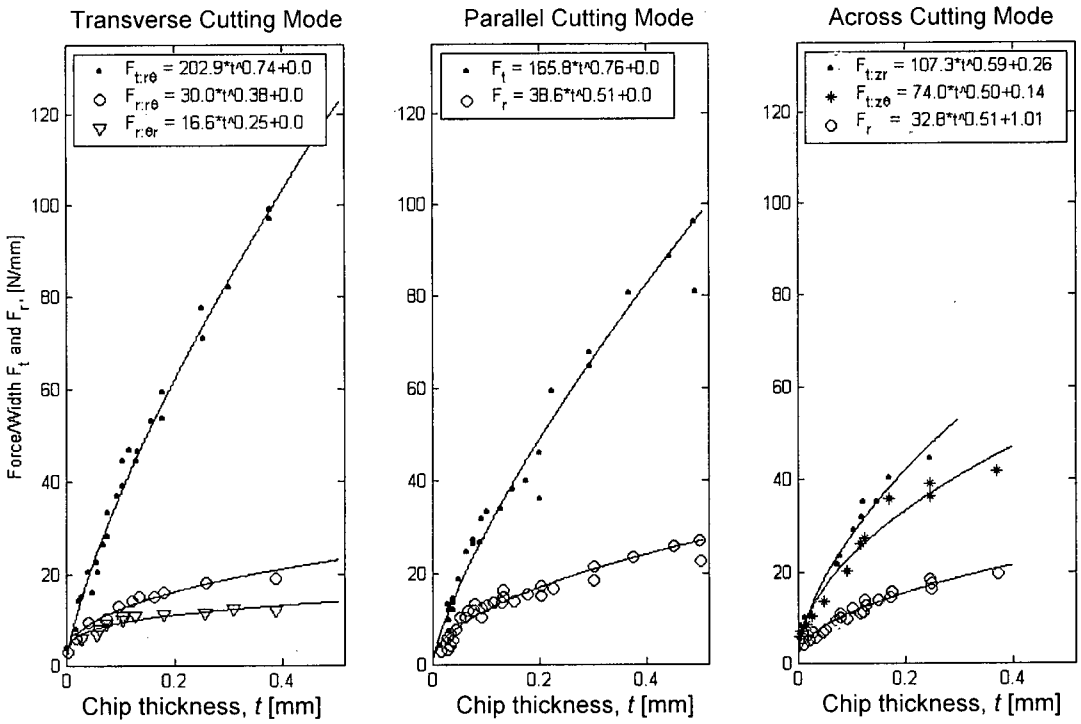

Figure 4.4 Orthogonal cutting data from Wiggins [1978] for $\alpha = 10°$.
Equations for lines of best fit. Least squares optimization used to fit data points.

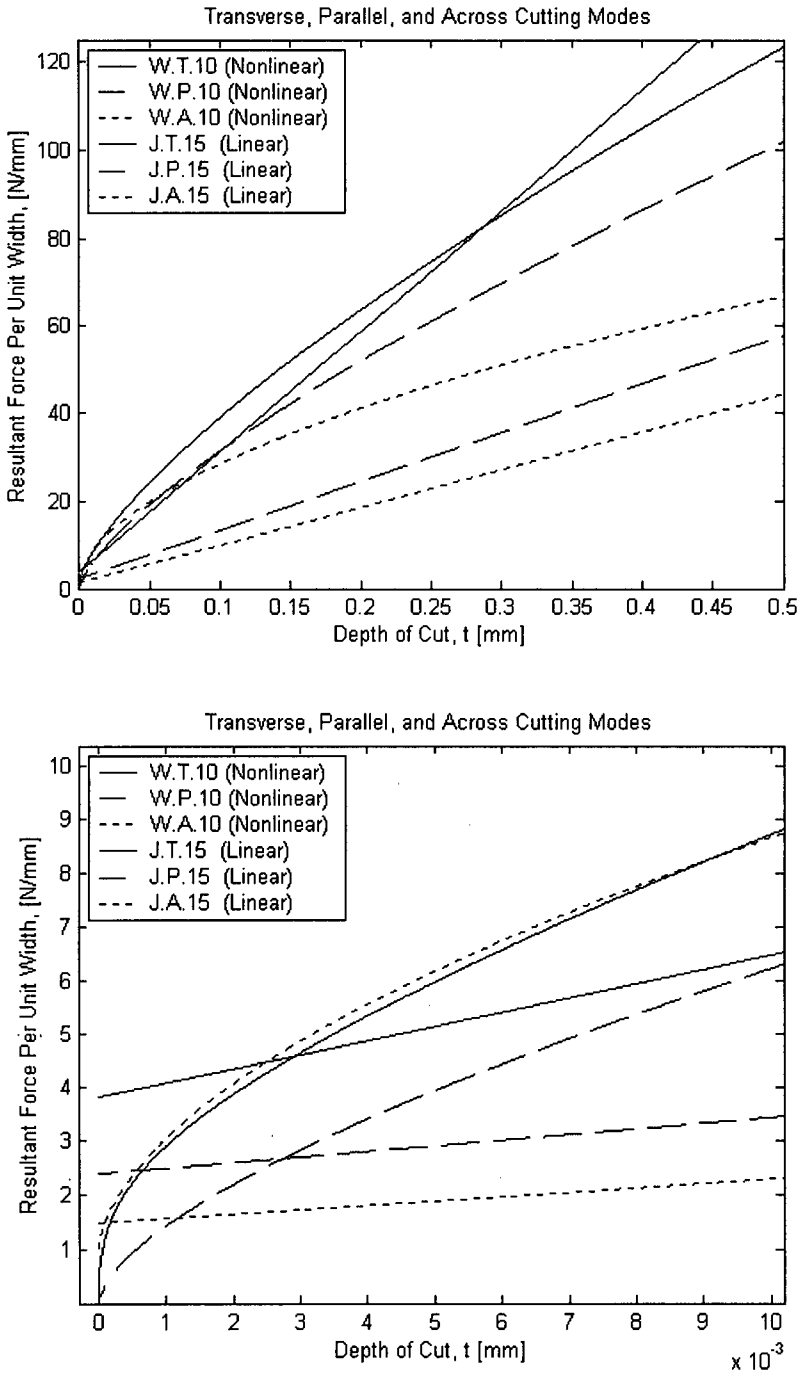

Figure 4.5 Resultant force curves plotted for large ($0<t<500\mu m$, top) and small ($0<t<10\mu m$, bottom) ranges of cutting depth.

Non-linear and linear curves represent the orthogonal cutting data from Wiggins [1978] for $\alpha = 10°$ and from Jacobs [1974] for $\alpha = 15°$, respectively.

Legend key (i).(ii).(iii) = (author).(cutting-mode).(rake-angle):
(i) W/J = Wiggins/Jacob, (ii) T/P/A = Transverse/Parallel/Across, (iii) 10/15 = 15°/10°.

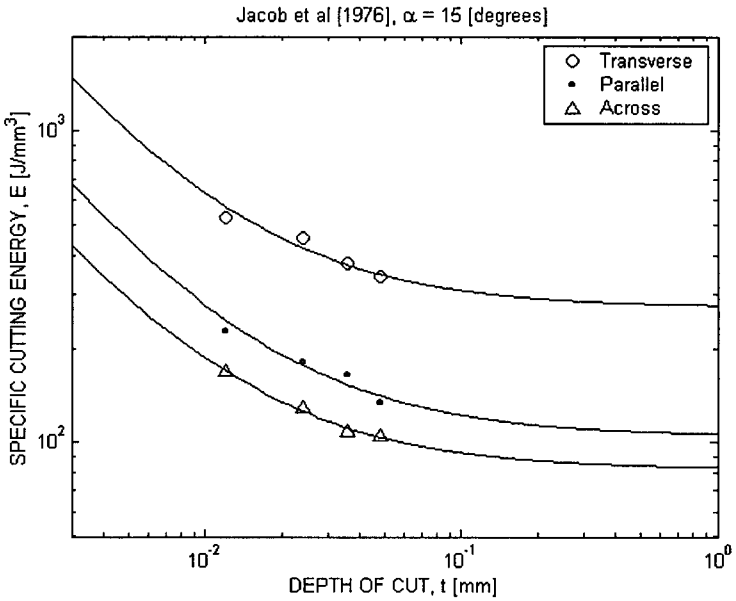

Figure 4.6 Specific cutting energy from the orthogonal cutting data of Jacobs [1973, 1974] for $\alpha = 15°$. Curves represent fitted force data (F_t/t where $F_t = K_{tc}t^l + F_e$, see Figure 4.3).

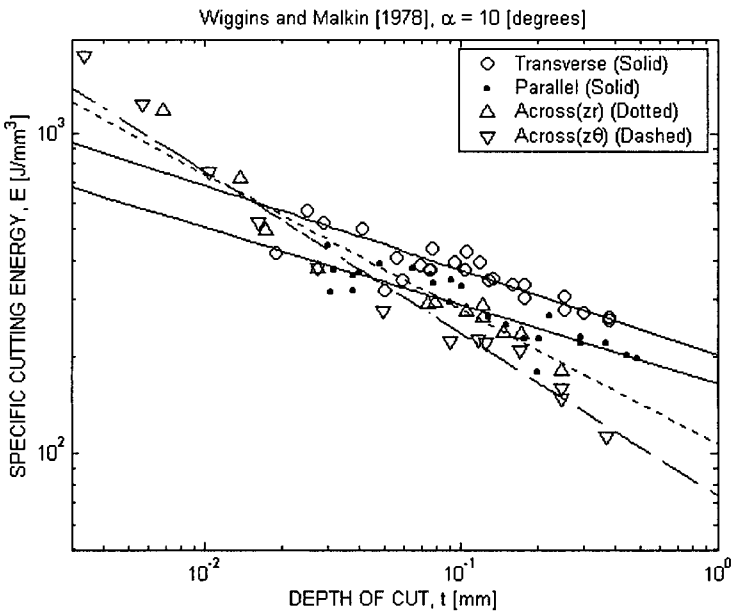

Figure 4.7 Specific cutting energy from the orthogonal cutting data of Wiggins [1974, 1978] for $\alpha = 10°$. Curves represent fitted force data (F_t/t where $F_t = K_{tc}t^{nc} + F_e$, see Figure 4.4).

4.2.2 *Variation of Specific Cutting Energy with Specimen Orientation.*

It has been experimentally shown in the cutting of anisotropic materials such as fibre reinforced composites [Puw 1996, Mahdi 2001], wood [McKenzie 1961], and bone [Jacobs 1974, Wiggins 1978], that the cutting mechanism and specific cutting energy are strongly correlated with the cutting direction with respect to the material anisotropy. In the milling process, the cutting edges are continuously revolving about the axis of the tool and the orientation of each cutting edge is continuously changing with respect to the direction of anisotropy. Therefore the materials' specific cutting pressure as experienced by any particular cutting edge also varies with the direction of the edge velocity [Puw and Hocheng 1993, 1996].

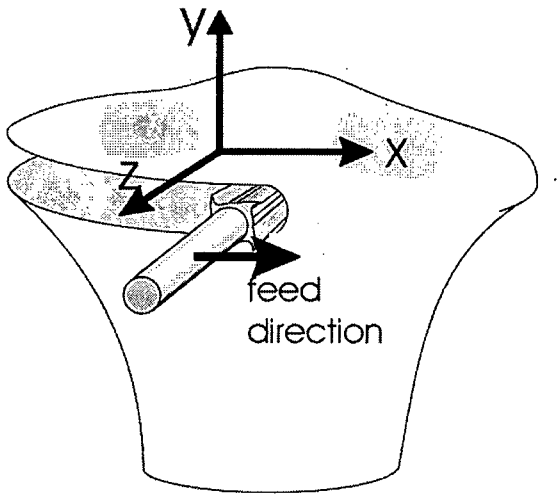

Figure 4.8 Coordinate system for milling tibial plateau.
Feed direction is medio-lateral (x) with predominate osteon direction parallel to y.

The complex composite structure of the cortical and cancellous bone at the epiphysis makes this analysis difficult. To help simplify the problem, we can neglect the bone porosity and consider the anatomy at the cutting site to be a transversely orthotropic field of cortical bone with the predominate osteon direction aligned with the anatomic axis of the bone (y axis) and the feed direction of the mill parallel to the medio-lateral axis (x axis, see figure 4.8) [Reilly 1975]. The cross-sectional area of the mill lies in the frontal plane and for the case of full immersion bone milling the orthogonal cutting mechanisms vary with the tool rotation as follows: at $\theta = 0$, the edge velocity is normal to the predominate osteon direction and the cutting mode is transverse; at $\theta = \pi/2$, the edge velocity is parallel to the osteon direction and the cutting mode is parallel; at $\theta = \pi$, the edge velocity is once again normal to the osteon direction and the transverse cutting mode

is now restored (figure 4.9). The instantaneous forces per unit width acting tangential ($F_* = F_t$) and perpendicular ($F_* = F_r$) to the tool velocity on each tooth segment at these principal orientations are:

$\theta = 0, \pi$: $$\delta F_*(T,t) = K_{*c,T} t^{n_{*,T}} + K_{*e,T} \quad \text{[N/mm]} \quad (3a)$$

$\theta = \pi/2$: $$\delta F_*(P,t) = K_{*c,P} t^{n_{*,P}} + K_{*e,P} \quad \text{[N/mm]} \quad (3b)$$

where T and P denote the (transverse and parallel) cutting mode, and K_{*c}, K_{*e}, and n_* are the constant parameters obtained from the orthogonal bone cutting data. For milling perpendicular to the axis of continuous fibre reinforced composites, Puw [1993, 1996] approximated the cutting forces in feed (x) and normal (y) directions with the following empirical formula:

$$F_x(\theta) = F_{t,T} \cos\theta + F_{r,P} \sin\theta \quad \text{[N/mm]} \quad (4a)$$

$$F_y(\theta) = F_{r,T} \cos\theta - F_{t,P} \sin\theta \quad \text{[N/mm]} \quad (4b)$$

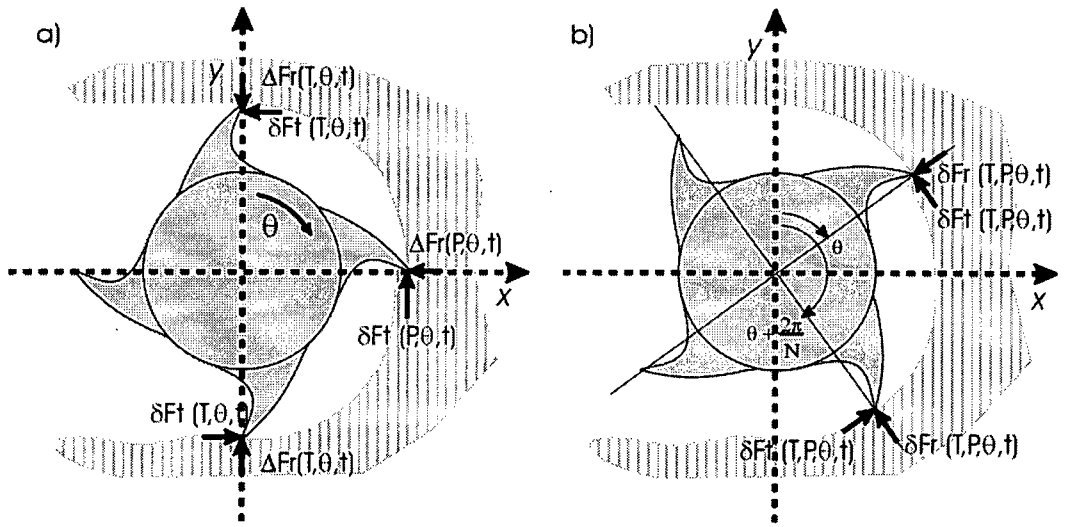

Figure 4.9a,b. Full immersion milling: a) cutting in the orthogonal directions; b) Cutting at an intermediate orientation.
P and T denote cutting energies for parallel and transverse cutting mechanisms.

Many mathematical models have been developed to estimate the variation of mechanical properties in bone as a function of specimen orientation relative to the principle directions [Reilly

1975, Wagner 1992]. The complex hierarchical structure of bone makes this a very challenging task. Although experimental values of Young's modulus have been collected at various orientations to the predominate osteon direction, we could find no such data for the specific cutting energy of bone. The micro-hardness of lamellar bone has been measured [Ziv 1996] in many different orientations and although hardness has been recently correlated to cutting forces in the orthogonal machining of fibreboard [Dippon 2000], this relationship remains to be investigated in bone. Hankinson [1921] introduced a simple empirical criterion to describe the ultimate compressive strength of wood (which is an extremely anisotropic material) at various orientations to the fibre axis. Reilly and Burstein [1975] used this empirical criterion to describe the ultimate strength of bone at orientations between the principal directions. Since no other cutting theory exists, we use their criterion here to approximate the specific cutting pressure at intermediate orientations to the principal directions. The relation is as follows:

$$K_*(\theta) = \frac{K_T K_P}{[K_T \sin^n(\theta) + K_P \cos^n(\theta)]} \qquad [\mathrm{N/m^2}] \quad (5)$$

where $K(\theta)$ is the off-axis specific cutting pressure at some angle of rotation θ, K_T and K_P are the transverse and parallel specific cutting pressures, respectively, and n is any number. The following plot illustrates the variation in the specific cutting pressures obtained from the orthogonal data of Jacobs [1974] as a function of θ, with $n = 2$.

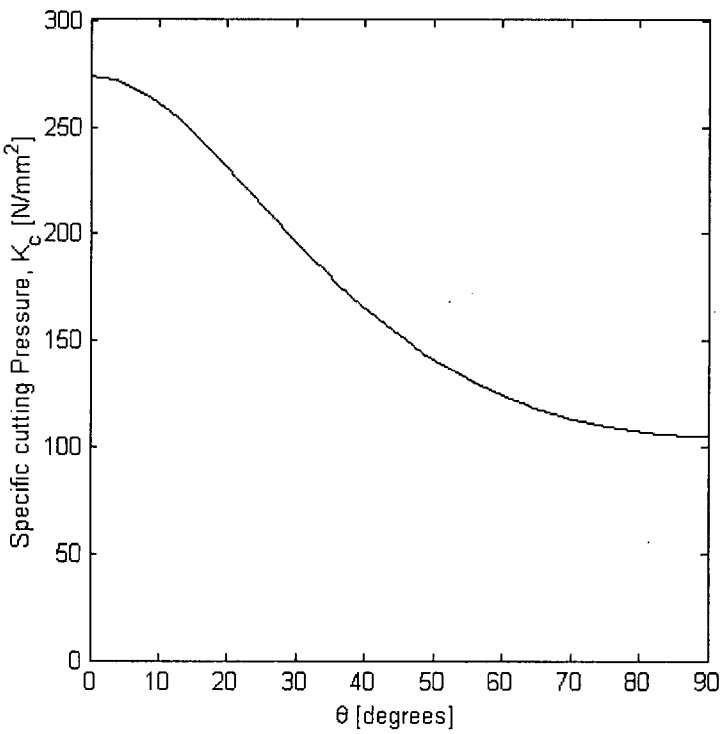

Figure 4.10. Variation in specific cutting pressure as a function of orientation (θ).

4.2.3 Chip Geometry in Milling.

From Equation (2) it can be seen that the uncut chip thickness (t) is a key element in predicting milling forces. In metal cutting research, several authors have previously examined the problem of estimating forces from chip geometry in milling. Martellotti [1941, 1945] was the first to study the kinematics of the milling process and derived the equations of motion of the cutter path as well as the uncut chip thickness as functions of the process parameters. Although Martellotti showed that the true path of a milling tooth is trochoidal, a circular tooth path is a good approximation if the feed rate of the tool is much smaller than the rotational velocity of the mill, which is the case for most powered milling operations. The instantaneous uncut chip thickness can therefore be expressed as a function of the angular position of the cutting edge, θ, and the feed per tooth c:

$$t(\theta) = c\sin(\theta) \qquad \text{[mm]} \quad (6)$$

$$c = 60f/(\omega N) \qquad \text{[mm]} \quad (7)$$

where ω is the rotation velocity (RPM) and f is the feed velocity [mm/s] of the cutter, and N is the number of cutting teeth.

For full immersion milling, where the entry and exit angles for each tooth are $\theta_{st} = 0$ and $\theta_{ex} = \pi$, respectively, the uncut chip thickness varies periodically with the rotation of the mill; from zero (at $\theta = 0$) to a maximum value of c (at $\theta = \pi/2$) and then back to zero (at $\theta = \pi$). An edge is considered to be in the 'cutting zone' (shaded region, figure 4.11) when $0 \leq \theta \leq \pi$. For $\pi < \theta < 2\pi$, no cutting occurs and therefore the force on the tooth element is zero. For the case of half immersion down-milling, where the entry and exit angles into the workpiece are $\theta_{st} = \pi/2$ and $\theta_{ex} = \pi$, respectively, the chip thickness instantaneously jumps from 0 to c upon tooth entry and then decreases to zero as the tooth exits the workpiece. The reverse occurs in half immersion up-milling.

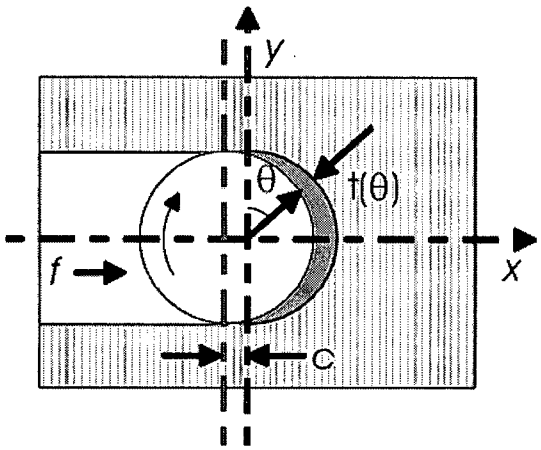

Figure 4.11. Chip thickness in full immersion milling: $t(\theta) = c \sin(\theta)$.

4.2.4 Milling Force Prediction Algorithm.

In the bone-milling algorithm presented here, the milling process is discretized into small angular rotations of $\Delta\theta$ and the forces acting on the mill are calculated at each incremental rotation. The milling tool is segmented into a series of axial slices (S_m) each of elemental thickness (Δz, see figure 4.12). For each axial slice (S_i), the algorithm determines which cutting flute segments ($J_{1...N}$) are currently engaged into the bone and calculates the normalized tangential and radial forces acting on each immersed flute segment. A flute segment is considered to be engaged and cutting into the bone if $\theta_{st} \leq \theta_j \leq \theta_{ex}$, otherwise the force is zero. The tangential and radial cutting force contributions for each edge element (calculated from Equations 3 and 5) are then resolved into force components in the feed (medio-lateral, x) and normal (proximal-distal, y) directions:

$$\delta F_{x_j}(\theta) = -\delta F_{t_j}(\theta)\cos\theta_j - \delta F_{r_j}(\theta)\sin\theta \qquad \text{[N/mm]} \quad (8a)$$

$$\delta F_{y_j}(\theta) = \delta F_{t_j}(\theta)\sin\theta_j - \delta F_{r_j}(\theta)\cos\theta \qquad \text{[N/mm]} \quad (8b)$$

The total forces acting on each axial slice in the feed and normal directions are simply:

$$\Delta F_{x_S} = \sum_{j=1}^{N}[\delta F_{x_j}(\theta_j)\times\Delta z] \quad \text{and} \quad \Delta F_{y_S} = \sum_{j=1}^{N}[\delta F_{y_j}(\theta_j)\times\Delta z] \qquad \text{[N]} \quad (9)$$

where N is the total number of cutting flutes. These elemental cutting forces may be lumped at the upper or lower boundaries of each axial slice.

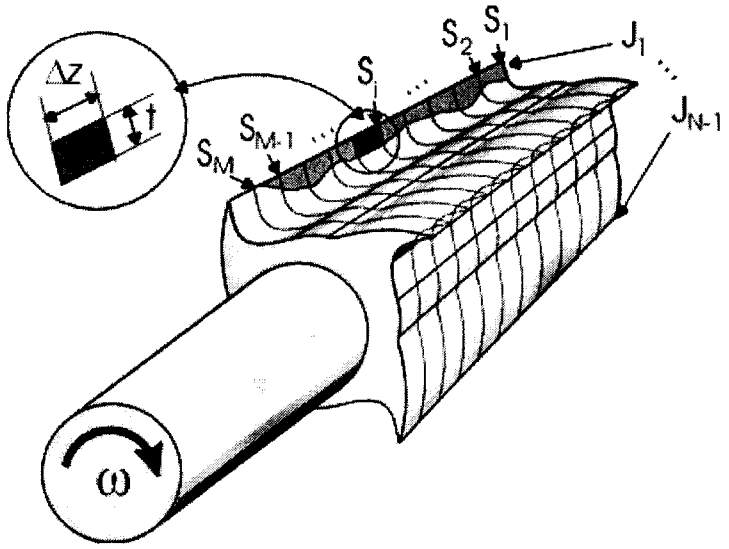

Figure 4.12. A milling tool with J_N cutting flutes and S_M axial segments

4.2.5 Cutting System Deflection.

Similar to previously developed milling deflection models, the deflection of the cutting tool as a result of the applied cutting forces is assumed to be instantaneous; i.e. only the static deflections are considered here. The dynamic effects of the system inertia, machine tool vibrations, and cutting process damping are neglected [Sutherland 1986, Budak 1994, Feng 1996, Altintas 2000].

The cutting tool is modeled as an elastic beam cantilevered at the collet and at the attachment bearings located some distance along the tool axis. The model does not consider any compliance in the bearings or between the tool collet/attachment and the bone, although the system compliance of the robotic tool holder or manual cutting guide could be approximated as a spring/damper system supporting the tool collet [Altintas 2000]. Since the deflection of slender milling tools under cutting forces is of interest here, the cutting error resulting from the inaccuracies of the guidance system is not considered. The axial compliance of the milling tool and the compliance of the bone itself in the cutting zone are also neglected.

The time-varying distribution of elemental cutting forces acting along a slender mill will cause time-varying deflections of the tool during the cutting process. At any particular instant in time, the static deflection of an individual axial slice can be calculated from the instantaneous force distribution. The deflection of axial segment S_k (that is a distance z_k from the free end of the mill, see figure 4.13) in the direction normal to the finished bone surface (y) caused by an elemental

force applied at axial slice m can be calculated by the cantilever beam equation [Budak and Altintas 1994]:

$$\delta_y(z_k,m) = \begin{cases} \dfrac{\Delta F_{y,m} v_m^{\,2}}{6EI}(3v_m - v_k), & 0 < v_k < v_m \\ \dfrac{\Delta F_{y,m} v_m^{\,2}}{6EI}(3v_k - v_m), & v_m < v_k \end{cases} \quad \text{[mm]} \quad (10)$$

where E is Young's Modulus, I is the area moment of inertia of the tool, and $v_k = l - z_k$, with l being the length of the cutter extending from the face of the attachment bearings. The area moment of inertia of the cutter can be approximated by $I = (\pi d_e^4)/64$, where $d_e = s \times d_o$ is the effective diameter of the cutter, d_o is the outer diameter of the cutting flutes and s is a scaling factor (usually $\cong$ 0.8). The total deflection at axial slice S_k can be calculated by the superimposition of the deflections produced by all M elemental forces acting along the mill axis [Altintas 2000]:

$$\delta_y(z_k) = \sum_{m=1}^{M} \delta_y(z_k,m) \quad \text{[mm]} \quad (10)$$

The deflection in the feed (x) direction can be found similarly.

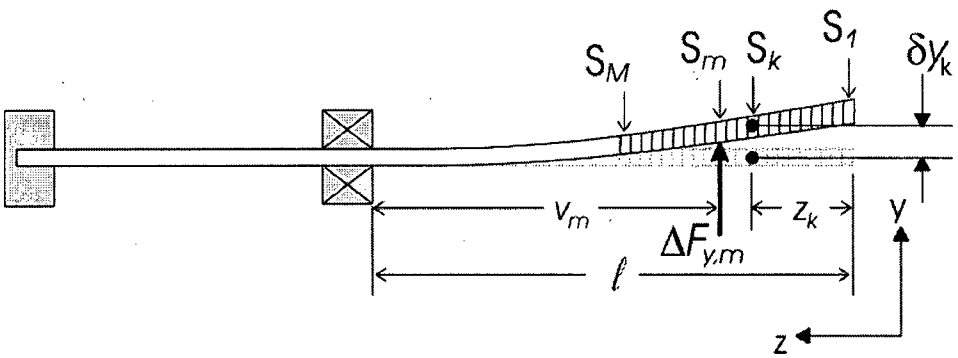

Figure 4.13. Deflection of axial element k due to force at m.

4.2.6 Surface Error Generation.

Bone cutting errors in orthopaedic surgery can result from a number of sources including the malpositioning and/or compliance of the guidance instrumentation, as well as the deflection of the cutting tool itself. Even the cutting mechanism governing the material removal process can affect the surface finish of the bone. In this study, the deflection of slender cutting tools under applied cutting forces is assumed to be the primary factor affecting the bone surface finish.

The surface error induced by the cutting tool deflection is defined as the deviation of the finished surface measured from the desired resection surface. This deviation is measured along the surface normal of the desired resection plane (y axis). The finished bone surface is generated when the cutting edge of any particular element is directly on the bone surface (i.e. $\theta_j = \pi$). The deflection of the element in the y direction, $\delta_y(z_k)$, at this instant defines the machining error at the location. At any other instant, the cutter deflection will cause errors on surfaces that will be machined away later, thus not affecting the finished surface accuracy [Feng 1996, Altintas 2000].

4.3 Simulations

The objective of this section is to simulate the effects of varying cutting conditions on the calculated milling forces and tool deflections for cutting tools of different form. The cutting conditions (feed rate, axial depth of cut, and milling tool) used in the previous chapter are also simulated. By simulating a variety of different cutting conditions, we can identify optimal machining parameters for maximum resection accuracy.

4.3.1 Material and Structural Properties of Bone Milling Tools

In this study, the cutting mechanics of two milling tools of varying geometry are simulated. The first tool is modelled after a commercially available orthopaedic bone mill (Midas Rex, # M10, TX, USA) having an outside diameter of 3.1mm, a total length of 100mm, and two straight cutting flutes extending 35mm axially from the tip. The second is a similar tool equipped with four cutting flutes. The material's elastic modulus and tool's structural stiffness were obtained by measuring the load-displacement curve of the circular shaft and cutting flute regions of the tool. A laser sensor was used to measure the displacement of the cantilevered tool under loads applied with a 10-500 gram mass set (figures 4.14 and 4.15).

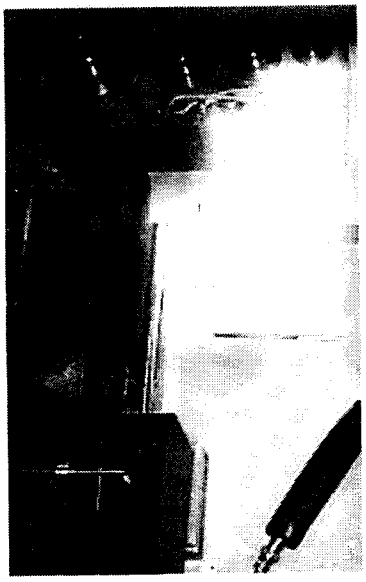

Figure 4.14. Laser sensor and mass set.

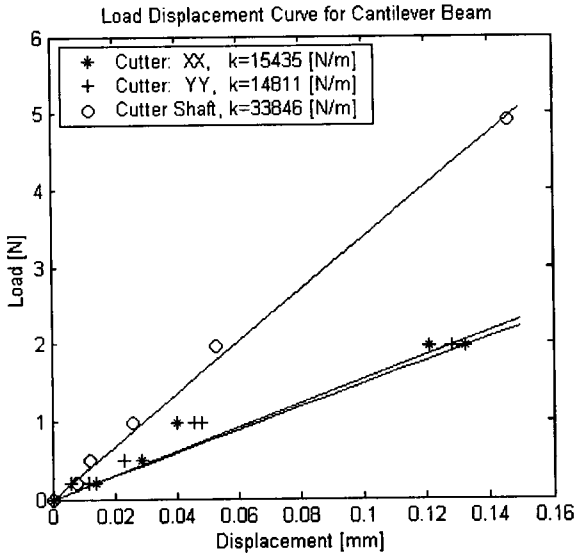

Figure 4.15. Load/Deflection lines of shaft and cutting flute regions of the M-10 bone mill (XX = across flutes, YY = along flutes).

The Young's Modulus of the material was calculated from the slope of the shaft's load displacement curve using the cantilevered beam equation (3.11), and was found to be E = 197 GPa. There was no difference is the structural stiffness of the cutter measured along and across the straight flutes (figure 4.15). The effective diameter of the mill due to the cutting flutes was found to be d_e = 2.54mm (s = .82) when supported at a distance of 35mm from the tip, and this increased to d_e = 2.76mm (s = .89) at 55mm from the tip. The geometric dimensions were measured with an ordinary engineering calliper, and are included in table (4.1).

$$E = \frac{\Delta F}{\Delta x}\frac{L^3}{3I} \tag{11}$$

Table 4.1. Properties of the M10 cutting tool

Shaft diameter	3.1mm
Effective diameter at 35mm	2.54mm
Effective diameter at 55mm	2.76mm
Flute length	35mm
Gauge Length	100mm
Number of cutting flutes (N_f)	2
Young's Modulus	197GPa
Rake angle	~0°

4.3.2 Cutting Conditions

The simulated cutting conditions will determine the relative cutting times and surface accuracies for different cutting tools or techniques, and therefore a criterion for selecting the appropriate cutting conditions must be established. The condition used to evaluate all milling tools and cutting techniques is a constant rate of bone removal (i.e. a tool cutting twice as deep will move twice as slow). The bone volume removal rate (*BVR*) is defined by:

$$BVR = f \times d_o \times DOC \qquad [\text{mm}^3/\text{s}] \quad (12)$$

where *DOC* is the axial depth of cut [mm]. We could find two studies, one milling and one sawing, that report *BVR* values for bone cutting in TKA. Fadda [1998] tested the surface accuracy of two kinds of standard bone milling tools (7.0mm and 12.5mm in diameter). Partial immersion milling was performed on porcine femurs using a *BVR* of 50mm^3/s and a robotic tool holder (f=2mm/s, d_o=5mm, *DOC*=5mm). Ark [1997] constructed an apparatus that applied a constant load on an oscillating saw, and measured the BVR in porcine femurs for four different TKA saw-blades of varying length and tooth geometry. Under a 6.86 N applied load, the average *BVR* value for all blades was ~45±15 mm^3/s. Consequently, a nominal BVR value of 50 mm^3/s will be used to govern the feed rate (f) for each milling tool (cutting at a depth of *DOC* with diameter d_o for full immersion milling).

4.4 Simulation Results

All simulations were carried out with an angular integration angle ($\Delta\theta$) of one degree and an axial slice thickness (Δz) of one millimetre. The force signatures the feed (x) and normal (y) directions for the two and four fluted cutting tools are presented in figures 4.16-4.19. Each force component is calculated from one of the three different force models. The first two force models use the non-linear and linear *F/t* relationships described by Wiggins [1978] and Jacobs [1974], respectively, with the Hankinson [1921] orientation criterion. The last force model uses the linear *F/t* relationship with the Puw and Hocheng [1996] orientation criterion for milling perpendicular to the fibre axis of fibre reinforced composites (also called fibre reinforced plastics, or FRP). These models are respectively labelled non-linear, linear, and FRP in the figures.

4.4.1 *Effect of Force Model and Number of Cutting Flutes on Force Predictions.*

All force models predict a periodic force signature (with frequency equal to the tooth passing frequency) in the feed and normal directions for both cutting tools. However, the shape of each force signature is different for all models, directions, and tools (see figure 4.16-3.17). The non-linear model produces a continuous force function while the linear models produce curves that are discontinuous at the tooth entry and exit angles. Although the chip thickness is zero for full immersion milling at these angular positions, the linear models have a constant frictional force or edge force (F_e) when cutting at all depths greater than or equal to zero. Since this force is reversed with respect to the feed direction at tooth entry and exit, the resulting discontinuity is most extreme in this direction. The linear curves produced with the Hankinson ('linear') and the Puw-Hocheng ('FRP') empirical orientation criteria for anisotropic materials are very similar. Note that this would also be the case for the non-linear and FRP curves had the non-linear force equations been used for both models. Therefore, only the 'non-linear' and 'linear' models will be discussed hereafter.

The non-linear model predicts that maximum forces are highest for the two-fluted cutter, while the linear model predicts slightly higher maximum forces with the four-fluted cutting tool. While doubling the number of flutes decreases the chip thickness by half for each cutting edge, the total frictional forces are doubled since there is twice the number of teeth in the cutting zone. Also, note that the even though the chip thickness is largest at $\theta = 90°$, the force curves for both tools peak at positions some angle away from this apogee. This is due to the higher specific cutting energy in the transverse direction.

4.4.2 *Effect of Feed Rate, Rotational Speed and Axial Cutting Depth on Cutting Forces.*

The effect of feed rate on the force components per millimetre of axial depth of cut for the two and four fluted cutting tools is illustrated in figures 4.16 and 4.17, respectively. Both models predict that the maximum force magnitudes increase with feed rate. However, the extent of the increase in force is not consistent over the two models. As the feed rate approaches zero, the non-linear model tends to zero, while the linear model tends to an asymptotic force value. This is due to the frictional forces that are independent of chip thickness. Notice that the feed-force relationship is not linear for either force model (i.e. when the feed is doubled the force is less than doubled). This is due to the decrease in specific cutting energy with the increase in chip thickness (see figures 4.6 and 4.7).

The effects of cutting speed (v) on specific cutting energy were not included in the force model due to the lack of data available. However, the model predicts that the effect of rotational speed (ω) on cutting force is inverse to that of feed rate (since both variables affect the chip thickness, see Equation 7). For instance, as the rotational speed tends to infinity, the non-linear model tends to zero, while the linear model that includes a friction force term tends to the same asymptotic force value. This trend is similar to the force-rotational speed relationship measured in drilling [Jacobs 1976]. The force signature plots for increasing rotational speed are similar to those for decreasing feed rate (figures 4.16 and 4.17) and therefore are not presented.

The effects of axial cutting depth and feed velocity on the net cutting forces, for a constant bone volume removal rate of 50 mm^3/s and cutting speed of 20000 RPM, are shown in figures 4.18 and 4.19 for the double and four fluted cutters. All models predict significantly decreased forces for both cutting tools in both directions when cutting at smaller axial depths of cut and larger feed rates. Note that as the axial cutting depth tends to zero, the frictional forces in the linear model also tend to zero (i.e. the forces acting at the tip or face of the cutting tool are not included in either model). Therefore, both models predict zero cutting forces at zero depth of cut.

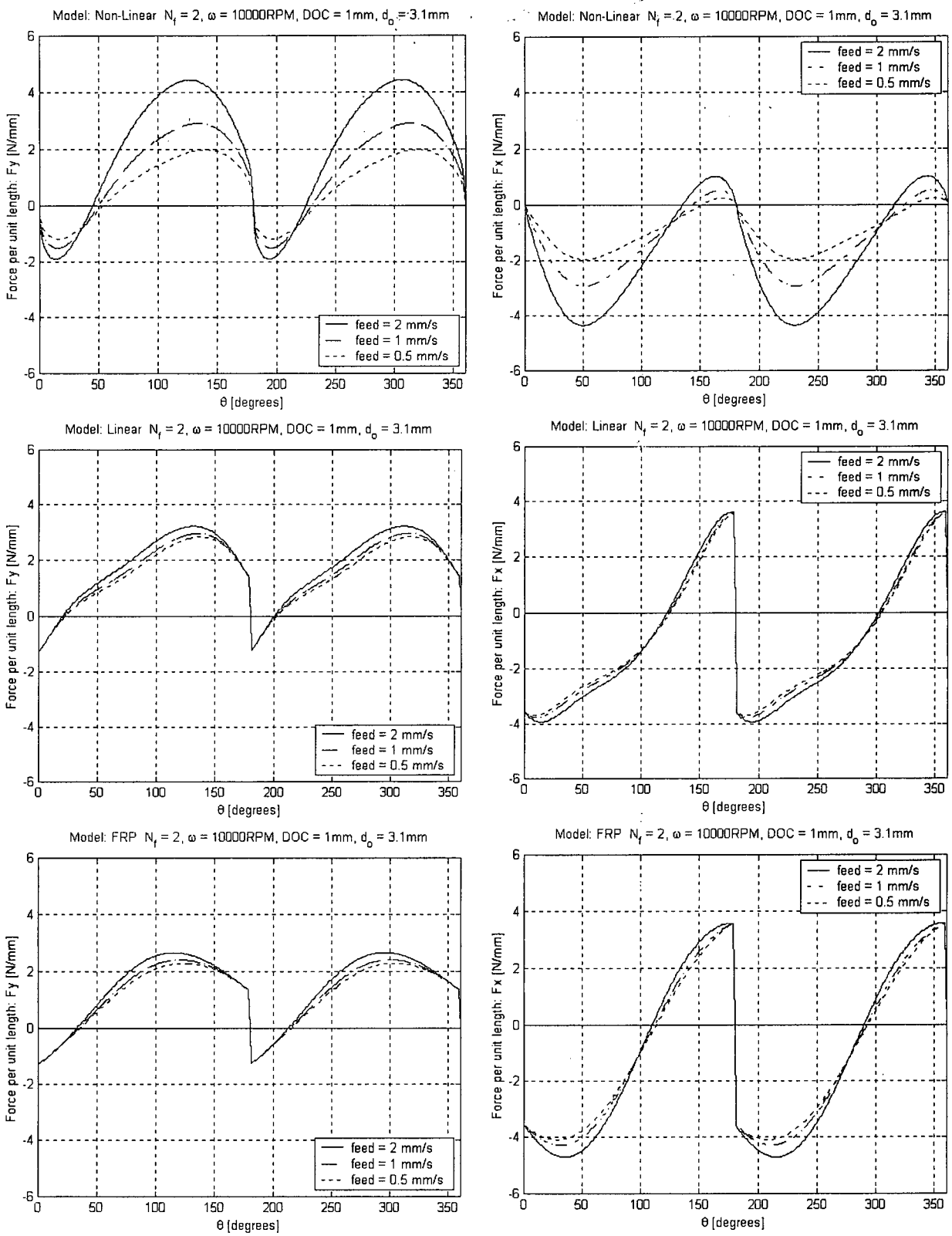

Figure 4.16. Normal (Fy [N/mm], column 1) and feed (Fx [N/mm], column 2) forces per unit axial depth of cut for a **two** fluted cutter (N_f = 2, ω = 10000RPM, DOC = 1mm, d_o = 3.1mm) as a function of rotation angle (θ°) for three feed rates [*feed* = 0.5 (- - -), 1.0 (- – -), 2.0 (—) mm/s].

Forces are simulated with the non-linear (row 1), linear (row 2) and linear FRP (row 3) models.

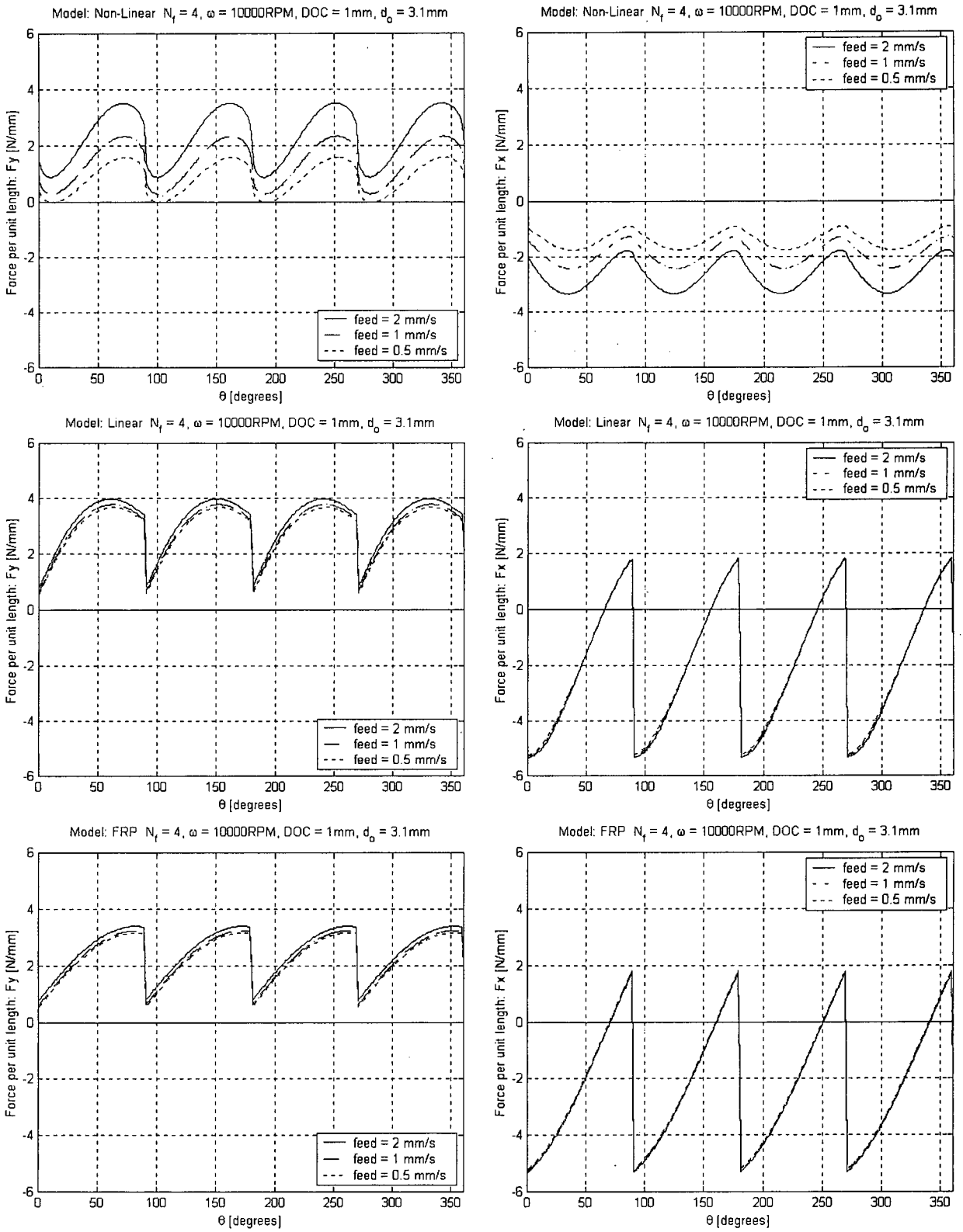

Figure 4.17. Normal (F_y [N/mm], column 1) and feed (F_x [N/mm], column 2) forces per unit axial depth of cut for a **four**-fluted cutter (N_f = 4, ω = 10000RPM, DOC = 1mm, d_o = 3.1mm) as a function of rotation angle (θ°) for three feed rates [*feed* = 0.5 (- - -), 1.0 (– – -), 2.0 (—) mm/s].

Forces are simulated with the non-linear (row 1), linear (row 2) and linear FRP (row 3) models.

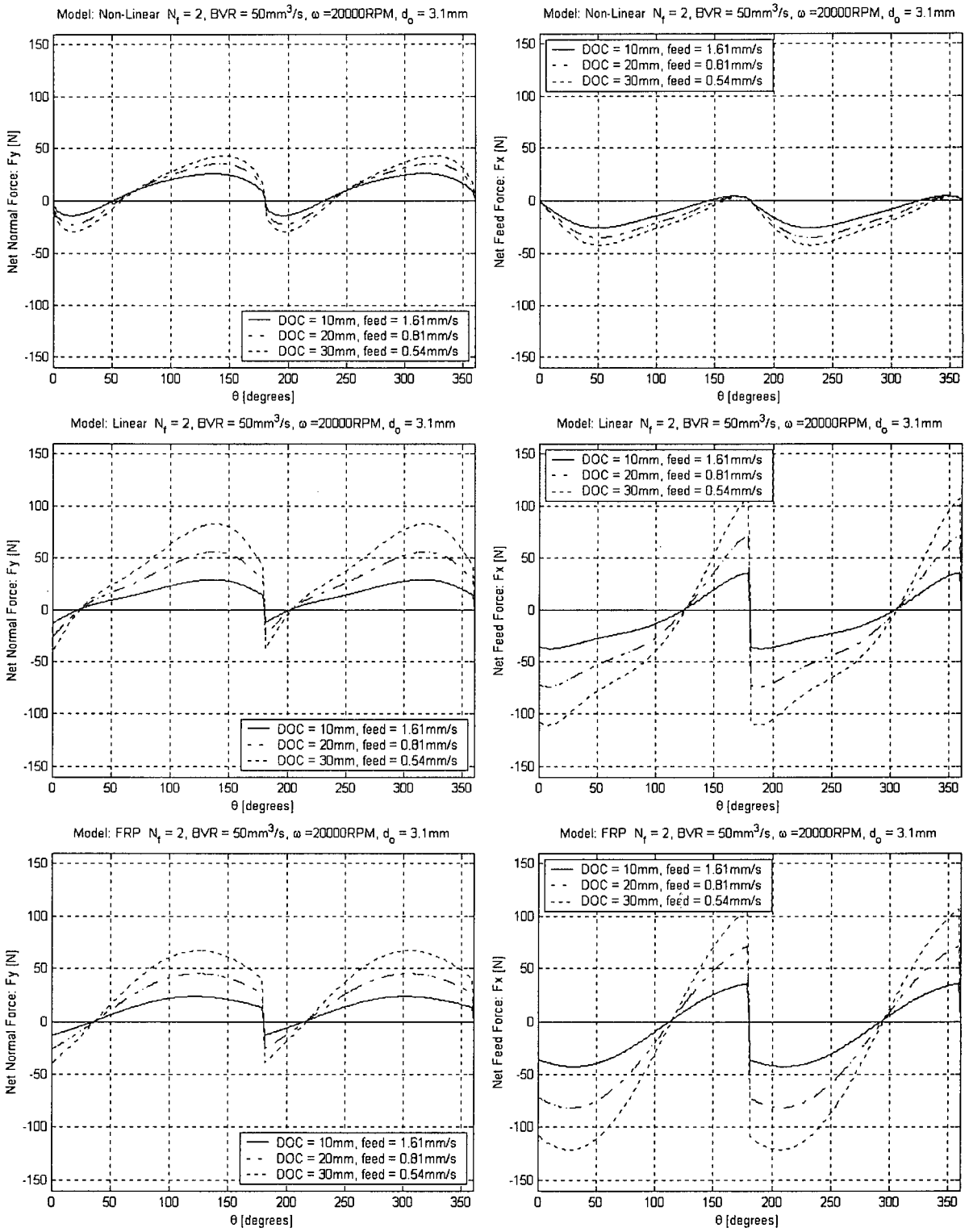

Figure 4.18. Net normal (F_y [N], column 1) and feed (F_x [N], column 2) forces for a **two** fluted cutter (N_f = 2, BVR = 50mm^3/s, ω=20000RPM, d_o=3.1mm) as a function of rotation angle (θ°) for three combinations of DOC [mm] / *feed* [mm/s]: [(- - -) 30/0.54; (- – -) 20/0.81; (—) 10/1.61] Forces are simulated with the non-linear (row 1), linear (row 2) and linear FRP (row 3) models.

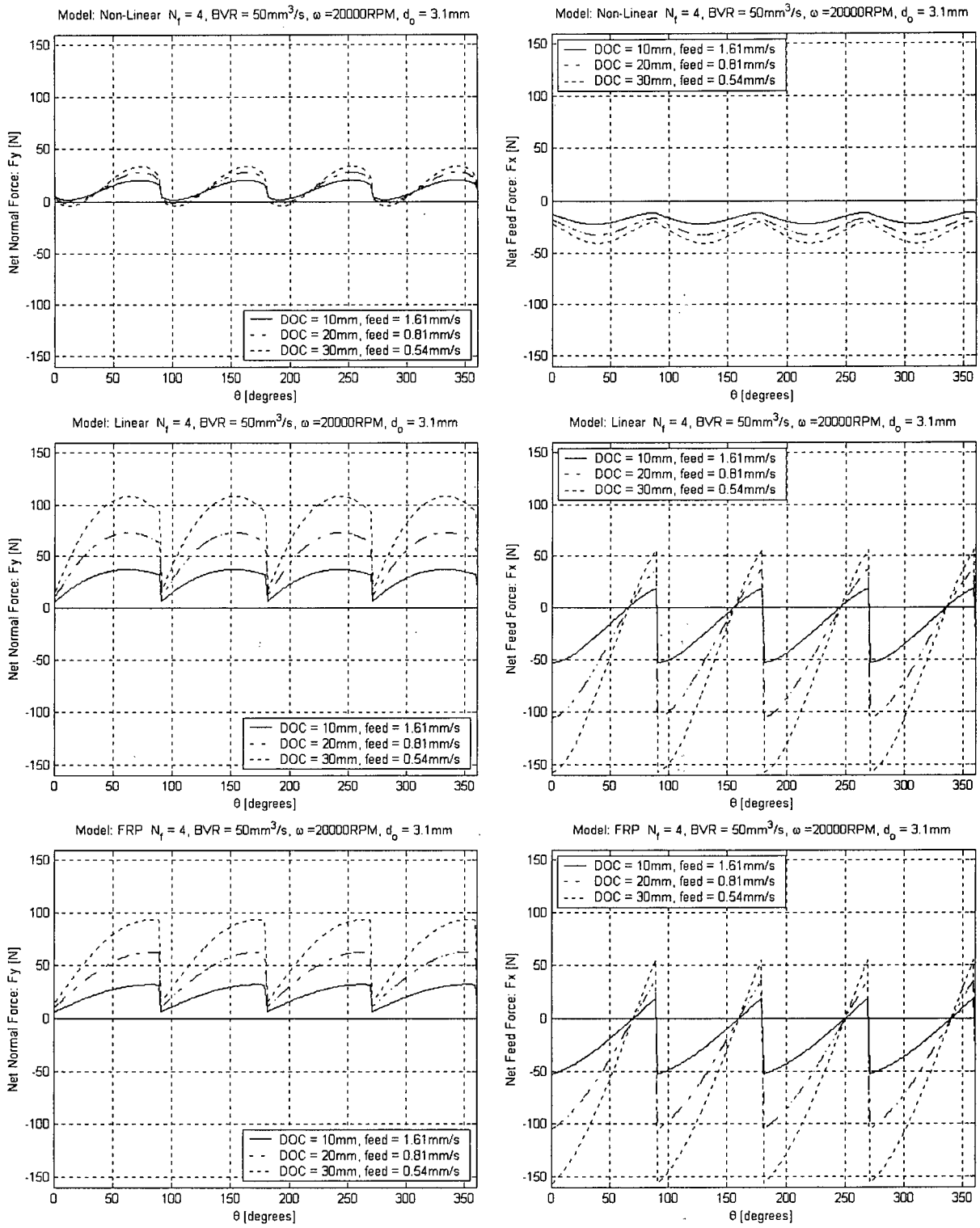

Figure 4.19. Net normal (F_y [N], column 1) and feed (F_x [N], column 2) forces for a **four** fluted cutter (N_f = 4, BVR = 50mm^3/s, ω=20000RPM, d_o=3.1mm) as a function of rotation angle (θ°) for three combinations of DOC [mm] / *feed* [mm/s]: [(- - -) 30/0.54; (– – -) 20/0.81; (—) 10/1.61]. Forces are simulated with the non-linear (row 1), linear (row 2) and linear FRP (row 3) models.

4.4.3 Cutting Tool Deflection.

The tool deflections are calculated for a constant rate of bone volume removal (50mm^3/s) and rotational speed (20000RPM), and for two combinations of axial cutting depth and feed rate (DOC-f: 35mm-0.46mm/s and 5mm-3.23mm/s). The maximum (δ_{max}) and minimum (δ_{min}) tool deflections, as well as the tool deflections while an edge is in the surface generating zone (θ = 170,180, and 190°), are presented in figures 4.20-4.21. The total tool deflection (δ_{max}-δ_{min}) is measured at the tip of the tool. To reduce the number of plots, only deflections resulting from forces applied with the non-linear force model are presented.

The deflection of the two-fluted cutting tool is illustrated in figure 4.20. When the cutter is operated at its standard exposed length of L_a = 35mm (upper row, figure 4.20ab), the total tool deflection is ~0.9mm and ~0.7mm when cutting at DOC-f = 35mm-0.461mm/s, and at DOC-f = 5mm-3.23mm/s, respectively. When the cutter is operated at the extended length of L_a = 55mm (lower row, figure 4.18cd), the total tool deflection is increased to ~4mm and ~2mm when cutting at DOC-f = 35mm-0.461mm/s, and at DOC-f = 5mm-3.23mm/s, respectively. The deflection at θ = 180° is zero for both cutting techniques (i.e. for the different DOC-f combinations).

Similar diagrams for the four-fluted tool are presented in figure 4.21. For both cutting techniques, the tip deflection at θ = 180° is ~0.2mm (upper row, figure 4.21ab) and ~0.5mm (lower row, figure 4.21cd) when operating at the standard and extended tool lengths, respectively. For each cutting technique (DOC-f = 35mm-0.461mm/s, and 5mm-3.23mm/s) the total tool deflections are on the order of ~0.5mm and ~0.3mm when operating at the standard length, and ~2mm and ~1mm when operating at the extended length, respectively.

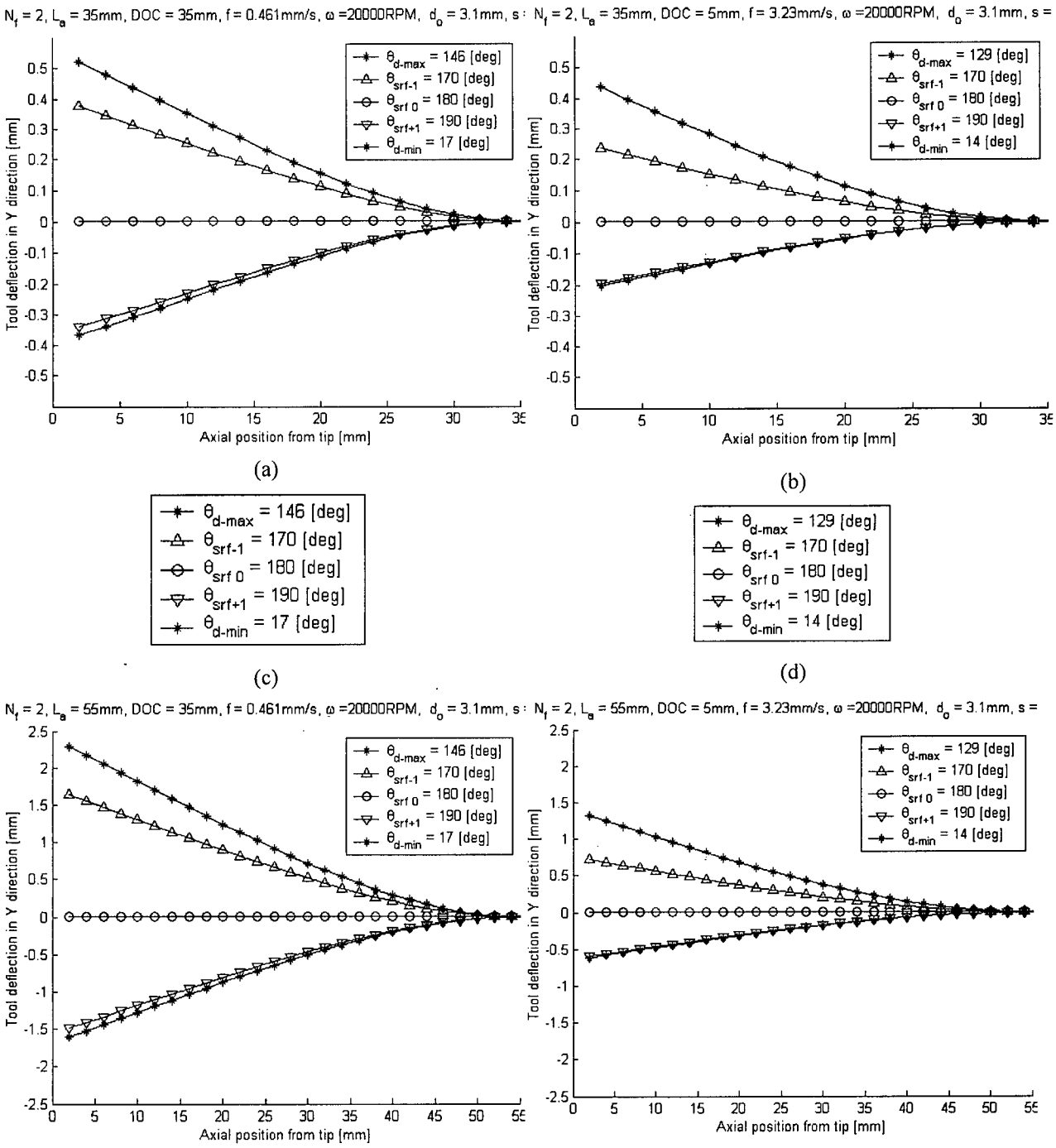

Figure 4.20abcd. Tool deflection in direction Y [mm, *vertical axis*] (normal to the bone surface) along the axial position from tip [mm, *horizontal axis*] for a **two**-fluted cutting tool cutter ($N_f = 2$, ω=20000RPM, d_o=3.1mm) at different angular positions (θ) within one cycle of rotation
(specifically, when the deflections are at a maximum $\theta_{d\text{-}max}$[-*-], minimum $\theta_{d\text{-}min}$[-*-], and when the cutting flute is in the surface generating zone θ = 170° [-△-], 180° [-○-], and 190°[-▽-]).

Deflections are calculated for two cutter lengths measured from the attachment bearing:
(*upper row*: L_a = 35mm, s = 0.82), and (*lower row*: L_a = 55mm, s=0.89),
and for two axial depths of cut (DOC)-*feed* combinations:
(*left column*: 35mm-0.46mm/s) and (*right column*: 5mm-3.23mm/s).

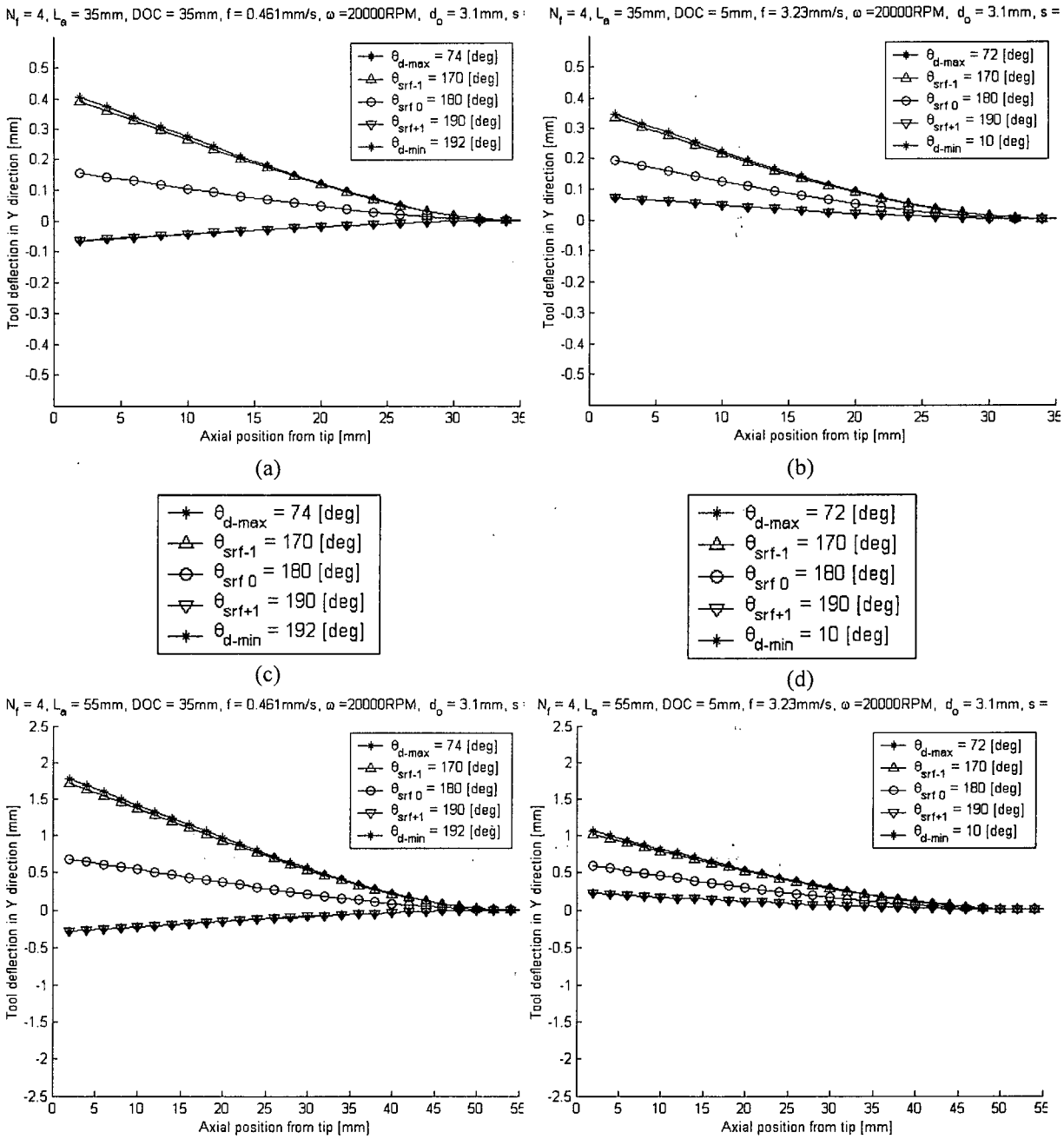

Figure 4.21abcd. Tool deflection in direction Y [mm, *vertical axis*] (normal to the bone surface) along the axial position from tip [mm, *horizontal axis*] for a **four**-fluted cutter ($N_f = 4$, ω=20000RPM, d_o=3.1mm) at different angular positions (θ) within one cycle of rotation
(specifically, when the deflections are at a maximum $\theta_{d\text{-}max}$[-*-], minimum $\theta_{d\text{-}min}$[-*-], and when the cutting flute is in the surface generating zone θ = 170° [-Δ-], 180° [-o-], and 190°[-▽-]).

Deflections are calculated for two cutter lengths measured from the attachment bearing:
(*upper row*: L_a = 35mm, s = 0.82), and (*lower row*: L_a = 55mm, s=0.89),
and for two axial depths of cut (DOC)-*feed* combinations:
(*left column*: 35mm-0.46mm/s) and (*right column*: 5mm-3.23mm/s).

4.5 Discussion

4.5.1 Model Validation

This work presents the first model for predicting forces in bone milling and for quantifying the interrelationships of cutting feeds, depths, and forces for cutters of varying form. Since no cutting force data was experimentally acquired in this work, it is of interest to compare these results to other previously measured cutting data. As mentioned in the introduction, we could only find one study that investigated the mechanics of bone milling, although this study used 'bone sculpting' burrs of rather complex geometry rather than conventional milling tools.

Krause [1982] investigated the effects of cutting depth, feed and speed on maximum cutting temperatures and feed forces with two high-speed rotary burrs. One bur was spherical in shape with 12 helical flutes spiralled along its axis (Hall #21 burr) and the other was oblong or elliptical in shape with 12 straight flutes (Hall #7 burr). Milling was performed parallel to the longitudinal axis of bovine femurs at three feed velocities (1.8, 3.7, 6.35 mm/s) with two high-speed air turbines (20,000 RPM and 100,000 RPM pneumatic milling motors). Three axial cutting depths (.127, .254, .508 mm) were used for the spherical burr while only one depth (.254mm) was used for the elliptical burr. It should be noted that the values of 20,000 and 100,000 RPM correspond to the 'free running speed' or 'no load speed' at maximum operating pressure as specified by the manufacture, and the that actual operating speeds of the air turbines was not measured during machining. However, it was stated that during the tests the air turbines often came close to stalling (and even stalled completely on occasion [Kelly 1976]), indicating that the motors were operating at a significantly slower speed during the cutting tests. Indeed, high-speed air turbines are known to quickly decelerate to 25% of their maximum free running speed under loading [Richards 1999].

The cutting parameters including the milling orientation with respect to the osteon direction (parallel-transverse-parallel cutting mode) were entered into milling the simulation program. To simplify the degree of complexity we made the following assumptions. Since the diameter of the burrs were large (~5mm) with respect to the axial cutting depths tested, the curved profile of the immersed portion of the tool was neglected and the cutter was approximated by the average diameter in this region (~2mm). Although cutting with helical flutes is actually an oblique as opposed to an orthogonal cutting process (i.e. three dimensional as opposed to two) we approximate the cutting forces with the orthogonal data since no oblique bone cutting studies exist. Since the rake angle of the cutting edges were not specified, the orthogonal force data for α

= 10° and α = 15° from Wiggins [1978] and Jacobs [1975] were used for the non-linear and linear models, respectively. Although no information regarding the data processing of the raw force signal was given in the paper (nor were any sample strip chart recordings presented in the thesis), this was discussed in a personal communication with the author (Krause 2002). The measured signal was an oscillating force and the reported values were an average of the maximum force regions of the periodic force signal. Therefore, the published data is compared with the maximum forces obtained from the simulations using the non-linear and linear force models.

The measured and simulated force values at the no load speed for burr #21 are presented in figure 4.22. At the no load speed of 20,000 RPM (figure 4.22a), the linear force model best approximates the magnitude of the measured forces, although the model fails to predict the effect of increasing feed velocity. This is due to the edge forces (F_e) that dominate the magnitude of the predicted force at small chip thickness (i.e. at high rotational speeds). This is also the case at 100,000 RPM (figure 4.22b), with no change in the linear model force predictions. The non-linear model, however, better predicts the feed/force relationship, with the simulated force values increasing with feed rate and cutting depth for both cutting speeds. The trend of decreased cutting force at increased rotation speeds is also captured with the non-linear model. Since the non-linear model seems to better represent the cutting depth/feed/speed interrelationship, this model is used in the following comparisons with the measured values.

The simulated force values for bur #21 are presented in figure 4.23 for various percentages of the no load speed (20%, 50%, and 80% NLS). Even at reduced cutting speeds, the simulated values consistently underestimate the 20000RPM cutting data, although they generally bracket the measured ones at the 100000 RPM test speed. This is also case for burr #7 (figure 4.24). We believe that this is probably due to the different chip removal mechanism that occurs when machining bone at high-speeds. Studies report that when machining at high-speeds (~100000RPM free running speeds) the generated bone chips are so thin that they are 'vaporised' into the surrounding atmosphere [Nogler 1999, Malvisi 2000]. However, when cutting at lower speeds, bone chips have a tendency to stick to the tool and build up in the grooves between cutting teeth, causing increased compressive forces between the bone chips and uncut bone surface. An increase in cutting force due to a poor chip removal mechanism at lower cutting speeds has also been reported in bone drilling [Wiggins 1976, Saha 1982], and this problem is commonly termed 'clogging'.

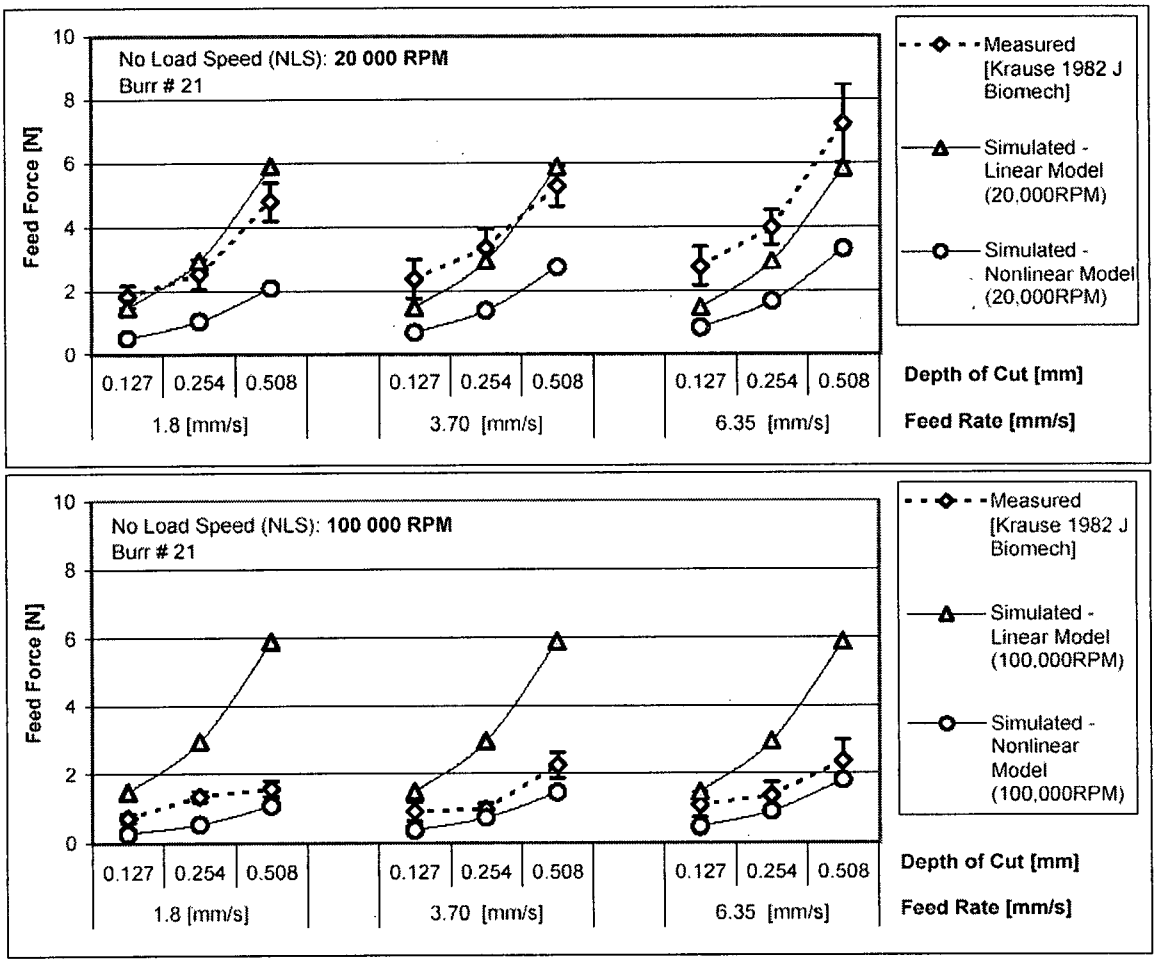

Figure 4.22ab. Measured and simulated feed force values for bur #21 at 20000RPM (upper plot) and 100000RPM (lower plot).

Measured values taken from Krause [*J. Biomechanics.* 1982] and simulated values based on linear [Jacobs: *J. Biomechanics.* 1974. α=15°] and non-linear [Wiggins: *J. Biomech. Eng.* 1978. α=10°] orthogonal force data.

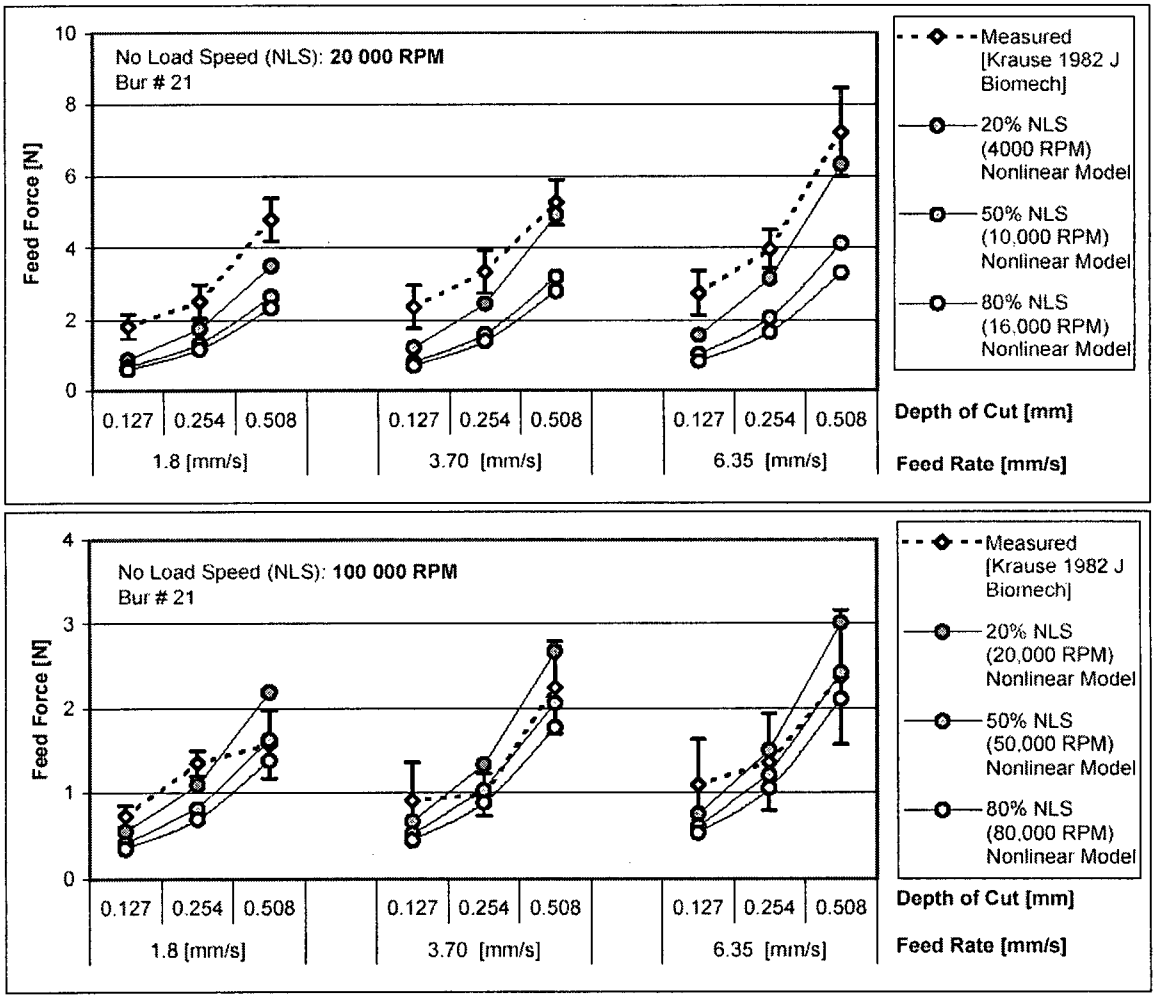

Figure 4.23ab. Measured and simulated feed force values for bur #21.

Simulated force values are for various percentages of the no load speed (20%, 50%, and 80% NLS) and measured force values are at the 20000RPM (upper plot) and 100000RPM (lower plot) no load speeds.

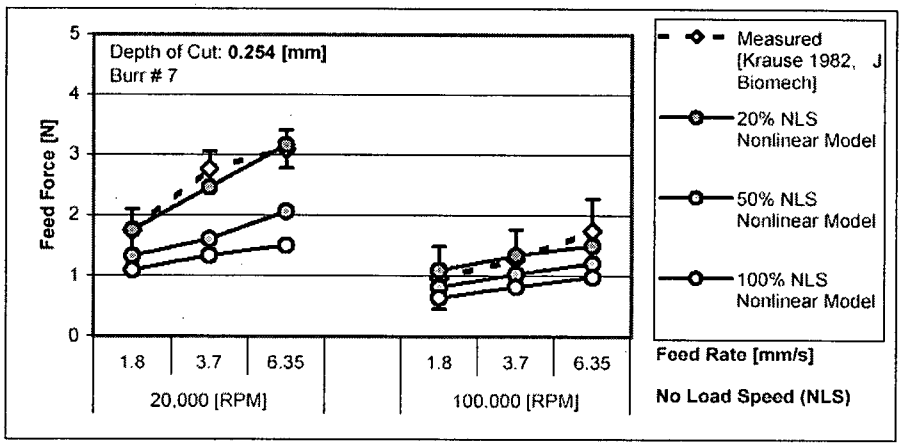

Figure 4.24. Measured and simulated feed force values for bur #7 at a constant cutting depth of 0.254mm, for three feed rates.
Simulated force values are for various percentages of the no load speed (20%, 50%, and 100% NLS).

Figure 4.25 compares the effect of axial cutting depth on the average increase in feed force for the measured (Exp.) and non-linear (Sim.) force values at the no load speeds. The percentage increase in feed force for each increase in cutting depth is averaged over all feed rates for each cutting speed. Although the model predicts a direct linear relationship between force and cutting depth (i.e. the feed force will double when the depth of cut is doubled), the measured feed force increases by only ~40% when the depth of cut is increased from 0.127 to 0.245 mm. Since the cutting depth is very small, this discrepancy may be due to the forces acting on the tip or end face of the tool, which are analogous to a grinding or face-milling operation. The surface area of the face or tip of the cutting bur that is in contact with the bone is about 8x the surface area of the axial portion of the cutting bur (i.e. the portion where the cutting flutes are actually doing the cutting). The model does not include tip effects since the primary objective is to simulate long cutting tools with large aspect ratios (i.e. where the axial cutting depth is relatively large compared to the cutter diameter). From figure 4.25 it can be seen that for both cutting speeds, the average increase in feed force begins to approach the predicted value of 100% as the cutter depth is further increased into the bone and the forces at the tip become relatively less significant.

Figure 4.26 compares the effect of feed rate on the average increase in feed force for the non-linear and measured values at the no load cutting speeds. For each increase in feed rate the percentage increase in feed force is averaged over all cutting depths. The non-linear model predicts that the average increase in feed force as a result of increased feed rate is in the range of

~15-30%, and the averaged experimental values fall within this range. The model also predicts that the increase in force as a result of increased feed rate is much less than that for increased cutting depth, and the experimental data support this assertion.

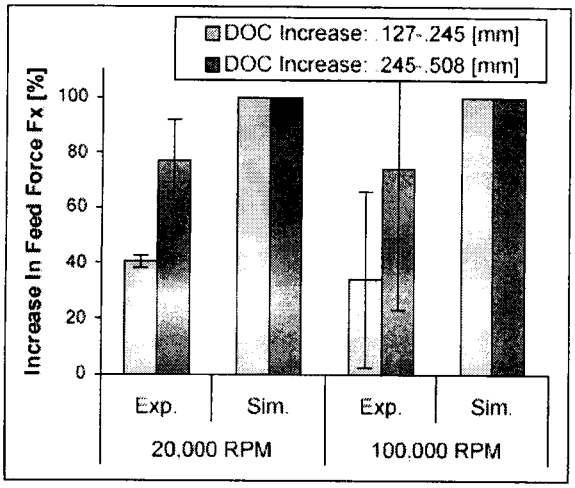

Figure 4.25. Percentage increase in feed force as a result of increasing axial depth of cut (DOC) for the measured (Exp., Krause. 1982) and simulated (Sim., non-linear force model) force values at the no load speeds.

Forces averaged over each increase in feed rate for each cutting speed.

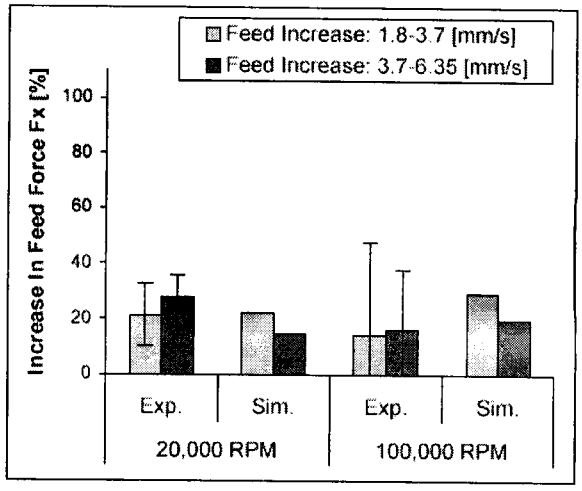

Figure 4.26. Percentage increase in feed force as a result of increasing feed rate for the measured (Exp: from Krause. 1982) and simulated (Sim: non-linear force model) force values at the no load speeds.

Forces averaged over each increase in axial DOC for each cutting speed.

4.5.2 Optimal Resection Tool

The force signatures and resulting tool deflections for two milling tools (one 2-fluted and one 4-fluted tool) were simulated and the total tool deflection became greater for both tools as each was extended further into the bone. The double fluted tool had a total deflection of ~1mm when cutting at the standard exposed length of 35mm, and this increased to ~4mm when the exposed tool length was extended to 55mm (figure 4.20ac). This suggests that the tool would remove excess bone and produce a poorer resection surface in the posterior regions of the transection. However, when the straight cutting flute is generating the bone surface at $\theta = 180°$, the static deflection model predicts that the deflection is zero at this point since no teeth are in the cutting zone at that instant (hence no cutting forces) and no surface errors occur. This prediction is consistent with the current static deflection models used in metal cutting research [Budak and

Altintas 1994, Feng 1996, Altintas 2000], where it is rationalized that the cutting errors that occur at other rotation angles will be machined away with the rotation of the tool and therefore only the deflection at $\theta = 180°$ is of importance.

Although the static deflection model predicted that the total deflection of the 4-fluted cutter was about half that of the 2-fluted cutter (~0.5mm at 35mm and ~2mm at 55mm, figure 4.21ac), the tip deflection at $\theta = 180°$ is not zero but a positive value. This positive deflection at $\theta = 180°$ was not reduced even when the cutting forces and total defections were optimized by modifying the cutting conditions (figure 4.21bd). This suggests that the tool would tend to leave excess bone at the back of the cut, resulting in an implant with a positive alignment bias in the sagittal plane. A negative alignment bias in the sagittal plane (i.e. excess bone removed at the back of the resection) is also possible if the feed direction was reversed. This could also cause frontal plane alignment errors if the surgeon were to mill from the centre regions of the transection outwards toward the medial and lateral cortices (since the cutting direction is reversed on one side the bias would be reversed from positive to negative on that side as well). These conditions are commonly referred to as up- and down-milling in the manufacturing industry and are known to respectively cause under- and over-cutting surface errors when cutting with tools that have multiple flutes in the cutting zone at the instant when an edge is generating the finished surface (i.e. at $\theta = 180°$) [Budak 1994, Altintas 2000].

The stiffness of the cutter determines the magnitude of the tool deflection under the applied cutting loads. The stiffness of a commercially available cutter was measured and found to be reduced by ~50% in comparison to the circular shaft portion of the tool, and this is due to the influence of the cutting flutes (figure 4.15). This effect was simulated by scaling the outside diameter of the cutter by ~0.8 to ~0.9, depending on the extended cutter length. If the effect of the cutting flutes cannot be avoided, selecting a tool of larger diameter would be an effective means of reducing the tool deflection. For instance, if we approximate the tibial plateau as a 60mm diameter circle with a corresponding ~3000mm^2 resection area, a 3.1mm diameter tool would necessitate a resection time of ~3min, assuming a constant bone removal rate of 50mm^3/s. Increasing the tool diameter by 25% (~0.8mm) would result in a 25% increase in resection time (~45sec) if the bone volume removal rate remains unchanged. However, since the moment of inertia is proportional to the tool diameter to the power of four ($I = (\pi d_e^4)/64$), this 25% increase in diameter (and 45 second increase in resection time) would reduce the tool deflection by over 60%.

4.5.3 Optimal Resection Strategy

The results of this study suggest that an increase in feed rate and decrease in cutting depth will be most effective in reducing forces and optimizing accuracy without compromising resection time. This advantage can be attributed to the decrease in specific cutting energy with increasing chip thickness (i.e. increased feed rate) [Wiggins 1974, 1978]. Wiggins and Malkin [1976] have also shown that the specific cutting energy of bone decreases in drilling operations when the feed rate is increased at any given rotational speed for several drill point geometries. Straight-line relationships were obtained when the specific cutting energy were plotted against feed rate on log-log coordinates, with higher specific energies obtained at lower feed rates. Since less energy is required to drill at higher feed rates, the authors suggested that lower temperatures and less thermal damage should occur in this case.

Although metal cutting theory (i.e. shear plane or Merchant analysis) does not predict an increase in specific cutting energy with decrease in cutting depth, several researchers have observed and attempted to explain this phenomenon [Backer 1952, Armarego 1962, Oxley 1989]. Backer [1952] reasoned that as the depth of cut is reduced the probability of finding dislocation sources in the material is also reduced and as a result the flow (or shear) stress and hence, the specific cutting energy, will increase. Although a fracture rather than shear mechanism has been observed in bone cutting, Backer's theory may still be applicable to bone. Upon examining micrographs obtained from interrupted cutting tests, Wiggins [1974, 1978] identified the cutting mechanism in the bone machining process to occur in a series of discrete fractures. They observed under several different machining conditions that the fractures propagated along weak planes within the bone matrix, such as between adjacent osteons. Krause [1987] also observed a tendency for cracks to propagate along the cement lines between lamellae during cutting, and these are known to be a weaker structural element within the bone matrix [Lui 1999]. Therefore, it is reasonable to assume that the probability of the fracture surface encountering a weaker plane to propagate across would reduce with the cross-sectional area of the cut. This would result in an increase in specific cutting energy at smaller cutting depths.

The profile of the tool cutting edge has also been regarded as an important factor contributing to the 'size effect' phenomenon [Armarego 1962]. Even a 'sharp' tool has some degree of dulling and this may become increasingly significant at smaller cutting depths. Both the nose radius of the cutting edge and the contact between the tool clearance face and the finished surface (and the resulting frictional forces) may contribute to the observed increase in specific cutting pressure by

making a proportionally greater contribution to the measured cutting forces at small depths of cut [Oxley 1989].

4.5.4 Temperature Considerations

Utilizing the decrease in specific cutting energy to optimize a cutting technique can not only improve resection quality by reducing cutting forces and tool deflections, but also by reducing bone temperature elevations. Cutting at a lower specific cutting energy reduces the energy expended in cutting the bone and hence the amount of energy turned into heat. Matthews and Hirsch [1972] measured the temperature distribution around holes machined in cortical bone by drilling at different feed rates (by varying the applied load). They found that the maximum temperatures measured at each thermocouple were significantly reduced for every case of increased feed rate (or applied load). In bone milling, the amount of heat generated is dependent on the cutting forces and frictional forces at the cutting edges, and therefore can be related to the number of revolutions completed and the number cutting flutes used when cutting bone [Krause 1982]. While the number of cutting edges is fixed for a particular tool, the number of revolutions completed in cutting a certain volume of bone is determined by the feed rate and the operating speed. An increase in feed rate would reduce the contact time between the bone and the cutting teeth and the number of revolutions required to make the cut. Krause [1982] measured the temperatures in cortical bone during milling at several feed rates and cutting depths and found that increasing the feed rate decreased the temperature elevations for all cutting depths tested. Since increasing the feed rate decreased the contact between the bone and the cutting edges, the frictional forces and the amount of heat generated were reduced. Decreasing the rotational speed also had a similar effect, however, it was felt that "the increase in feed rate had a greater effect on the temperature response than the rotational speed so that cutting with a 100,000 RPM tool is satisfactory if a fast feed rate is used."

4.5.5 Study Limitations

There have been several assumptions made and factors neglected in the development of this model. These include factors influencing the force predictions, such as the effects of cutting velocity on the specific cutting energy and frictional forces, as well as the rigid tool assumption in calculating the force signatures. In addition, factors directly influencing the tool deflection and accuracy predictions such as the cutting tool dynamics were neglected. These are discussed below.

4.5.5.1 Effect of cutting speed

Bone is a viscoelastic material and we would therefore expect it to exhibit different properties when cutting at different velocities. Krause [1976, 1987] investigated the effect of cutting velocity on the specific cutting energy of bone in an orthogonal cutting study that aimed at optimizing the design and operating characteristics of oscillating and reciprocating saws. Cuts on bovine femora were performed with tools having negative rake angles (0° to -30°) at low (1.27 to 25.40 mm/s) and high (105.9 to 409.2 mm/s) cutting speeds. For all test cuts, the depth of cut was held constant at 0.07mm and the cutting direction was across the osteons. The specific cutting energy increased slightly with increasing velocity at low cutting speeds, and then decreased at a higher rate with increasing velocity at high cutting speeds. The radial force component remained essentially constant over the velocity range tested. Krause deduced that a critical cutting velocity probably exists around 50mm/s, where the fracture or crack propagation mechanics change from a controlled to catastrophic nature.

Pal [1986] measured cutting forces in bovine tibiae while cutting transverse to the principle osteon direction with positive rake angles (0 to 30°) at three different cutting depths and velocities (t = 0.05, 0.10, 0.15mm; v = 0.5, 16.6, 31.8, mm/s) and found no significant differences in resultant forces for the three velocities tested.

Aside from the few conditions studied, the non-linear relationship between cutting forces and velocity remains largely uncharted. Little data is available on how the relationship varies at other cutting depths, speeds and orientations relative to the bone anisotropy. Therefore, the effects of cutting velocity on cutting forces were not included in the model developed here.

4.5.5.2 Frictional effects

Living bone is a wet, fibrous substance and this makes the modelling of frictional forces in the bone cutting process an exceedingly difficult task. When forces are experimentally acquired as in, for example, an orthogonal cutting or milling process, the cutting forces are always confounded with the frictional forces that act on the clearance and rake faces of the tool. In metal machining analysis, the forces acting on the tool are often resolved into four components, where each component is either normal or tangential to the rake or clearance face of the tool. The force components acting on the clearance face are identified by plotting the measured cutting forces against depth of cut and extrapolating back to zero depth [Thomson 1953, Armarego 1969, Altintas 2000]. The force intercept, called the edge force, is removed by subtracting its value

from all the data and a coefficient of friction, μ, between the workpiece and tool material, is then determined from the ratio of the normal and tangential forces acting on the rake face of the tool.

Several investigators have found that the coefficient of friction is dependent on the cutting conditions and have attempted to explain this phenomenon by considering the distribution of stresses on the rake face of the tool [Armarego 1969, Altintas 2000]. By assuming two stress distributions on the rake face, one of high decreasing normal stress and one of constant shear stress, two separate regions of sticking and sliding friction exist. The coefficient of friction in the sticking region is not constant but dependent on the magnitude of the normal load (friction adhesion theory says that plastic deformation occurs at the interface contact asperities under high normal loads, which affects the area of contact and the extent of bonding between the two metallic surfaces; the 'welded' asperities must then be sheared to produce relative motion). The value of μ in this sticking region is lower than that for sliding friction conditions, and the μ value measured in metal cutting is therefore assumed to be an average value based on both the sticking and sliding regions. A change in the cutting conditions can alter the relative area of each stress region, and thus, the measured force and μ values. For example, increasing the rake angle α reduces the overall normal load on the rake face causing a decrease in the area ratio of sticking to sliding regions, which increases the measured value of the coefficient of friction.

The coefficient of friction has also exhibits dependence on cutting conditions when machining wet bone. Krause [1987] reported that μ increased with the tool rake angle and the cutting speed. It should be noted that Krause did not account for the edge effects acting on the tool clearance face when calculating μ since only one depth of cut was tested. However, the measured variation of μ with cutting speed suggests that a more accurate model should incorporate the effects of cutting speed on frictional forces. In the mechanistic approach to force prediction the measured force values are directly related to the cutting speed and feed through empirical constants calibrated for each tool geometry [Jacobs 1976, Wiggins 1976]. Prediction of the cutting forces in this manner is accurate and convenient since the variation of both the cutting and frictional forces with the cutting conditions are incorporated into the exponential and scaling constants. Unfortunately this process is extremely time consuming and costly and therefore more fundamental relationships rather than empirical ones are needed to reduce the work involved.

In the generalized model developed here, both the cutting and frictional forces were considered to be independent of cutting speed. The linear force model included edge forces at zero cutting depth (F_e>0), while these were not significant for the non-linear model (F_e=0). Like many metal

cutting researchers [eg. Oxely 1989], Wiggins [1978] neglected the edge forces and presented the cutting data with straight lines on log-log coordinates. Although Jacobs [1974] reported a linear resultant force-depth of cut relationship with significant edge forces obtained when extrapolating to t=0, upon inspection of the force components we can see that a non-linear relationship would also produce a good fit to the cutting force data (see figure 4.3). This can also be seen from the specific energy log-log plots, where the extrapolated linear force model does not predict the specific cutting energy beyond the tested cutting depths as measured by Wiggins and Malkin (figures 4.6 and 4.7). This suggests that simply using an invariant step function to model the friction force while the edge is in the cutting zone is not representative of the actual mechanics governing the process. This is also evident from the comparison with the milling data, where the linear model failed to predict the effect of increased cutting feed and speed due to the effect of the friction forces (figure 4.22). Clearly, more detailed force data obtained by milling at several feeds and speeds is necessary to further the development of a more accurate model for predicting cutting and frictional forces.

4.5.5.3 Rigid chip size

Like previously developed milling force and accuracy models, the force signatures for each milling tool are generated assuming a completely rigid system and the surface error is then calculated based on the generated forces [Kline 1982, DeVor 1983]. This assumption of a rigid milling system for the calculation of forces has produced good results for cutting systems whose deflections are small [for example, Budak and Altintas 1994]. However, when milling with slender cutters like those simulated in this study, the deflections may become large and have a significant effect on the chip size and thus cutting forces and surface error.

Sutherland and Devor [1986] incorporated the inherent cutting system flexibility into a previously developed milling force and surface error model [Kline 1982]. They used an iterative procedure to balance the forces and deflections generated during the milling process. Both the rigid and flexible models were then used to predict the forces and surface errors measured in a series of experiments using both short (rigid) and long (flexible) milling tools. The two models were also used to simulate tools with and without the condition of cutter 'runout' (where the tool axis is slightly misaligned or offset with the spindle axis, causing an alternating oversized and undersized chip thickness with each half revolution). The rigid and flexible models produced virtually identical force signatures for the short tools and for the long tools with no runout. However, for milling with long tools with cutter runout, the flexible model produced force

signatures more representative of the measured data. Since system deflections temper the effect of cutter runout, the rigid force model consistently over-predicted the maximum forces while the flexible milling model predicted lower and more accurate maximum forces and surface errors as measured with the long tools with runout.

For this study we adopted a rigid system model to generate the force signatures for each milling tool simulated. Since tool runout was not considered here, we believe that a rigid model is adequate for predicting reasonably accurate tool deflections for the simulated cutting conditions. Not incorporating the system flexibility into the force prediction algorithm only produces more conservative force and surface error estimates, since machine tools tend to deflect in a manner that decreases the chip size and the cutting force.

4.5.5.4 Cutting tool dynamics

Accurately predicting cutting tool deflections and surface errors necessitates consideration of the dynamic aspects of the cutting process. This is especially important when machining with slender milling tools as they are known be susceptible to dynamic phenomena such as mode coupling and self-excited chatter [King 1985, Altintas 2000]. The dynamics of the machining process were not included in the model developed here since we believe that it is important to first establish a good static model before incorporating dynamic effects, and therefore this is left for future work. For a preliminary investigation on the vibration characteristics of the cutting tool used in this thesis, the interested reader is referred to Appendix A.

4.6 Conclusions

In summary, a generalized milling model for predicting forces and accuracy was developed and implemented in a series of bone milling simulations. The simulation results indicate that for optimal resection accuracy, smaller cutting depths and larger feed rates should be practiced. This is based on the observation that when machining a certain volume of bone in the form of chips, it is more efficient to cut thicker chips of smaller width, rather than thin chips of larger width, since the specific cutting energy decreases with the uncut chip thickness. Krause [1982] experimentally verified that this milling strategy results in reduced feed forces and temperature elevations in bovine bone.

The optimized resection strategy reduced the total tool deflections by ~50% in the simulations, without any increase in estimated resection time. However, even with this optimized resection strategy, the cutting tools simulated were not stiff enough to keep maximum deflections within the gap limits necessary for bony ingrowth in cementless surgery, which should be less than 0.3-0.5mm [Carlsson 1986, 1988]. Therefore it is recommended that the diameter of the milling tool be increased from 3.1mm to ~4mm, which would increase the estimated three minute resection time by ~45 seconds. It is also recommended that a two-fluted cutting tool be used instead of a four-fluted tool, since the latter had a tendency to over or under cut bone (depending on the cutting direction), which could affect frontal and sagittal plane implant alignment.

Chapter 5: Conclusions and Future Work

5.0 Thesis Summary

Achieving precise bone cuts and implant alignment have always been vital to the technique of total knee arthroplasty (TKA), and several clinical studies have noted higher incidences of implant loosing and failure when frontal plane alignment is outside a 3° window [Insall 1985, Moreland 1988, Hsu 1989, Jeffery 1991, Ritter 1994]. Passive computer-assisted TKA systems are being developed with the long-term objective of reducing frontal plane alignment variability to ~1° SD, so that the surgeon can almost always align implants within a 3° window. This is a very challenging task considering the number of sources of variability in the procedure, including registering the hip, knee, and ankle centres, positioning and mounting the cutting guides, manually implementing the bone cuts and cementing the prosthesis into position. In addition, all of these steps have to be performed with due consideration to balancing the soft tissues which support the joint. This thesis is limited to considering the variability due to manually implementing the bone cuts.

In the first of the three studies completed, we measured the alignment accuracy and variability of surgeons implementing a planar bone cut relative to a positioned guide with an oscillating saw. Open and slotted cutting guides were used to evaluate proximal tibial, distal femoral, anterior and posterior femoral resections in the frontal and sagittal planes. Three expert and five training orthopaedic surgeons performed a total of eighty-five resections on 19 cadaveric femurs and tibiae. As a group, surgeons with extensive TKA experience exhibited significantly less variability in the frontal plane (varus/valgus alignment errors) than less experienced surgeons, with respective standard deviations of 0.4° and 0.8° SD. Variability in the sagittal plane was significantly higher (~1.3° SD) than in frontal the frontal plane for both surgeon groups. We also detected a tendency for the saw blade to deflect away from the guide surface in the sagittal plane for cuts guided by open surface guides, resulting in a bias of ~1°. Slotted cutting guides reduced the variability for experienced surgeons and eliminated the bias in the sagittal plane for both experience groups but did not significantly improve frontal plane alignment errors.

This laboratory experiment revealed that manual bone sawing (which is only one of many potential sources of error in TKA) can contribute up to 1.5° SD of variability to frontal plane implant alignment (taking $\sqrt{2}$ × SD at the 95% upper confidence limit to account for the two independent cuts made on either side of the knee joint). In the sagittal plane, bone sawing can

contribute over 2° SD of variability in addition to significant bias effects. These contributions may be even higher in the operating room due to the more taxing surgical conditions and the reduced access, stability, and visibility of the bone. Indeed, several surgeons have noted that it is difficult to constrain the oscillating saw-blade to the guide surface and consistently achieve accurate resections in the clinical setting [Lennox 1988, Laskin 1991, Minns 1992, Mont 1997].

In light of this, we designed a milling technique that gives surgeons better control of the cutting tool, allowing them to physically prevent deviations of the cutting instrument from the resection plane. We evaluated the technique by implementing a total of 50 proximal tibial and distal femoral resections on porcine knees with a specially designed 'open' type of cutting guide. To provide an indication of how sensitive the technique was to surgical experience, expert surgeons and untrained operators were recruited to perform the resections, though none of the operators had any previous experience with this particular technique. Since animal bones were used for this study, we also asked the four operators to perform a total of 35 resections with the conventional sawing technique and open cutting guides, and compared these values to those obtained *in vitro* in chapter two. The effect of surgical experience on sawing variability was evident in the frontal plane, and the untrained operators performed slightly worse than the training surgeon group, and considerably worse than the expert surgeon group (1.0° vs. 0.8° vs. 0.4° SD). Sagittal plane sawing precision was also consistent with the sawing trends found *in vitro*, with a variability of ~1.2° SD and a significant bias of ~1° for all groups.

The milling instrumentation proved effective and significantly reduced the cutting variability for the untrained operators. The milling variability was estimated at 0.32° and 0.68° SD in the frontal and sagittal planes, respectively, with no significant bias in either plane. One drawback to the new technique was that resection time was increased for the novice operators, though it is expected that this will diminish as the surgeon becomes more comfortable with the technique. In addition, many surgeons note that additional time is spent in surgery revising inaccurate bone cuts [Lennox 1988, Minns 1992], so the milling technique may save some time in that respect.

This study indicated that it is possible to achieve sub-degree cutting variability with manual instrumentation even for operators without any surgical expertise. However, this work should only be considered as a pilot study until an evaluation is performed on cadaveric specimens with all relevant soft tissues retained.

To make this tool as clinically useful as possible, it is also important that the optimal cutting speeds, feeds, depths, and tools be determined. Unfortunately, no models exist in the literature for determining optimal resection parameters or tools and these are often arbitrarily selected. To further develop the milling technique, we formulated a model for predicting bone-milling forces with the objectives of minimising tool deflections and optimizing cutting accuracy. The model is based on the specific cutting energy of cortical bone, which we estimated from orthogonal cutting tests reported in the literature. We used both linear and non-linear models of the cutting process, along with corrections for the anisotropy of bone, to estimate the instantaneous cutting forces in milling operations as a function of the cutter orientation and other surgical parameters. In particular, we simulated a milling process in which the cutting tool was fully immersed in the bone and the tool was treated either as rigid or flexible.

For a given set of input parameters, the non-linear force model correlated well with corresponding experimentally acquired milling force data from the literature. The linear model, however, had limited applicability to machining operations that are characterized by very thin chips (i.e. high-speed milling). The results of the study indicate that smaller cutting depths and larger feed rates should be used to minimize the loading on the tool, and Krause [1982] experimentally verified that this strategy results in reduced feed forces and temperature elevations in bovine bone.

For our milling technique, we predict that resection surface errors (estimated by solving for the quasi-static deflection of the slender milling tool in the direction normal to the cutting surface) can be substantially reduced without any increases in resection time by simply optimizing the surgical parameters (i.e. increasing the feed – depth of cut ratio). The optimized resection strategy reduced the total tool deflections by ~50% in the simulations without any predicted increase in estimated resection time. However, even with this optimized resection strategy, the cutting tools simulated were not stiff enough to keep maximum deflections within the gap limits necessary for bony ingrowth in cementless surgery. Therefore, I recommend that the diameter of the milling tool be increased by ~30%, which may increase the resection time by a similar fraction. Alternatively, the cutter could be redesigned so that the cutting teeth do not reduce the stiffness of the tool to the extent seen in this thesis. I also recommend that a two-fluted cutting tool be used instead of a four-fluted tool, since the latter has a tendency to over- or under-cut bone (depending on the cutting direction), which could affect frontal and sagittal plane implant alignment.

I would emphasize that these findings are the results of preliminary tests and the novel milling technique and force prediction model must be validated before they are used clinically. The following section describes what subsequent steps are recommended to continue this work.

5.1 Future Work

- Bone-milling model validation: To validate the orthogonal bone milling model, milling experiments should be undertaken in cortical bone at several operating speeds and feeds with cutters of relatively simple geometry and the force signatures measured for each case. Cutting tools should be rigid (i.e. not slender) with 2 to 4 cutting teeth, each of known geometry angle (preferably with 10° clearance angle and 0° rake angle) and zero degree helix angle (straight flutes). The cutting tests should be performed in such a manner that the generated bone chips are free to escape from the cutting zone and not influence the measured cutting forces. A substantial depth of cut should also be used so that end effects at the tip of the tool are not significant in relation to the measured loads. Alternatively, a slice of bone could be machined so that the tool tip projects from the far side, thereby avoiding end effects entirely. Thick slices of bone or large cutting depths will also reduce the difficulty associated with measuring small force values accurately. In addition, the sampling rate and dynamics of the load cell must also be taken into account when acquiring high-speed force data (i.e. high frequency, low magnitude), as these can considerably affect the measured forces. Once these steps are undertaken we can establish the most suitable milling model for predicting forces, and then build on this to incorporate more complicated effects such as cutter end effects or oblique cutting situations.

- Cutting tool dynamics: Our current technique uses a static assessment to estimate cutter deflection and surface errors, but milling is a dynamic process and ignoring inertial and vibrational phenomena may result in markedly erroneous predictions (for example, under certain conditions the effects of chatter are known to dominate tool deflections in metal milling processes). Therefore, a dynamic analysis of the cutting process must also be undertaken. Vibrational, centripetal and gyroscopic effects should all be incorporated into the model to determine the most stable and optimal tool stiffness and operational conditions. The behaviour of the cutting tool should be investigated at all operating speeds and axial lengths, and in particular near the resonant frequencies of the tool structure.

- Cadaver testing: Finally, a complete and thorough evaluation should be undertaken where the safety and clinical feasibility aspects (as well as the accuracy and variability) of the technique are assessed by qualified TKA surgeons. A representative population of fresh cadaver knees of various sizes must be tested, with incisions made and soft tissues exposed as in a typical procedure. Cuts and recuts should be performed with a positioned guide approximating typical surgical conditions.

In summary, I have demonstrated markedly improved cut accuracy and precision for untrained operators when making bone cuts using a milling tool rather than a conventional bone saw, and we therefore expect that a milling technique will be a necessary component in future high-accuracy computer-assisted surgical systems.

References

1. Altintas Y. Manufacturing Automation: metal cutting mechanics, machine tool vibrations, and CNC design. *Cambridge University Press*. Cambridge UK. 2000
2. Ark TW, Thacker JG. McGregor W. Rodeheaver GT. Edlich RF. Innovations in oscillating bone saw blades. *Journal of Long-Term Effects of Medical Implants.* 7(3):279-268, 1997
3. Armarego EJA, Brown RH. On the size effect in metal cutting. *Int. J. Prod. Res.* (1):75-99, 1962
4. Armarego EJA, Brown RH. The Machining of Metals. *Prentice-Hall International*. New Jersey. 1969.
5. Backer, W.R. Marshall, E.R. Shaw MC. The size effect in metal cutting. *Trans. ASME* 74: 61-71, 1952
6. Bai B. Baez J. Testa N. Kummer FJ. Effect of posterior cut angle on tibial component loading. *J Arthroplasty*. 15:916, 2000
7. Brugioni DJ. Andriacchi TP. Galante JO. A functional and radiographic analysis of the total condylar knee arthroplasty. *J Arthroplasty*. 5:173, 1990
8. Brys DA. Lombardi AV Jr. Mallory TH. Vaughn BK. A comparison of intramedullary and extramedullary alignment systems for tibial component placement in total knee arthroplasty. *Clin Orthop* 263:175, 1991
9. Budak E, Altintas Y. Peripheral milling conditions for improved for dimensional accuracy. *Int. J. Mach. Tools Manufac.* 34(7): 907-918, 1994
10. Carlsson L. Rostlund T. Albrektsson B. Albrektsson T. Branemark PI. Osseointegration of titanium implants. *Acta Orthopaedica Scandinavica.* 57(4):285-9, 1986
11. Carlsson L, Rostlund T, Albrektsson B, Albrektsson T. Implant fixation improved by close fit. Cylindrical implant – bone interface studied in rabbits. *Acta Orthopedica Scandinavica.* 59: 272-275, 1988
12. Coller JP. Mayor MB. Surprenant VA. Dauphinais LA Surprenant HP. Jensen RE. Biological Ingrowth of Porous-Coated Knee Prostheses. in Goldberg VM (ed): Controversies of total knee arthroplasty. *Raven Press* N.Y. chap 10, 1991
13. Cooke, T.D., Saunders, G., Siu, D., Yoshioka, Y., & Wevers, H. Universal bone cutting device for precision knee replacement arthroplasty and osteotomy. *J. Biomed Eng,* 7(1), 45-50, 1985
14. Coull R. Bankes MJK. Rossouw DJ. Evaluation of tibial component angles in 79 consecutive total knee arthroplasties. *The Knee.* 6:235-237, 1999
15. Davies BL, Harris SJ Lin WJ, Hibberd, Middleton R, Cobb JC. Active compliance in robotic surgery – the use of force control as a dynamic constraint. *Proc Instn Mech Engrs.* 211H, 285292, 1997
16. Delp SL. Stulberg SD. Davies B. Picard F. Leitner F. Computer assisted knee replacement. *Clin Orthop* 354:49, 1998
17. Devor RE. Sutherland JW. Kline WA. Control of surface error in end milling. *11th North American Manufacturing Research Conference Proceedings*. May:356, 1983
18. Dippon J. Ren H. Amara FB. Altintas Y. Othogonal cutting mechanics of medium density fiberboards. *Forest Products Journal.* 50(7):25-30, 2000
19. Dorr LD. Boiardo RA. Technical considerations in total knee arthroplasty. *Clin Orthop.* 205:5, 1986

20. Ewald FC. Jacobs MA. Walker PS. Thomas WH. Scott RD. Sledge CB. Accuracy of total knee replacement component position and relation to bone-cement interface reaction. P. 117. In Dorr LD (ed): The Knee. Papers of the First Scientific Meeting of The Knee Society. *University Park Press*; Baltimore, 1985

21. Fadda M. Marcacci M. Toksvig-Larsen S. Wang T. Meneghello R. Improving Accuracy of Bone Resections Using Robotics Tool Holder and a High Speed Milling Cutting Tool. *J. Medical Eng. & Tech.* 22(6):280-4, 1998

22. Feng HY. Menq CH. A Flexible ball-end milling system for cutting force and machining error prediction. *Journal of Manufacturing Science and Engineering.* 118:461-469. 1996

23. Giraud JY. Villemin S. Darmana R. Cahuzac JP. Autefage A. Morucci JP. Bone cutting. *Clin. Phys. Physiol. Meas.* 12(1):1-19, 1991

24. Hankinson. Investigation of crushing strength of spruce at varying angles of grain. *U.S. Air Service* Information Circular No. 259, 1921

25. Hofmann AA. Bachus KN. Wyatt RW. Effect of the tibial cut on subsidence following total knee arthroplasty. *Clin Orthop* 269:63, 1991

26. Hsu HP. Garg A. Walker PS. Spector M. Ewald FC. Effect of knee component alignment on tibial load distribution with clinical correlation. *Clin Orthop* 248:135, 1989

27. Hungerford DS. Kenna RV. Krackow KA. The porous-coated anatomic total knee. *Orthop Clin North Am* 13:103, 1982

28. Hungerford DS. Krackow KA. Kenna RV. Alignment in total knee arthroplasty. p. 9. In Dorr LD (ed): The Knee. Papers of the First Scientific Meeting of The Knee Society. *University Park Press*, Baltimore, 1985

29. Inkpen KB. Precision and accuracy in computer-assisted total knee replacement. Master's Thesis. *University of British Columbia.* 1999

30. Inkpen KB, Hodgson AJ, Plaskos C, Shute C, McGraw RW: Accuracy and Repeatability of Bone Cutting and Ankle Digitization in Computer-Assisted Total Knee Replacements. In: Delp SL (ed): Medical Imaging and Computer Assisted Intervention (MICCAI'00). Lec. Notes Comp. Sc.V1935. *Springer-Verlag.* p.1163, 2000

31. Insall JN: Technique of total knee replacement. p. 23. In Dorr LD (ed): The Knee. Papers of the First Scientific Meeting of The Knee Society. *University Park Press*, Baltimore, 1985

32. Jacobs CH. The Machining Characteristics of Bovine Bone. Master's Thesis. *University of Vermont.* 1973

33. Jacobs CH, Pope MH, Berry JT, Hoaglund F. A study of the bone machining process – Orthogonal cutting. *J. Biomechanics.* (7):131-136, 1974

34. Jacobs CH, Pope MH, Berry JT, Hoaglund F. A study of the bone machining process – Drilling. *J. Biomechanics.* (9):343-349, 1976

35. Jeffery RS. Morris RW: Coronal alignment after total knee replacement. *J Bone Joint Surg Br* 73:709, 1991

36. Jenny JY. Boeri C. [Navigated implantation of total knee endoprostheses--a comparative study with conventional instrumentation]. [German] *Zeitschrift fur Orthopadie und Ihre Grenzgebiete.* 139(2):117-9, 2001

37. Kagan A II: Mechanical causes of loosening in knee joint replacement. *J Biomech* 10:387, 1977

38. Kelly J. The mechanical and thermal effects of a high speed rotary burr on bovine bone. M.S. Report. *Clemson University* 1976.

39. King RI. Handbook of high speed machining technology. *Chapman and Hall.* New York N.Y. 1985

40. Kline WA. DeVor RE. Shareef JR. The prediction of surface accuracy in end milling. *ASME Journal of Engineering for Industry*. 104:272, 1982

41. Krakow KA, Hungerford DS: Sequence of reconstruction and alignment in total knee arthroplasty. in Goldberg VM (ed): Controversies of total knee arthroplasty. *Raven Press* N.Y. chap 20, 1991

42. Krackow, KA. Bayers-Thering M. Phillips MJ. Mihalko WM. A new technique for determining proper mechanical axis alignment during total knee arthroplasty: progress toward computer-assisted TKA. *Orthopedics*. 22(7), 698-702. 1999

43. Krause WR, Bradbury DW, Kelly JE, Lunceford EM. Temperature elevations in orthopaedic cutting operations. *J. Biomechanics*. 15(4):267-275, 1982

44. Krause WR. Orthogonal Bone Cutting: Saw design and Operating Characteristics. *J. Biomech. Eng.* 109:263-271, 1987

45. Krause WR. Bioengineering Consultants Ltd. Personal telephone communication. Feb 06, 2002

46. Laskin RS: Bone Resection Techniques in Total Knee Replacement. p. 55-74. In Laskin RS (ed.): Total Knee Replacement. *Springer-Verlag* London Limited, 1991

47. Leitner, F., Picard, F., Minfelde, R., Schulz, H.J., Cinquin, P., & Saragaglia, D. Computer Assisted Knee Surgical Total Replacement. In J. Troccaz, E. Grimson, & R. Mosges (Eds.), CVRMed - MRCAS Proceedings '97: Grenoble, France: *Springer-Verlag*. 1997

48. Lennox DW. Cohn BT. Eschenroeder HC Jr: The effects of inaccurate bone cuts on femoral component position in total knee arthroplasty. *Orthopedics* 11:257, 1988

49. Lotke, P.A., Ecker, M.L. Influence of positioning of prosthesis in total knee replacement. *J.Bone Joint Surg.* 59A(1), 77-79. 1977

50. Lui D. Weiner S, Wagner HD. Anisotropic mechanical properties of lamellar bone using miniature cantilever bending specimens. *J Biomech.* 32:647-654, 1999

51. Marcacci M. Dario P. Fadda M. Marcenaro G. Martelli S. Computer-Assisted Knee Arthroplasty. In Taylor RH et al (ed): Computer-integrated surgery: technology and clinical applications. Cambridge, Mass.: *MIT Press.* p41. 1996

52. Mahdi M. Zhang L. A finite element model for the orthogonal cutting of fiber-reinforced composite materials. *Journal of Materials Processing Technology*. 113:373-377, 2001

53. Malvisi A. Vendruscolo P. Morici F. Martelli S. Marcacci M. Milling versus Sawing: Comparison of Temperature Elevation and Clinical Performance During Bone Cutting. In: Delp SL (ed): Medical Imaging and Computer Assisted Intervention. *Springer-Verlag*. p1238, 2000

54. Matthews LS and Hirsch C. Temperatures Measured in Human Cortical Bone when Drilling. *Journal of Bone and Joint Surgery*. 54A(2):297-308, 1972

55. Martellotti ME. An Analysis of the milling Process. *Trans. ASME* 63:677-700, 1941

56. Martellotti ME. An Analysis of the milling Process, Part 2-Down milling. *Trans. ASME* 67:233-251, 1945.

57. Matsen FA. Garbini JL. Sidles JA. Pratt B. Baumgarten D. Kaiura R. Robot assistance in orthopaedic surgery: a proof of principle using distal femoral arthroplasty. *Clinical Orthopaedics and Related Research.* 296:178-186, 1993.

58. McKenzie WM. Fundamental Analysis of the Wood-Cutting Process. *University of Michigan.* Ann Arbor, 1961

59. Mielke RK. Clemens U. Jens JH. Kershally S. [Navigation in knee endoprosthesis implantation--preliminary experiences and prospective comparative study with conventional implantation technique]. [German] *Zeitschrift fur Orthopadie und Ihre Grenzgebiete.* 139(2):109-16, 2001

60. Minns RJ. Surgical instrument design for the accurate cutting of bone for implant fixation. Clinical Materials 10:207, 1992

61. Moctezuma JL. Schuster D. Gosse F. Schulz HJ. A new oscillating saw for robotic aided surgery. *Proc Instn Mech Engrs.* 211:301, 1997

62. Mont MA, Urquhart MA, Hungerford DS, Krackow KA. Intramedullary goniometer can improve alignment in knee arthroplasty surgery. *J Arthroplasty* 12:332, 1997

63. Moreland JR: Mechanisms of failure in total knee arthroplasty. *Clin Orthop* 226:49, 1988

64. Nogler N. Wimmer C. Lass-Florl C. Mayr E. Bach C. Krismer M. Is there a contamination risk for the surgical team through ROBODOC's high-speed bone cutter? Abstracts from CAOS. *Computer Aided Surgery* 4:223, 1999

65. Nuno-Siebrecht N, Tanzer M, Bobyn JD. Potential errors in axial alignment using intramedullary instrumentation for total knee arthroplasty. *J Arthroplasty* 15:228, 2000

66. Otani T. Whiteside LA. White SE: Cutting errors in preparation of femoral components in total knee arthroplasty. *J Arthroplasty.* 8:503, 1993

67. Oxely PLB. Mechanics of Machining: an analytical approach to assessing machinability. Ellis Horwood Ltd. Chichester England. 1989

68. Pal S. Bhadra N. Dutta S. Orthogonal cutting of bone. *Biomater. Med. Devices Artif. Organs* 14:124, 1986.

69. Piazza SJ. Delp SL. Stulberg SD: Posterior tilting of the tibial component decreases femoral rollback in posterior-substituting knee replacement: a computer simulation study. *J Orthop Res* 16:264, 1998

70. Plaskos C. Hodgson AJ. Inkpen KB. McGraw RW. Bone cutting errors in total knee arthroplasty. *J Arthroplasty.* 2002. In press.

71. Puw HY, Hocheng H. Milling force prediction for fiber-reinforced thermoplastics. *Proc. 114th ASME Winter Annual meeting, Machining of Advanced Composites.* 73-88, 1993

72. Puw HY, Hocheng H. Anisotropic model of milling force prediction for fiber-reinforced plastics. *Eng. Sys. Des. Analysis. ASME* 75(3):11-20, 1996

73. Rand JA, Bryan RS. Alignment in porous coated anatomic total knee arthroplasty. p. 111. In Dorr LD (ed): The Knee. Papers of the First Scientific Meeting of The Knee Society. *University Park Press*, Baltimore, 1985

74. Reilly D.T. Burstein A.H. The elastic and ultimate properties of compact bone tissue. *J Biomech.* (8):393-505, 1975

75. Richards F. State-of-the-Art Electric Handpiece for Dental Surgeons. *Medical Equipment Designer.* March 1999.

76. Ritter MA. Faris PM. Keating EM. Meding JB. Postoperative alignment of total knee replacement. Its effect on survival. *Clin Orthop* 299:153, 1994

77. Saha S, Pal S, Albright JA. Surgical Drilling: Design and Performance of an Improved Drill. *Journal of Biomechanical Engineering.* (104):245-252, 1982

78. Saragaglia D. Picard F. Chaussard C. Montbarbon E. Leitner F. Cinquin P. [Computer-assisted knee arthroplasty: comparison with a conventional procedure. Results of 50 cases in a prospective randomized study]. [French] *Rev. Chir. Orthop. Reparatrice Appar. Mot.* 87:18, 2001

79. Seki T. Omori G. Koga Y. Suzuki Y. Ishii Y. Takahashi HE. Is bone density in the distal femur affected by use of cement and by femoral component design in total knee arthroplasty?. *Journal of Orthopaedic Science.* 4(3):180-6, 1999

80. Sutherland JW. DeVor RE. An improved method for cutting force and surface error prediction in flexible milling systems. *J Eng. Ind.* 108:269-79, 1986

81. Teter KE. Bregman D. Colwell CW Jr. The efficacy of intramedullary femoral alignment in total knee replacement. *Clin Orthop.* 321:117, 1995

82. Tlusty J. MacNeil P. Dynamics of Cutting Forces in End Milling. *Annals of the CIRP*, 24(1):21-5, 1975

83. Toksvig-Larsen S. Ryd L: Temperature Elevation During Knee Arthoplasty. *Acta Orthop Scan.* 60:4 1989

84. Toksvig-Larsen S. Ryd L. Surface characteristics following tibial preparation during total knee arthroplasty. *J Arthroplasty* 9:63, 1994a

85. Toksvig-Larsen S. Kroon PO. Ryd L. Improved bone cutting using a semirotating saw – A cadaver study of the cut surface on tibial condyles. *Acta Orthop Scand.* 65(4):412-414, 1994b

86. Thomson EG Lapsley JT. Grassi RC. Deformation Work Absorbed by the workpiece during metal cutting. *Trans. Amer. Soc. Mech. Engrs.* 75:591, 1953

87. Van Ham G. Denis K. Vander Sloten J. Van Audekercke R. Van der Perre G. De Schutter J. Aertbelien E. Demey S. Bellemans J: Machining and accuracy studies for a tibial knee implant using a force-controlled robot. *Computer Aided Surgery.* 3(3):123-33, 1998

88. Wagner HD. Weiner S. On the relationship between the microstructure of bone and its mechanical stiffness. *J. Biomech.* 25(11):1311-1320, 1992

89. Walker PS. Garg A. Range of motion in total knee arthroplasty. A computer analysis. *Clin Orthop* 262:227, 1991

90. Wevers HW. Espin E. Cooke TD. Orthopedic sawblades. A case study. *J Arthroplasty.* 2:43, 1987

91. Whiteside LA. Amador DD. The effect of posterior tibial slope on knee stability after Ortholoc total knee arthroplasty. *J Arthroplasty* 3 Suppl:S51-57, 1988

92. Wiggins KL. Machining of Bone. PhD Thesis. *University of Texas.* Aug. 1974

93. Wiggins KL, Malkin S. Drilling of Bone. *J. Biomechanics.* 1976 (9)553-559.

94. Wiggins KL, Malkin S. Orthogonal machining of bone. *J. Biomech. Eng* 1978 (100)122-130.

95. Windsor RE, Scuderi GR, Moran MC, Insall JN: Mechanisms of failure of the femoral and tibial components in total knee arthroplasty. *Clin Orthop* 248:15, 1989

96. Ziv V. Wagner HD. Weiner S. Microstructure-microhardness relations in parallel-fibered and lamellar bone. *Bone.* 18(5):417-28, 1996

Appendix A: Determining the Resonant Frequencies and Optimal Operational Speeds for Bone Milling

A.0 Introduction

Dynamic loading of a cutting tool will produce a dynamic response and vibration of the tool, resulting in undesired cutter motion and dimensional errors from the cut surface or resection plane (cutting errors). The cyclic cutting loads exerted on the tool tip are a result of the varying chip thickness encountered at the rotating cutter tooth. The period or frequency of the cutting force is a function of the tools rotational velocity and the number of cutting teeth. Knowledge of the tools dynamic response over a range of operating frequencies is important to the surgeon because they can control and adjust the operating speed of the tool while cutting in surgery.

Structural resonance is characterized by relatively low dynamic stiffness which can lead to significantly increased dynamic response and vibration of structural elements. Quantitative knowledge of the frequencies, stiffness, damping, and mode shapes associated with structural resonance facilitates understanding of how forces are generated and transmitted throughout the mechanical system and can allow evaluation of vibration control modifications and treatments. Modal analysis techniques enable us to determine these dynamic characteristics of the system over a range of operating frequencies, including the resonance frequency. The dynamic characteristics can then be utilised to evaluate the stability and performance of the system over a range of cutting conditions.

In this chapter, the dynamic characteristics of a cutting tool are investigated with three different techniques: 1) a continuous or distributed parameter vibration model, 2) a finite element model 3) by experimental modal analysis. Transverse or flexural vibrations of the cutter are considered (as opposed to longitudinal or torsional vibrations) since motion in this direction will correspond to out-of-plane deviations of the tool and cutting errors on the prepared bone surface. In this study, the cutter is considered as a simple circular elastic shaft with no cutting teeth.

A.1 Theory

A.1.1 Distributed Parameter Model

The distributed parameter or continuous model considers the mass and elasticity of the object to be distributed throughout the structure as a series of infinitely small elements, where each of these of these infinite number of elements move relative to each other in a continuous fashion when the structure vibrates.

A.1.1.1 Natural Frequencies and Mode Shapes

At resonance, the structure vibrates at its natural frequency (ω_n). Since the number of natural frequencies of vibration is equal to its number of degrees of freedom (DOF) for that system, a continuous system will have an infinite number of natural frequencies. With each natural frequency is an associated natural mode shape that is assumed by the system during free vibration at that frequency. Although the complete solution to the free vibration problem requires determination of all natural frequencies and associated mode shapes, in practice it is often necessary to know only a few or even the first of the natural frequencies.

When any linear system (where the elastic restoring force is proportional to the deflection) executes free vibration in a single natural mode, each element of the system (except those at the supports and nodes) executes simple harmonic motion about its equilibrium position. All possible free vibration of any linear system is made up of superimposed vibrations in the normal modes at the corresponding natural frequencies. The total motion at any point of the system is the sum of the motions resulting from the vibration in the respective modes. There are always nodal (stationary) points in each of the normal modes of vibration of any system. For the fundamental mode, which corresponds to the lowest natural frequency, the supported or fixed points of the system usually are the only nodal points; for other modes, there are additional nodes.

A.1.1.2 Solution of Natural Frequencies and Mode Shapes

The classical method of solving any vibration problem is to set up one or more equations of motion (Newton's second law). For a continuous system partial differential equations must be solved (ordinary differential equations are obtained for discretized systems having a finite number of DOF). A detailed derivation of the governing equations of motion, along with the solution for the cutting model is presented.

A.1.1.3 Modelling the Tool

We can model the structure as an elastic circular shaft with simple built-in and pin supports at the tool chuck and bearing attachments, respectively (figure A.1a). The built-in support at the chuck can sustain moments and loads while the pin support at the attachment bearing prevents lateral displacements only (figure A.1b). The total length of the cutter, measured from the chuck end, is constant and equal to the supported length plus the free length ($L_t = L_s + L_f$).

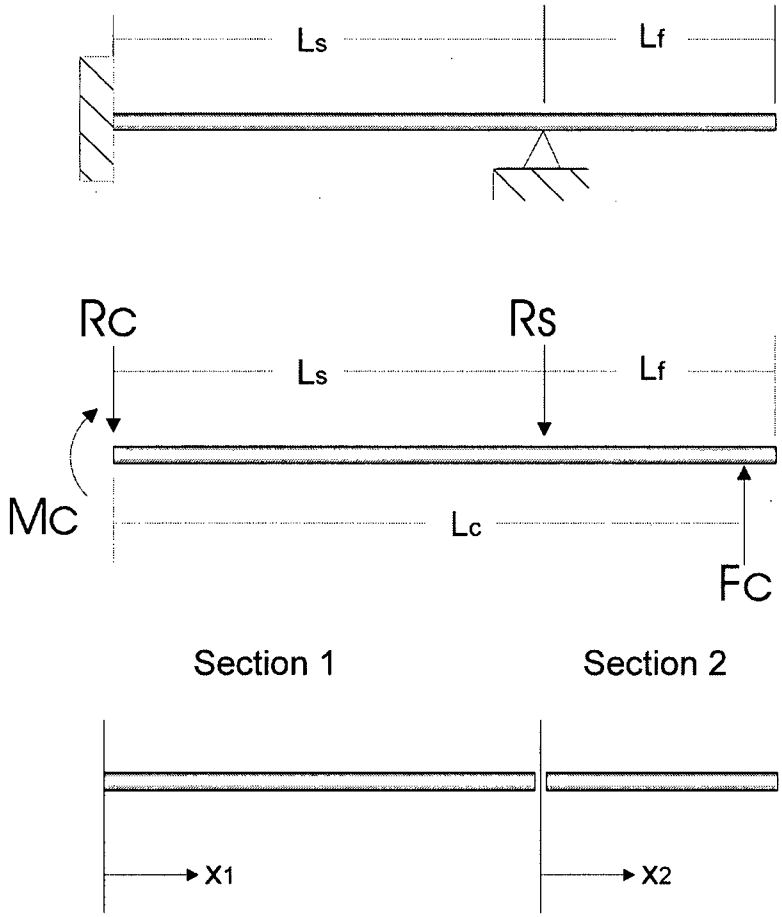

Figure A.1abc. Tool Model: cantilevered at the tool chuck and pin supported at the tool attachment bearing.

For a continuous beam with multiple supports, the section between each pair of supports (and between the support and the free end) can be considered as a separate beam with its origin at the left support section (figure A.1c).

The solution of this model is found be imposing the following boundary conditions at the ends of each beam section:

1. zero deflection (y = 0) and slope (y' = 0) at the chuck ($x_1 = 0$)

2. continuity of deflection (y), slope (y'), moment (y''), and shear (y''') at the point joining sections 1 and 2 ($x_1 = L_s$, $x_2 = 0$)

3. zero moment (y'' = 0) and shear (y''' = 0) at the free end ($x_2 = L_f$)

Substituting these eight boundary conditions into the assumed system solution gives eight equations which can be reduced to a system of five equations of the form $[A]_{5x5}[x]_{5x1} = [0]_{5x1}$, where [x] is a vector of constants to be determined, and [A] is a function of the natural frequency, stiffness, geometry and mass of the beam. Setting the determinate of [A] to zero ($|A|=0$) gives the characteristic equation of the system. If the material and geometric properties of the beam are known, the beam's natural frequencies of vibration can be identified from the roots of this characteristic equation.

A.1.1.4 Equations of Motion for Slender Beams

For a slender beam or shaft (where the diameter of the shaft is small in comparison with its length) the effects of shear deformation and rotational inertia (about the axis perpendicular to the axis of the shaft, not the spinning of the shaft itself) can be neglected. The curvature at each section of the beam can therefore be related solely to the bending moment at that section:

$$EI(x)\frac{\partial^2 y}{\partial x^2} = M(x,t) \tag{A.1}$$

where E is Young's elastic modulus of the beam and $I(x)$ is the cross-sectional area moment of inertia. Equation A.1 is valid for small deflections only, and for beams that have a high slender ratio since the effects of shear deflection and rotation of the cross-sections are neglected.

A model of bending vibration can then be derived from examining the forces on an infinitesimal element of the beam. By summing the shear forces on a single beam element ($\delta V/\delta x$) and equating them to the product of the mass of the element ($S\rho\delta x$, S = cross-sectional area, ρ = density) and the acceleration ($\delta^2 y/\delta t^2$) in the lateral direction:

$$\frac{\partial V}{\partial x} = -S\rho\frac{\partial^2 y}{\partial t^2} \tag{A.2}$$

If moments are taken about a point on the beam, $V = (\delta M/\delta x)$. Other terms containing differentials of higher order can be neglected. Substituting this into Equation A.2 gives $-\delta^2 M/\delta^2 x = S\rho^*(\delta^2 y/\delta^2 t)$. Substituting Equation A.1 gives:

$$-\frac{\partial^2}{\partial x^2}\left(EI\frac{\partial^2 y}{\partial x^2}\right) = S\rho\frac{\partial^2 y}{\partial t^2} \tag{A.3}$$

This is the basic equation for the lateral vibration of beams.

A.1.1.5 Solution for a Beam of Constant Cross-Section

The solution of equation A.3, if *EI* is constant, is of the form $y = X(x)\,[\cos(\omega_n t + \phi)]$, where X is a function of x only. Substituting into Equation A.3 and differentiating,

$$X''''(x) = \frac{\omega_n S\rho}{EI}X(x)$$

if we let:

$$\kappa^4 = \frac{\omega_n{}^2 S\rho}{EI} \tag{A.4}$$

then:

$$X''''(x) = \kappa^4 X(x) \tag{A.5}$$

where X is any function whose fourth derivative is equal to a constant multiplied by the function itself. One suitable function is:

$$\begin{aligned} X = {} & A(\cos\kappa x + \cosh\kappa x) + B(\cos\kappa x - \cosh\kappa x) \\ & + C(\sin\kappa x + \sinh\kappa x) + D(\sin\kappa x - \sinh\kappa x) \end{aligned} \tag{A.6}$$

For beams having various support conditions (i.e. deflection X, slope X', moment X'', shear X''') the constants (A-D) can be found from the boundary conditions.

$$\begin{aligned} X' = {} & \kappa[A(-\sin\kappa x + \sinh\kappa x) + B(-\sin\kappa x - \sinh\kappa x) \\ & + C(\cos\kappa x + \cosh\kappa x) + D(\cos\kappa x - \cosh\kappa x)] \end{aligned} \tag{A.7}$$

$$\begin{aligned} X'' = {} & \kappa^2[A(-\cos\kappa x + \cosh\kappa x) + B(-\cos\kappa x - \cosh\kappa x) \\ & + C(-\sin\kappa x + \sinh\kappa x) + D(-\sin\kappa x - \sinh\kappa x)] \end{aligned} \tag{A.8}$$

$$\begin{aligned} X''' = {} & \kappa^3[A(\sin\kappa x + \sinh\kappa x) + B(\sin\kappa x - \sinh\kappa x) \\ & + C(-\cos\kappa x + \cosh\kappa x) + D(-\cos\kappa x - \cosh\kappa x)] \end{aligned} \tag{A.9}$$

For a continuous beam with multiple supports, the section between each pair of supports can be considered as a separate beam with its origin at the left support section (figure A.1c). Since the deflection is zero at the origin of each section ($X_{1,2}(0) = 0$, therefore $A_{1,2} = 0$), Eqn A.6 reduces to:

$$X_{1,2} = B_{1,2}(\cos \kappa x - \cosh \kappa x) + C_{1,2}(\sin \kappa x + \sinh \kappa x) + D_{1,2}(\sin \kappa x - \sinh \kappa x)$$

for sections 1 and 2 of the beam.

The boundary conditions for each beam section are:

Beam Section	**Location Along Beam**	**Support Conditions**
1	$x_1 = 0$	$X_1(0) = 0$ $X_1'(0) = 0$
1	$x_1 = L_s$	$X_1(L_s) = 0$ $X_1'(L_s) = X_2'(0)$ $X_1''(L_s) = X_2''(0)$ $X_1'''(L_s) = X_2'''(0)$
2	$x_2 = (0)$	$X_2(0) = 0$ $X_2'(0) = X_1'(L_s)$ $X_2''(0) = X_1''(L_s)$ $X_2'''(0) = X_1'''(L_s)$
2	$x_2 = (L_t - L_s) = L_f$	$X_2''(L_f) = 0$ $X_2'''(L_f) = 0$

A.1.1.6 Determination of Constants

The boundary conditions at $x_1 = 0$ ($X_1 = X_1' = 0$) require that $A_1 = 0$ and $C_1 = 0$.

The boundary condition at $x_2 = 0$ ($X_2(0) = 0$) requires $A_2 = 0$.

$x_1 = L_s$	$X_1(L_s) = 0$	$B_1(\cos \kappa L_s - \cosh \kappa L_s) + D_1(\sin \kappa L_s - \sinh \kappa L_s) = 0$
$x_1 = L_s$	$X_1'(L_s) = X_2'(0)$	$B_1(-\sin \kappa L_s - \sinh \kappa L_s) + D_1(\cos \kappa L_s - \cosh \kappa L_s) = 2 C_2$
$x_1 = L_s$	$X_1''(L_s) = X_2''(0)$	$B_1(-\cos \kappa L_s - \cosh \kappa L_s) + D_1(-\sin \kappa L_s - \sinh \kappa L_s) = -2 B_2$

$x_2 = L_f \qquad X_2''(L_f) = 0 \qquad B_2(-\cos \kappa L_f - \cosh \kappa L_f) + C_2(-\sin \kappa L_f + \sinh \kappa L_f) + D_2(-\sin \kappa L_f - \sinh \kappa L_f) = 0$

$x_2 = L_f \qquad X_2'''(L_f) = 0 \qquad B_2(\sin \kappa L_f - \sinh \kappa L_f) + C_2(-\cos \kappa L_f + \cosh \kappa L_f) + D_2(-\cos \kappa L_f - \cosh \kappa L_f) = 0$

Rearranging the equations in the form Ax = 0, where [x] is the vector of constants, [0] is the zero vector, and [A] is a 5x5 matrix that is only a function of κ

[A]					x	[x]	=	[0]
$\cos\kappa L_s - \cosh\kappa L_s$	$\sin\kappa L_s - \sinh\kappa L_s$	0	0	0		B_1		0
$-\sin\kappa L_s - \sinh\kappa L_s$	$\cos\kappa L_s - \cosh\kappa L_s$	0	-2	0		D_1		0
$-\cos\kappa L_s - \cosh\kappa L_s$	$-\sin\kappa L_s - \sinh\kappa L_s$	2	0	0	x	B_2	=	0
0	0	$-\cos\kappa L_f - \cosh\kappa L_f$	$-\sin\kappa L_f + \sinh\kappa L_f$	$-\sin\kappa L_f - \sinh\kappa L_f$		C_2		0
0	0	$\sin\kappa L_f - \sinh\kappa L_f$	$-\cos\kappa L_f + \cosh\kappa L_f$	$-\cos\kappa L_f - \cosh\kappa L_f$		D_2		0

We can solve for κ by setting the determinant of A to zero. The natural frequencies can then be determined by solving for ω_n in Equation A.4

$$\omega_n = \kappa^2 \sqrt{\frac{EI}{S\rho}}$$

A.1.2 Finite Element Model

The finite element model is constructed from a series of ten nodal points equally distributed along the length of the structure and connected by nine beam elements. Each beam element has a constant cross-section, stiffness, and density. Constraints are applied at the chuck (node # 1: y=0, dy/dx = 0) and attachment bearing (node # 5,6,7: y=0). The two attachment configurations (plus one intermediate configuration) are simulated by decreasing the node # of the applied constraint (fig #). The model was implemented on the ANSYS Finite Element Solver software.

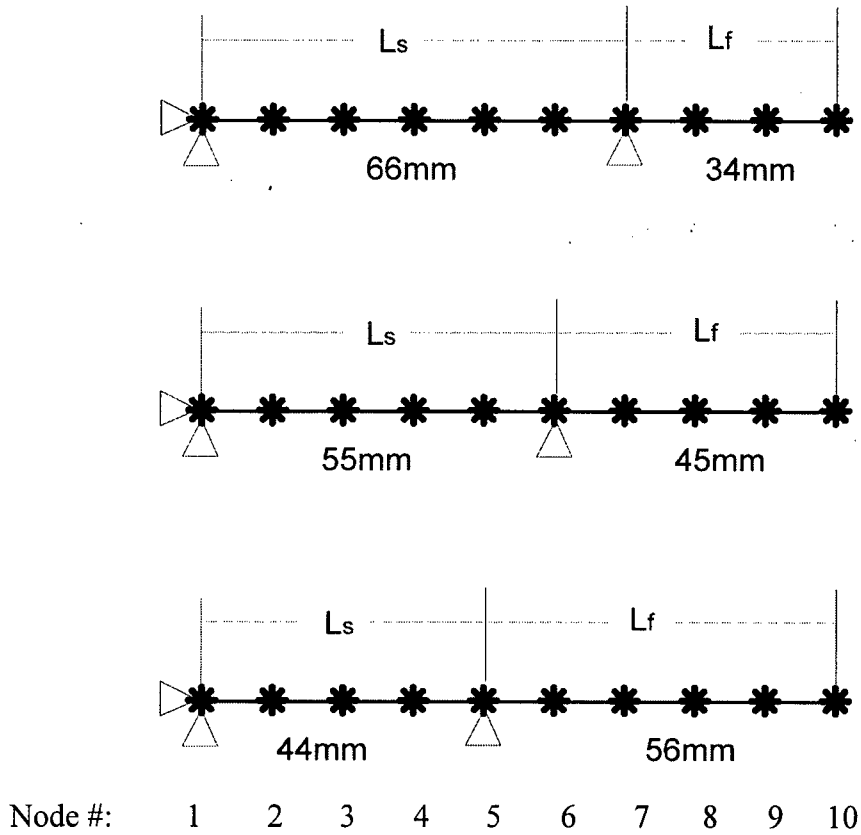

Figure A.2. Finite Element Model.

A.1.3 Experimental Modal Analysis: Impulse Response Technique

Modal analysis tests enable the dynamic characteristics of complex structures to be determined experimentally and are useful for verifying theoretical models of the structure. In the impulse response technique, transient excitation of the structure is produced by approximating an impulse force input to the system through the use of an impactor or instrumented hammer (figure A.3), and the response of the structure is measured. In contrast to other experimental modal analysis techniques, impact testing is one of the simplest and fastest methods for exciting the structure into vibration and obtaining good frequency response estimates. However, the technique does place greater demand on the analysis phase of the measurement process as it can be particularly susceptible to measurement noise [Halvorsen 1977].

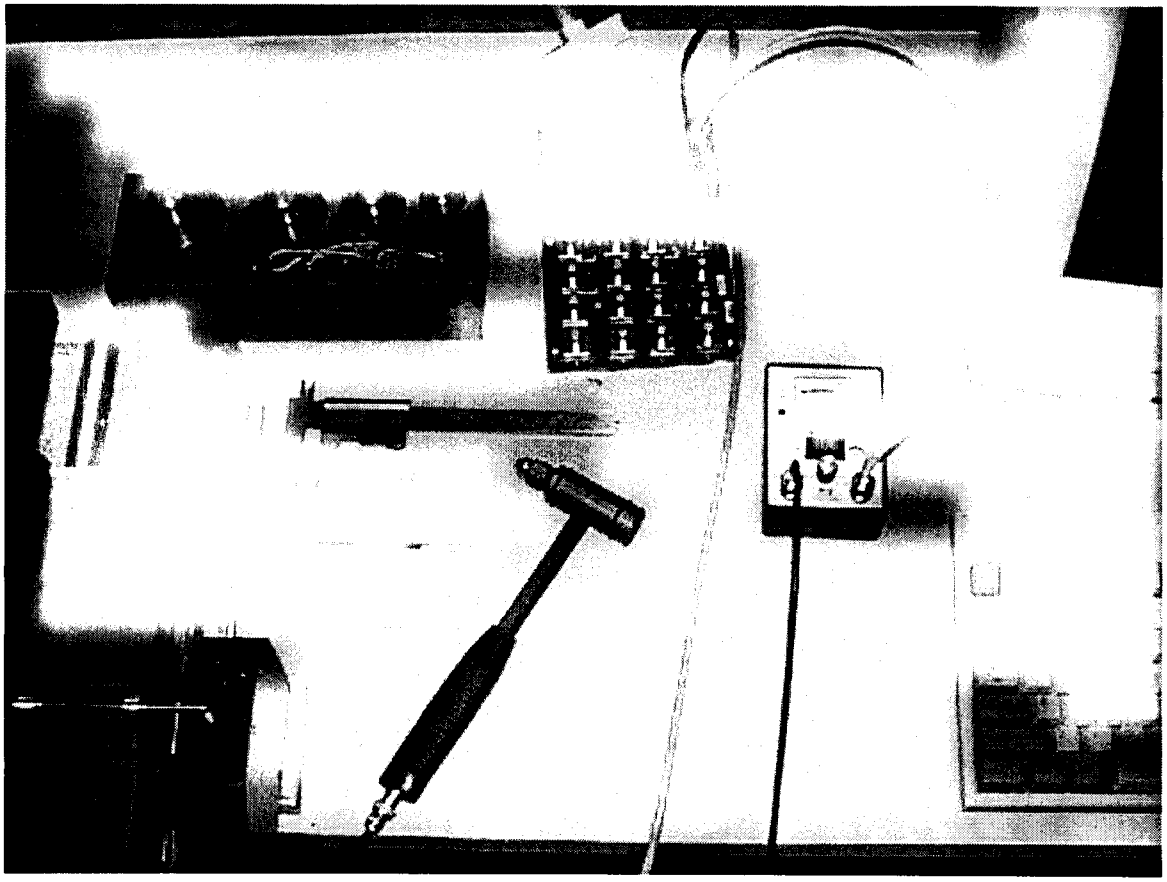

Figure A.3 Measurement set-up for impact tests. Laser displacement sensor and impact hammer instrumented with force sensor.

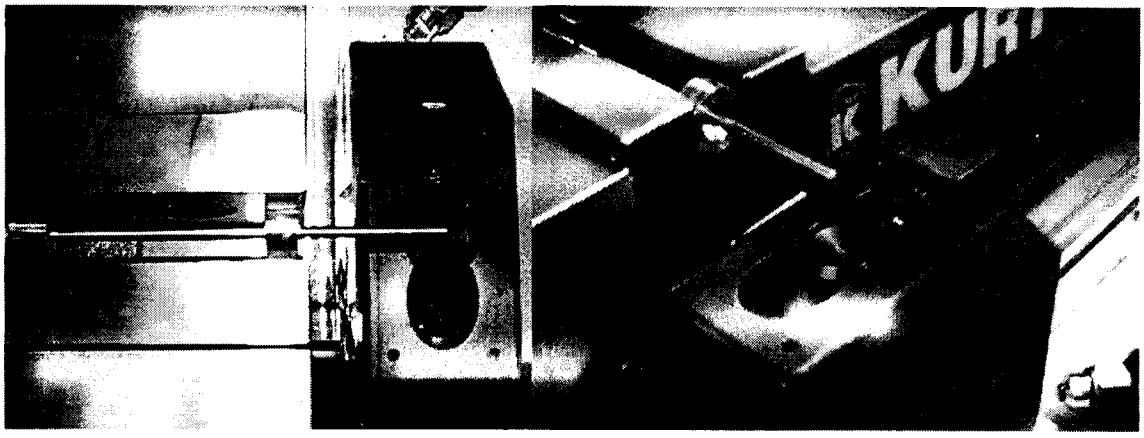

Figure A.4 Tool supported with cantilever and point supports machined from aluminium.

A.1.3.1 Frequency Response Function

The goal of modal testing is to measure the frequency response function (FRF) of the structure. For a single-input/single-output system, the FRF ($\Phi(j\omega)$) is simply the ratio of the Fourier transforms of the system output (or time response, $x(t)$) to the system input (or excitation, $f(t)$, figure A.5):

$$\Phi(j\omega) = X(j\omega)/F(j\omega) \tag{A.10}$$

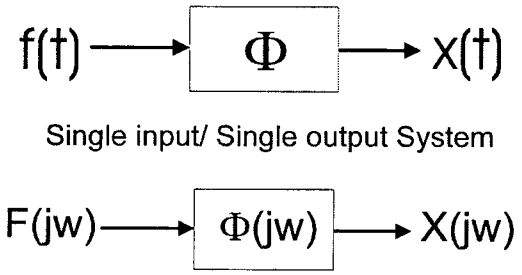

Figure A.5. Frequency Response Function (FRF).

From Equation A.10 we can see that the FRF is only valid at frequencies where the input force is non-zero.

Because the FRF is a complex function, it can be displayed in terms of its magnitude and phase, or its real and imaginary parts. Both sets of plots for a single DOF system are presented in figure A.4 and A.5 as function of the frequency ratio of the input force ($r = \omega/\omega_n$). The amplitude of the vibration of the structure in response to an applied unit load of varying frequency is illustrated in the magnitude plot (figure A.6a). As the frequency of the input force tends to zero ($\omega \rightarrow 0$), the magnitude of the FRF tends to the static flexibility of the structure (1/k). As the excitation frequency approaches the natural frequency ω_n ($r = 1$), the magnitude of the vibrations is at a maximum and the structure is at resonance. The natural frequency of the structure can be determined from the zero-crossing of the real part of the FRF.

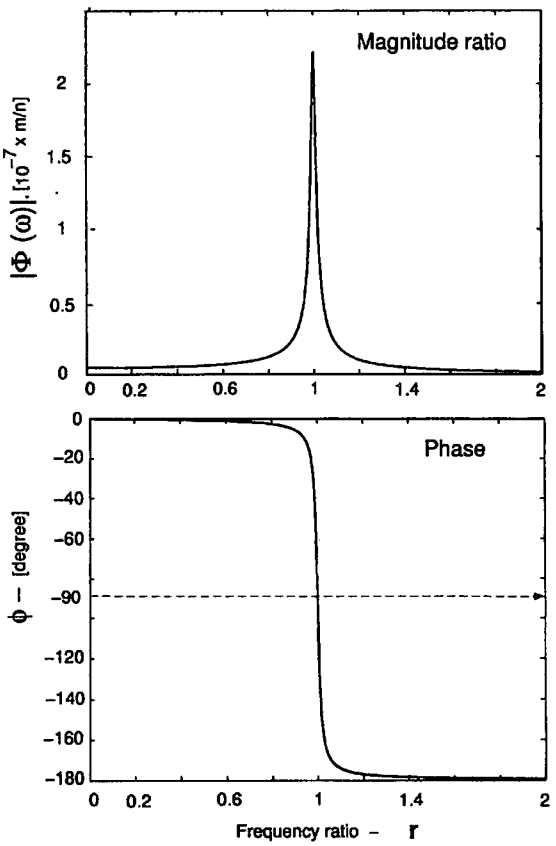

Figure A.6ab. Magnitude (a, upper) and phase (b, lower) plots of the FRF [Altintas 2000]

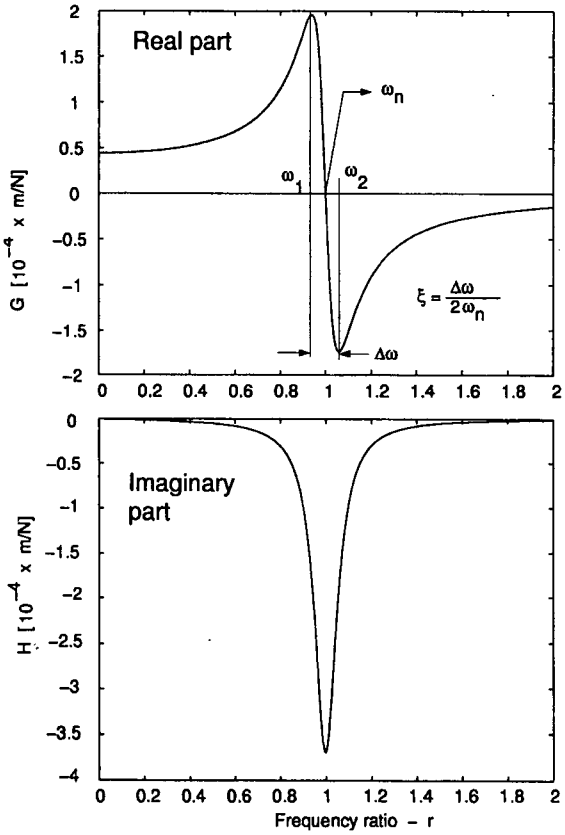

Figure A.7ab. Real (a, upper) and imaginary (b, lower) plots of the FRF [Altintas 2000]

A.2 Results

The following plots display the natural frequencies for three positions of the attachment bearing along the axis of the tool (Ls = 66, 55 and 44mm) as determined by the distributed parameter model, the finite element method, and the impact tests.

A.2.1 Distributed Parameter Model

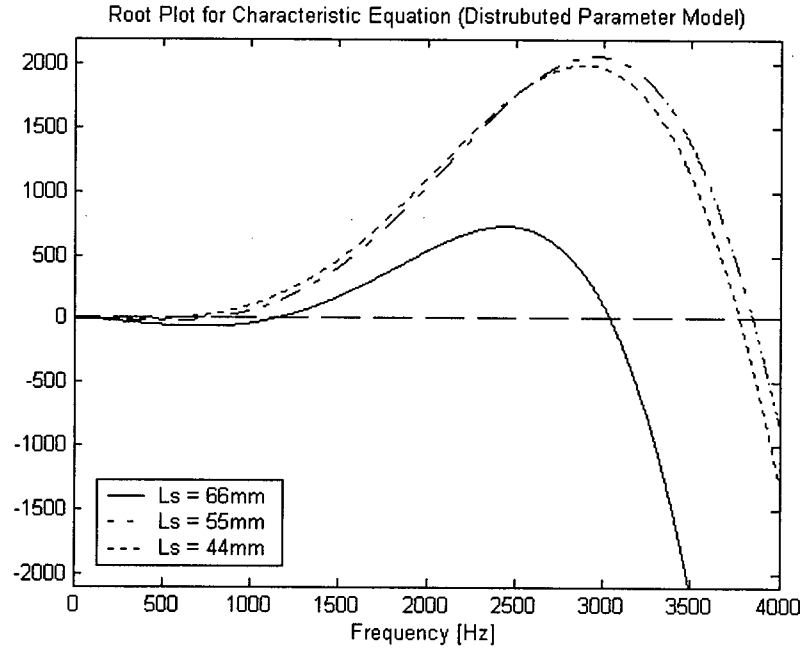

Figure A.8. Root plot for characteristic equation (distributed parameter model). Zero crossings indicate (first two) natural frequencies for three supported tool lengths (Ls, see figure A.1)

A.2.2 Finite Element Model

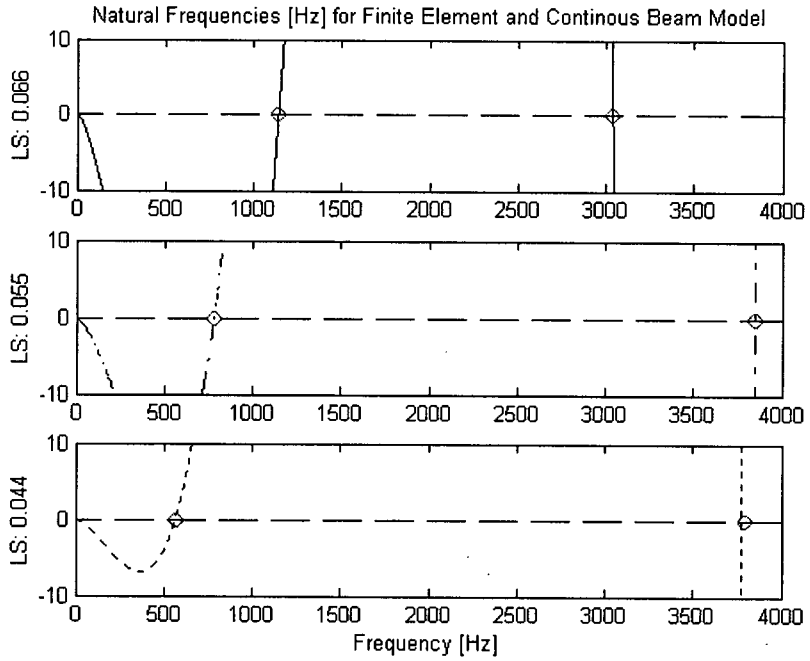

Figure A.9. Finite element solution (circles) plotted over the distributed parameter model solution (roots of the characteristic equation). Ls is the supported tool length (see figure A.1)

A.2.3 Impact Tests

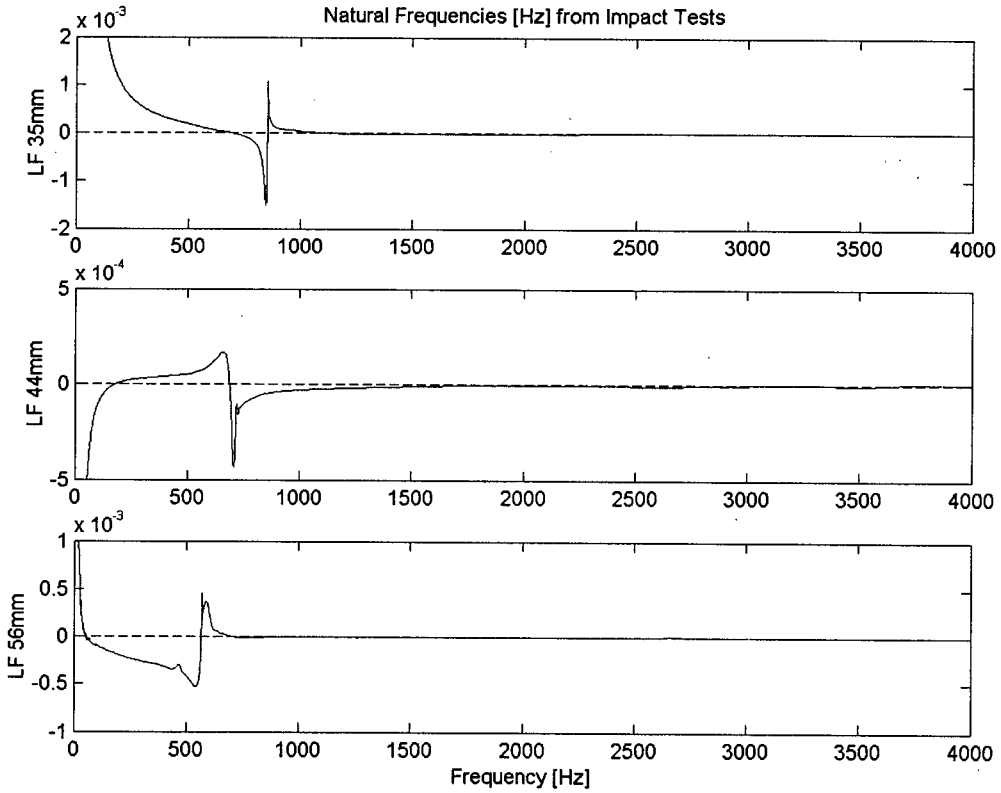

Figure A.10. Real part of transfer function as determined by Impact tests. Zero crossings indicate first natural frequencies. (LF is the unsupported tool length or length of free end, see figure A.1)

The real part of the transfer function as determined from the vibration experiments is plotted in figure A.10. The natural frequency can be found from the zero crossings of the curve. We can see that only the first natural frequency is identified from the impact test and the second natural frequency is not apparent. This is probably due to the use of a hammer to approximate an impulse. A hammer blow will always have a time duration associated with it, and although several different hammer tips and sizes were used to attain the shortest duration, this duration can limit the frequency range of the test [Halvorsen 1977]. Therefore, the higher natural frequencies of the tool should be determined from the continuous or FE model.

A.3 Discussion

Cutting tool vibrations can cause dimensional errors and poor surface finish on bone surfaces in implant surgery. In milling, the excitation frequency or forcing frequency due to the cutting force is dependent on the operating speed and the number of cutting teeth on the milling tool. As the excitation frequency approaches the natural frequency of the tool the vibration amplitude begins to grow. At resonance vibrations are at a maximum and the phase angle approaches -90°.

The deflection magnitude of a two-fluted cutting tool due to static and dynamic (vibrational) deformations, as a function of operating speed and feed rate, is plotted in figure A.11. The orthogonal data of Wiggins [1978] (α = 10°, cutting mode: transverse, parallel, transverse) is used to calculate the cutting forces. The deflections are for a 3.1mm diameter circular shaft that is extended 34mm past the support bearing. At low cutting speeds (less than 10,000 RPM) the high deflections are due to the static deformation of the tool under the high cutting loads. As the speed increases, the cutting forces and tool deflections decrease. When the periodic cutting forces approach the natural frequency of the tool (at ~1140 Hz or ~34200 RPM), the tool resonates in the first mode of vibration and deflections are at a maximum. As the speed is further increased, the amplitude of the vibrations decrease because the physical structure cannot respond to the high frequency disturbances. At ~90,000 RPM (or ~300 Hz), the second mode of vibration is excited and the vibrations are at a maximum again. It should be noted that although centripetal and gyroscopic forces are not considered here, these other dynamic effects would cause even larger tool deflections at the higher operating speeds.

Similarly, the deflection magnitude of the two-fluted cutting tool extended 56mm past the attachment bearing is plotted in figure A.12. The deflection magnitude at the low cutting speeds (less than 10,000 RPM) is increased due to the decreased stiffness of the structure. The first natural frequency of the structure is also decreased (ω_n ~ 560 Hz) and vibrations peak at ~17000 RPM. The second natural frequency is also shifted (ω_n ~ 3800 Hz) and is now beyond the 100000 RPM operating speed mark.

These results show that the cutting speed can dramatically effect the tool deflection and vibration effects should be considered when selecting an optimal cutting speed. Based on these results, I would recommend an operational speed of ~60000 RPM for the two fluted cutting tool considered here.

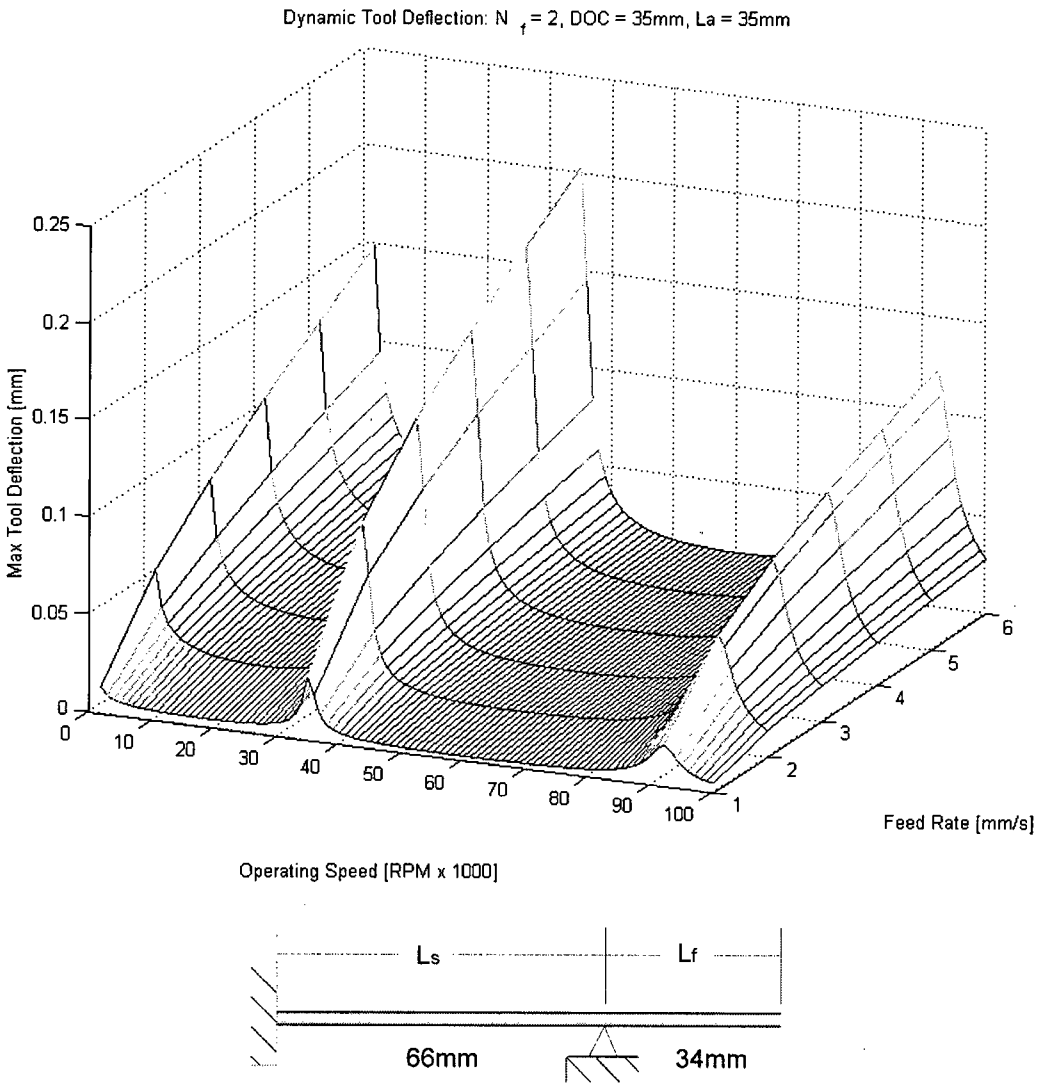

Figure A.11. Maximum tool deflections as a function of operating speed and feed rate for a 2-fluted milling tool (circular shaft) extended 34mm beyond the attachment bearing.

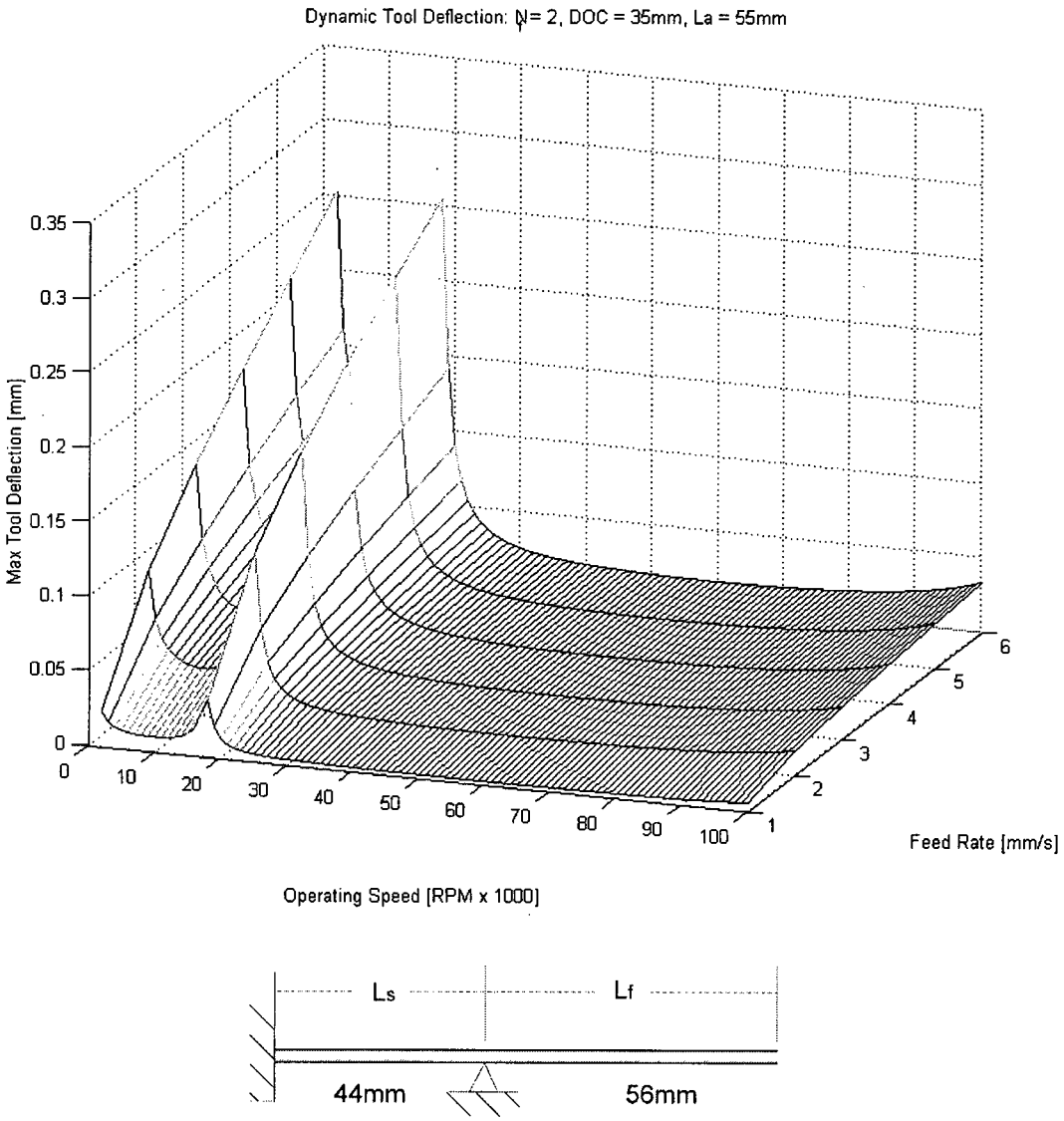

Figure A.12. Maximum tool deflections as a function of operating speed and feed rate for a 2-fluted milling tool (circular shaft) extended 56mm beyond the attachment bearing.

A.4 References

Altintas Y. Manufacturing Automation: metal cutting mechanics, machine tool vibrations, and CNC design. *Cambridge University Press*. Cambridge UK. 2000

Stokely WF. Vibration of Systems Having Distributed Mass and Elasticity. In: Shock and Vibration Handbook, edited by C. M. Harris and C. E. Crede. New York: *McGraw-Hill*, 1961

Halvorsen W.G. Brown D.L Impulse Technique for Structural Frequency Response Testing. *Sound and Vibration*. Nov. 1977

Appendix B:

A Passive Bone Milling Guide for Computer-Assisted Total Knee Replacements

Christopher Plaskos & Antony J. Hodgson

Department of Mechanical Engineering
University of British Columbia, Vancouver, BC, Canada
ahodgson@mech.ubc.ca

Abstract. In contrast to conventional bone sawing, robot guided milling can accurately position and execute bony resections relative to the essential biomechanical landmarks, while keeping temperature elevation and surface roughness under the critical values for bone necrosis and ingrowth into porous implants. This short paper describes a novel cutting guide for computer-assisted total knee replacement (TKR) that secures to the bone and passively constrains a high speed mill in the desired cutting plane. The benefits of milling are utilized while the invasive registration and immobil-ization issues (as well as cost and clinical feasibility) associated with robotic aided surgery are avoided. Preliminary results show that sub-degree accuracy is achievable with small forces transferred at the bone/guide interface.

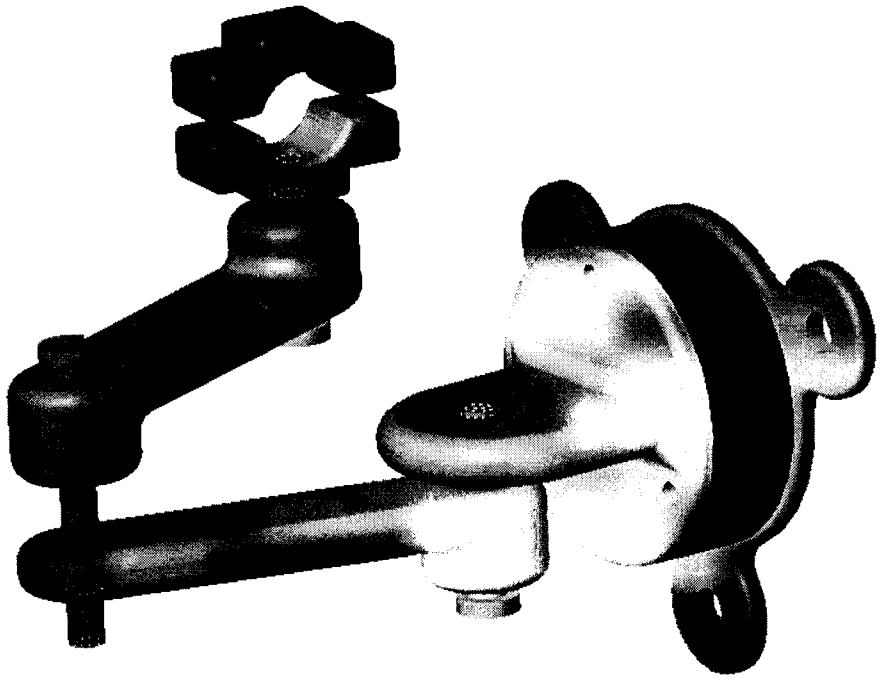

Figure B.1. Protoype Passive Cutting Guide

B.1. Introduction

The consequences of malalignment and inconsistent fixation of cementless implants in TKR have increased efforts in the field of computer-assisted surgery, aiming to improve the accuracy and repeatability of the procedure without introducing additional imaging requirements (such as preoperative CT scans) or invasive procedures (such as IM rods or preoperative fiducial pins). We have shown that bony resections carried out using conventional oscillating saws can produce significantly variable cuts, and can contribute as much as 90% of the total variance of frontal plane alignment when incorporated into a computer-assisted technique [1]. In comparison to oscillating saws, high speed milling tools have lower vibration and reaction forces. This work investigates the feasibility of realizing TKR resections with a high speed mill constrained to the desired cutting plane by means of a miniature two degree of freedom (DOF) passive arm secured to the bone.

B.2 Design and Methods

The prototype milling guide incorporates a planar arm with 3 revolute joints in parallel and an attachment for the milling tool and guide reference frame. The 2 DOF passive arm prevents the surgeon from tilting the cutting tool out of the desired cutting plane while still allowing the surgeon to feel the cutting forces and safely make the cut. Once the patient's mechanical axis (MA) is registered and the guide is mounted and calibrated, the pose of the cutting plane relative to the MA is manually adjusted by the surgeon under computer guidance. For this evaluation, a force/torque sensor (ATI Industrial Automation, NC, USA) was mounted at the bone/guide interface in order to quantify any excessive forces transmitted to the bone.

A pneumatic mill (Midwest Rhino XP, IL, USA) operating at 20000 rpm (40psi) was used with a 80mm side cutting tool (Midas Rex S4-218, TX, USA). Eleven cuts approximating primary resections and recuts were made on six rigidly clamped porcine specimens: 3 tibia and 3 femora (specimen mass ~90kg, average resection surface 15.4cm^2). Angular pose of the bone cut plane relative to the guide plane was measured with a Flashpoint 5000 localizer (Image Guided Technologies, CO, USA), as in [1]. The guide plane was calibrated before each cut by tracking the tool's motion within the cutting plane and fitting a plane to the points using a least squares criterion.

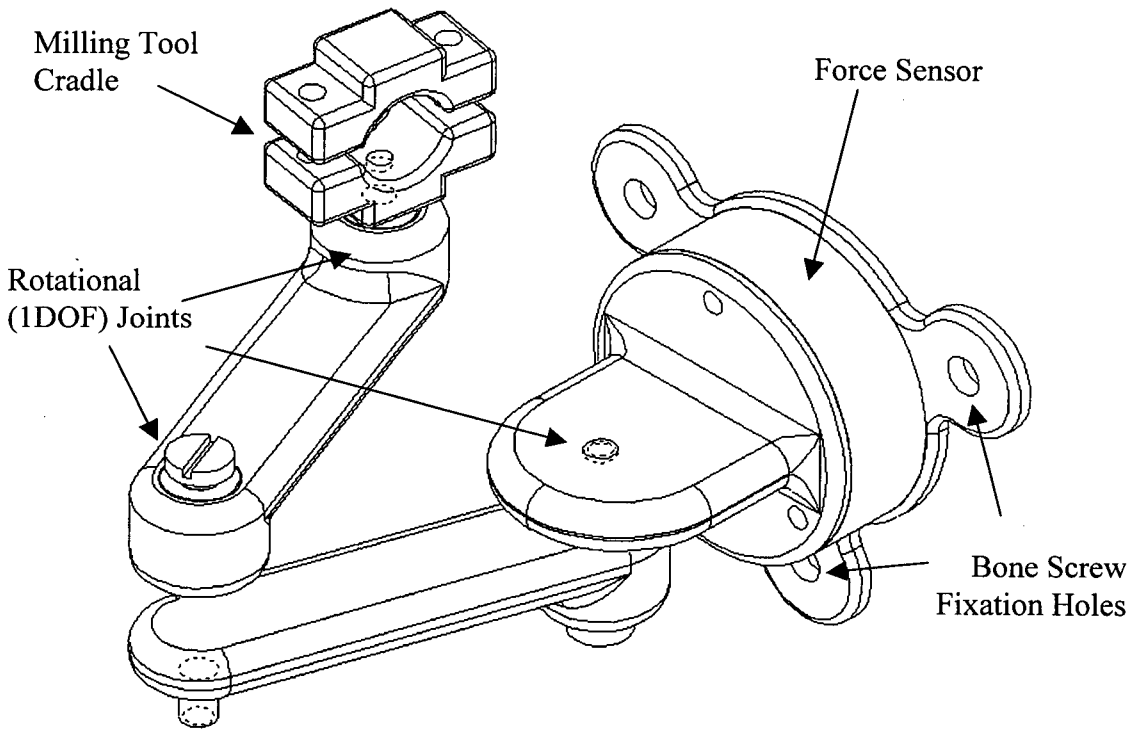

Figure B.2. Wire-view of 3 degree of freedom (DOF) prototype passive milling guide.

B.3 Results and Discussion

The angular accuracy (mean ± standard deviation, SD) in the frontal (varus/valgus) and sagittal (flexion/extension) planes for all cuts are presented in Table 1, along with the mean maximum and mean absolute force and torque values. The guide reference frame was tracked during the cutting task, and the average absolute perpendicular distance (along the guide plane normal, or proximal/distal direction) of each point tracked to those collected during calibration represent the proximal/distal error value. The frontal plane variance is limited to <0.1 $(°SD)^2$ with the largest variance residing in the sagittal plane. No significant bias was found in either plane (in contrast to the sagittal plane bias of ~1° found with sawing [1]). Force values are minimal in the plane of the guide and peak along the proximal/distal direction. Although histological and inter-user evaluation still remains, passive guidance appears to be an effective means of realizing accurate and repeatable resections in TKR.

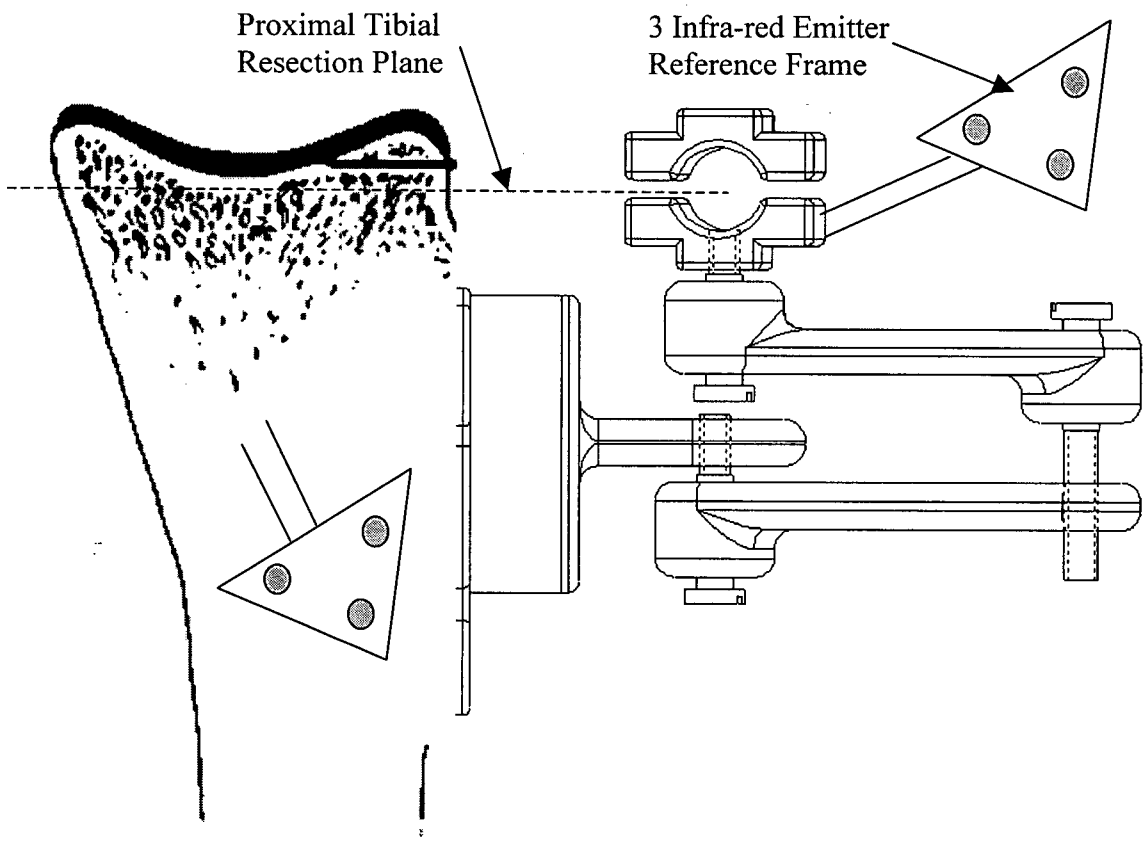

Figure B.3. Typical Tibial Plateau Resection

Table 1 [Mean ± SD]	Varus/Valgus	Flexion/Extension	Proximal/Distal
Error: [$n_{cuts} = 11$]	0.0 ± 0.25°	0.0 ± 0.43°	0.30 ± 0.21mm
Maximum Force [N]	2.7 ± 1.1	2.6 ± 0.9	4.7 ± 1.5
Maximum Torque [N·mm]	300.1 ± 80.0	246.3 ± 98.9	71.8 ± 30.9
Mean Abs. Force [N]	0.31 ± 0.1	0.37 ± 0.1	0.75 ± 0.1
Mean Abs Torque [N·mm]	60.5 ± 9.7	56.1 ± 7.2	11.6 ± 1.9

B.4 References

1. Inkpen KB, Hodgson AJ, Plaskos C, Shute C, McGraw RW: Repeatability and Accuracy of Bone Cutting and Ankle Digitization in Computer-Assisted Total Knee Replacement. In: Delp S, DiGioia A, Jaramaz B (eds): MICCAI 2000. Lecture Notes in Computer Science Vol. 1935, Springer-Verlag.1163-1172.